# THE INFLUENCE OF SOIL DEPTH MODELS ON SIMULATING SLOPE INSTABILITY THE CASE OF SOUTHERN DOMINICA

MULUGETA BEYENE DIBABA
February 2019

SUPERVISORS:
Dr. D.B.P. Shrestha (Dhruba)
Prof. Dr, V.G. Jetten (Victor)

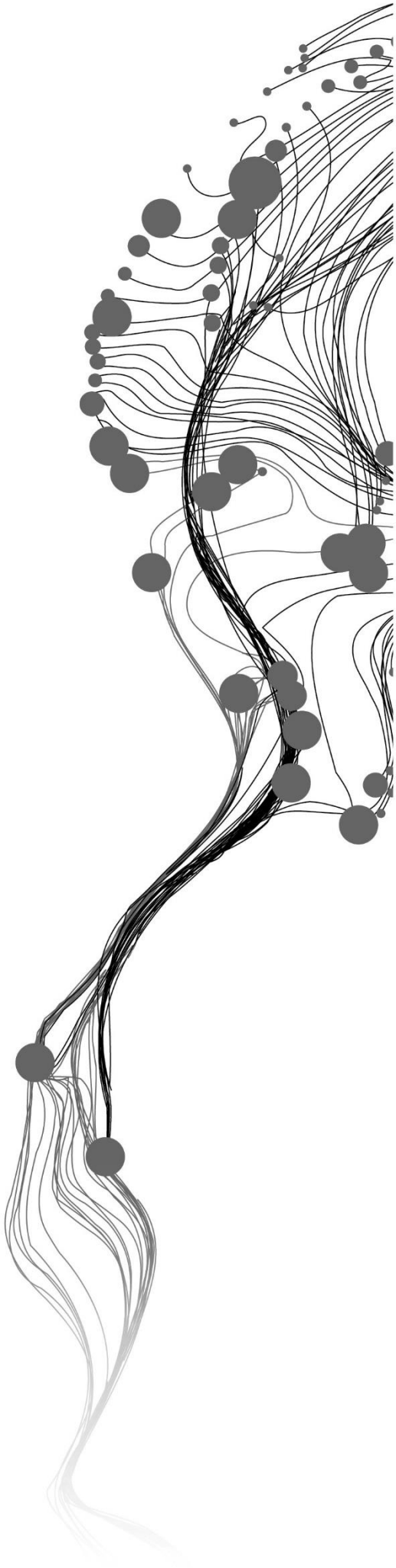

# THE INFLUENCE OF SOIL DEPTH MODELS ON SIMULATING SLOPE INSTABILITY
# THE CASE OF SOUTHERN DOMINICA

MULUGETA BEYENE DIBABA
Enschede, The Netherlands, [February 2019]

Thesis submitted to the Faculty of Geo-Information Science and Earth Observation of the University of Twente in partial fulfilment of the requirements for the degree of Master of Science in Geo-information Science and Earth Observation.

Specialization: Applied Earth Sciences (Natural hazards, risk and engineering)

SUPERVISORS:
Dr D.B.P. Shrestha (Dhruba)
Prof. Dr, V.G. Jetten (Victor)

THESIS ASSESSMENT BOARD:
Prof. Dr N. Kerle (Norman) (Chair)
Dr Jeroen Schoorl (Wageningen University & Research) (External Examiner)

# ABSTRACT

Dominica is one of the most active landslide-prone areas in the Caribbean islands. Landslides, which usually occur during tropical storms and hurricanes, can result in catastrophic loss of life and property damage. Hence, for any development effort in the area, one should take into account of landslide-prone locations to reduce its negative consequences. For slope stability assessment, soil depth is considered as an essential factor. In this study, the influence of soil depths, derived from different soil depth models, on slope instability was analysed. Unfortunately, dense soil depth sampling in the field was very challenging due to the inherent young volcanic nature of the island, rugged topography, very steep slopes and dense forest cover. Besides, the available DEM lacks terrain details and contain some artefacts. However, models which explain the spatial variability of soil depth is required for slope instability assessment. Hence, three different techniques namely decision tree, multiple linear regression and soil water balance were applied for estimating soil depths. All the soil depth models predicted deep soil within stream channels. Decision tree and multiple linear regression model predicted shallow to moderately deep soil on the slopes while the soil balance model predicted moderate to very deep soils. The predictive powers of each soil depth model were checked against the field measurements. The results show that the soil depth predicted using the decision tree gave higher correlations with surface topography. Following the soil depth simulations, landslide susceptibility assessment was carried out using the infinite slope model in which various soil depth maps were used as one of the input data layers while other data (shear strength of soil, soil hydraulic properties, data on land use, topography, etc.) were kept constant. Also, the role of rainfall in landslide trigger is considered, and its influence was checked by varying between normal and extreme values. Then the factor of safety obtained from the infinite slope model under both normal and extreme rainfall conditions was validated against existing landslide inventory data. The result shows that soil depth, obtained from the decision tree, showed a good correlation with the existing landslide inventory data. Furthermore, the influence of slope gradient on slope failure was checked, which showed that most slope failures were located on slope angles greater than 37 degrees.

Keywords: Soil depth, prediction, topographic variables, infinite slope, inventory landslide, model validation

# ACKNOWLEDGEMENTS

First and foremost, I would like to thank God, the Almighty, for his blessing and strength to undertake this research work. I would also want to take this opportunity to thank the Netherlands government for the Netherlands Fellowship Programme (NUFFIC) who covered every expense of my study under NFP Fellowships.

My sincere gratitude likewise goes to my supervisors, Dr Dhruba Shrestha and Prof. dr. V.G. Jetten (Victor) for their continuous guidance and support throughout this research work. This thesis work would have been unfeasible without their direction and scientific inputs. They were always there for me when I needed help.

My deepest appreciation also goes to all staffs of the Earth science department at ITC who are academically motivated and helpful at any time. I also thank Dr Cees Van Westen for his explanation and scientific input during our fieldwork in Dominica. Prof. dr. V.G. Jetten (Victor) has contributed a lot in understanding the details of this research problem during the fieldwork in Dominica, and I am grateful for that. I am also indebted to a team who worked with me on different problems in Dominica including Fernando, Aron, Bastian and Sobhan for a great moment and wonderful discussion we had.

I am also blessed with classmate friends and cheerful groups of fellow ITC students and am grateful for that. I will always remember my classmates (Mishi, Vincent, Lilian, Marcius, Fernando, Felippe, Kasimir, Aron, Ayu) for the wonderful discussion we made and from which I have learned a lot.

Last but not least, I am grateful to my families and friends who made me feel home when I am away from home.

# TABLE OF CONTENTS

# LIST OF FIGURES

# LIST OF TABLES

# 1. INTRODUCTION

## 1.1. Justification of the study

Landslide and flood are the most frequently occurring natural disasters followed by tropical storms and hurricanes across the world. Both landslide and flood in combined affected more than 78million people globally and caused economic damage of about 59billion USD in 2016 alone(Guha-sapir et al., 2016). Landslide mainly is a common hillslope process which causes loss of life and properties in mountainous areas of the world. Its frequency has also recently increased despite the lack of comprehensive information on the actual damage it caused(Gariano & Guzzetti, 2016). Landslides caused worldwide fatalities of 32,322 between the year 2004 and 2010. Likewise, the annual global economic loss due to geophysical disasters including landslides was estimated to be 32 billion USD in 2016 although this figure is ambiguous due to lack of detailed data (Guha-sapir et al., 2016).

The main triggers of a landslide are rainfall and earthquakes, and several other environmental factors contribute to the probability of landslides occurring (Segoni et al., 2011). Environmental factors constitute the complex interactions of topographic attributes, geological and anthropogenic factors of a given area (Matori & Basith, 2012; Mccoll, 2015). Topography initiates shallow landslides by controlling subsurface flow and through slope gradient(Montgomery & Dietrich, 1994). The demand for land due to population growth and urbanisations has forced people to settle on unstable slope regions (Di Martire et al., 2012). Then, people activities on unstable slopes like the construction of houses and roads aggravate slope instability. The global climate change has also significantly contributed to an increased slope instability of the last decades (Gariano & Guzzetti, 2016). Similarly, slope processes controlled by geomorphological, geological and hydrological factors indisputably induce slope instability and determine its distributions (Reichenbach et al., 2014).

Assessment of landslide causes is useful for mitigation and future development of hazardous areas(Mccoll, 2015). It involves mapping the probability of landslide occurrences using several environmental factors and different soil type related input parameters (Cascini et al., 2015; Sorbino et al., 2010). The role of soils in slope instability is undisputable because most of the slope failures happen through soil mass (Ran et al., 2012). Broadly speaking, slope instability could be modelled using an either physical based model which utilise the physical properties of materials that control geomorphological processes or using an empirical-statistical model which assumes slope instability to occur under the previous condition by using terrain attribute information derived from topographic data and land use data (Goetz et al., 2011). In the physical based model, infinite slope stability analysis method is widely used in many shallow landslide analysis, and it also considers soil depth as an input parameter (Montgomery & Dietrich, 1994; Kim et al., 2015; Ho et al., 2012; Gorsevski et al., 2006).

Many types of researches have proved the significance of soil depth information in improving slope instability assessment. However, accurate soil depth measurement is very challenging and difficult to obtain at a spatial point (Fu et al., 2011; Michel & Kobiyama, 2016). Because, the boundary between depth to a hard surface (soil depth) and underlying bedrock is mostly gradational as different lithologic units are characterised by different soil depth in different climatic zones (D'Odorico, 2000). Also, the rate of weathering variation with depth disturbs the sharp boundary between soil and rock. Another factor that makes soil depth measurement a challenging task is associations of depth variation with site-specific

nature that depends on soil forming factors and landscape history (Wilford & Thomas, 2013; Schaetzl, 2013).

Despite the challenges, we can still obtain soil depth information from road cuts, river cuts, borehole site and other human-made incisions and landslide scarps of an area. Various researchers used soil mechanical and soil hydrologic properties to define the boundary between soil and underlying rock. Catani et al. (2010) described soil depth as the depth to the first significant marked vertical change in the hydrological property of soils which can be determined based on field grain size description. Cascini et al. (2017) considered soil depth as the depth at which the first change in geotechnical properties of the soil occur that could be decided based on field strength measurements. Kuriakose et al. (2009) also described soil depth as depth to relatively consolidated surfaces (based on soil strength). Besides, the clue of soil depth can also be obtained from the influence of parent materials. For example; carbonate rocks like limestone are highly susceptible to weathering because they are chemically reactive while quartz-rich materials are more resistant to weathering. Hence, in a similar environment, carbonate rocks form thin soil whereas coarse-grained mafic materials form deep soils. On the other hand, basic volcanic rocks produce soil suitable for plant growth, so we can see vegetation difference, whereas soils formed from acidic volcanic rocks possess high quartz minerals and are stable in structure but low in fertility(Gray & Murphy, 1999).

Several soil parameters related to soil mechanical and hydraulic properties are required as an input in an infinite slope model to determine the influence of soil depth in landslide initiations. Soil strength parameters are either determined in the field (like cohesion) or analysed in the laboratory. However, parameters related to soil hydraulic properties are difficult and time-consuming to measure in the field, but it can be easily obtained from readily measured soil properties using a different method. One of the commonly used predictive functions of soil hydraulic properties is a pedo-transfer function (PTF)(Wosten et al., 2001). It is a predictive function of soil properties and variables from available soil information to parametrise soil process(Looy et al., 2017).

## 1.2. Background study

Prediction of soil depth spatial variability is essential for understanding and analysis of the slope process in a landscape (Lucà et al., 2014; Scull et al., 2003). Moreover, soil depth influences the spatial and temporal distribution of shallow landslides in mountainous areas (Montgomery & Dietrich, 1994; Segoni et al., 2011; Kim et al., 2016). Also, soil depth determines a depth of slope failure surface and volume depending on the subsurface flow of water and its connectivity through the soil mass(Sorbino et al., 2010; Lanni et al., 2012; Fan et al., 2016). Although soil depth plays a crucial role in slope stability analysis, its detail remains a challenging task because of the various factors influencing its spatial distribution. Kim et al. (2015) correlated soil depth spatial variation to local topographic units to improve landslide predictions. Still, it is unlikely for soil depth to be strongly correlated to unique topographic attributes because of its various factors which control its depth. Derose et al. (1991) suggested analysing soil depth relationships with all influencing landscape factors to have accurate soil depth information. Practically, accurate soil depth information is obtained only through direct measurements which is costly and time-consuming.

Many methods of soil depth estimation that have been developed through time are currently available. Several researchers used a single method while others compared different types of methods to get a good result. Tesfa et al. (2009) predicted soil depth using generalised additive and random forests statistical methods, but the result explained only 50% of the soil depth spatial variation within the catchment. Cascini et al. (2017) estimated soil thickness from topography and geological analysis for landslide analysis

which required the improvements of their results through geotechnical back analysis of failed slopes and geomorphological analysis. Sarkar et al. (2013) predicted soil depth from elevation, slope, aspect, slope curvature, topographic wetness index, distance from the streams and land use using a soil-landscape regression kriging model where the model result explained 67% of soil depth spatial variation. Kuriakose et al. (2009) compared multivariate statistical methods with geostatistical methods for predicting soil depth by applying regression kriging on environmental covariates of elevation, slope, aspect, curvature, wetness index, land use and distance from streams and obtained prediction result which explained 52% of soil depth variation.

It is evident that the existing methods of soil depth prediction are not universal, and the issue of soil depth mapping is still open for further research because of uncertainties on the details of hillslope interiors (Zhang et al., 2018). These uncertainties could be either input uncertainty or model uncertainty (Bishop et al., 2006). Furthermore, soil depth mapping can be conducted using decision tree models where a detailed soil survey is not practical. It involves the correlation of field depth observations and explanatory soil depth distribution variables like topographic variables (Taghizadeh-Mehrjardi et al., 2014). Besides, soil depth field observations and the topographic explanatory variables can be related based on the general principles of soil distributions on the slope. Montgomery & Dietrich, (1994) related soil distribution on the slopes to soil formation through weathering and soil removal by erosion processes where they described the process as a soil balance. Kuriakose et al. (2009) used the soil balance principle and tested it in Southern India by relating soil depth to environmental variables using a script to produce a soil depth map. In general, it is logical to relate soil depth to topographic variables which assumes a relatively shallow depth with relatively young soils and a strong influence of geomorphological processes (denudation and accumulation). However, the relationship between soil depth distributions and topography does not always exist as in the case of a deep weathered tropical soil under rainforest that has a strong surface process and deep volcanic deposit.

The present study area located in the Southern part of Dominica is one of the active landslide areas of the region. Previous studies on the area described the frequent extreme hurricane and tropical storm events as the main factor inducing landslides in the area. These studies are focused mainly on national scale landslide susceptibility assessment (De Graff et al., 2012; Zafra, 2015; van Westen, 2016), landslide dam failure (Jerome et al., 2010), and national flood hazard maps (Jetten, 2016). However, soil depth which was proved to be an essential factor in improving slope instability analysis (Lucà et al., 2014; Scull et al., 2003; Montgomery & Dietrich, 1994; Segoni et al., 2011; Kim et al., 2016; Sorbino et al., 2010; Lanni et al., 2012; Fan et al., 2016) was not given emphasis by the previous studies in the present study area. Therefore, this study assumes slope failure causes many damages unless identified in advance through slope stability analysis and the best way to improve the analysis result is by including soil depth as the principal input parameter because of slope failure sensitivity to soil depth. However, soil depth maps were produced using different techniques to get options of improved results because of the quality of existing DEM, size of the area, density and the spatial distributions of field soil depth points.

### 1.3. Factors influencing landslide occurrence: A Review

Every slope has the potential to fail at some point in time based on the magnitudes of stress resisting failure along an assumed failure surface. Hence, the stability of the slope is assessed based on the balance between opposing forces and driving forces whose relative ratio is expressed as a factor of safety(McColl, 2015). Popescu, (1994) classified factors that cause different stages of landslide stability into preparatory factors (factors that reduce stability over time) and triggering factors (factors that initiate movement) based on their function (Figure 1.1). Preparatory factors include antecedent rainfall, weathering, landcover,

(de)forestation and triggering factors like meteorological factors, earthquake and human factors (Gariano & Guzzetti, 2016).

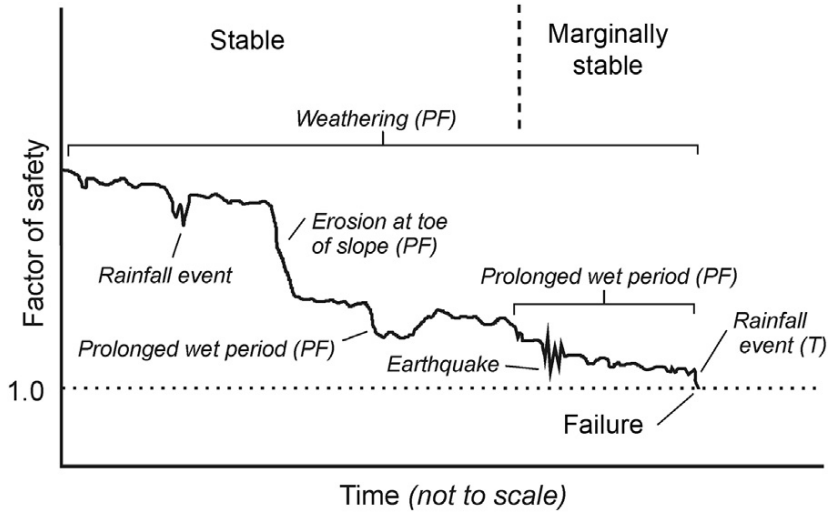


Figure 1.1 Example of how the factor of safety changes in time due to many factors. Source: (Popescu, 1994)

A list of main factors that play a role in landslide occurrences is presented as follow. The general overview of some of the factors was also highlighted under the background study subtopic above. Usually, each of the influencing factors can also act together in causing a landslide and hence, influence one another.

**i) Topography**

Local topography influences the occurrence and spatial distributions of landslide through both the concentrations of subsurface flow and slope gradient (Montgomery & Dietrich, 1994). The increase in slope gradient facilitates slope failure under the force of gravity and increases the likelihood of slope failure because of an increase in shear forces on a steep slope. Mccoll, (2015), argued slope geometry (slope height and steepness) which is determined by material strength is only a precondition for landslide occurrences, and failure occurs when a factor of safety drops either suddenly or gradually by internal or external factors. Then, the very steep slope nature of the present study area is a potential facilitator for landslide occurrences.

**ii) Geology**

Lithology and weathering characteristics of materials control geomorphology and together influence the likely distribution of landslides (Dai & Lee, 2003; Mccoll, 2015). Geological structures and other planes of weaknesses like cleavages, foliation, bedding plane and weathering horizon found within lithologic or weathered mass are even the primary landslides influencing factors, mainly when favourably dipping to the valley side of the slope (Mccoll, 2015). Although the lithological parent materials of the present area are volcanic in origin and closely related, the spatial variability of rainfall caused variations in weathering effectiveness and produced different soil types that influence landslide occurrence. The soil types of the area have significant differences in strength and closely related in texture based on the weathering intensity, time, age of volcanic source materials(Rouse et al., 1986).

**iii) Climate**

The long term climate changes (mainly temperature and rainfall) influence the occurrence of a landslide(Gariano & Guzzetti, 2016). They stated that an increase in rainfall intensity and frequency

increases landslide occurrences because it is a primary landslide trigger. However, long term rainfall pattern affects the occurrences of deep-seated landslide more than shallow slide(Mccoll, 2015). Temperature influences landslide occurrence in rock slopes by altering rock fracture openings due to icefall and avalanche, and deep-seated landslides by changing the hydrological cycle(Gariano & Guzzetti, 2016). The primary role of rainfall is to affect factors of shear stress and shear strength adversely. Hence, rainfall reduces soil strength and effective stress(through increased weight), increase river discharge and removes basal and lateral slope support, lubricates failure surface between minerals and facilitates slope failure(Crozier, 2010). Furthermore, rainfall infiltration into the soil slope causes groundwater fluctuations and leads to slope failures.

**iv) Earthquake**

Ground shaking by earthquakes cause deteriorations of slope material strength through particle rearrangement and reduce slope stability(Mccoll, 2015). Such a role was further elaborated that even though the present earthquake does not lead to failure, it will prepare the slope for the next event. Although the frequency of landslide changes after large earthquakes occur, the frequency of an earthquake is not the same as the frequency of climatic factors to cause frequent landslides(Gariano & Guzzetti, 2016). Earthquakes occurrence of Southern Dominica is mainly associated with volcanic complexes like Plat pays which is one of the active volcanic centres of the island. However, its cause of landslide occurrence lacks historical records (Degraff, 1987) or its intensity was not high enough to cause landslides compared to rainfall which is the major landslide influencing factor in the area(van Westen, 2016).

**v) Groundwater fluctuation**

Groundwater fluctuation is the most common dynamic trigger which affects landslide in the form of increasing slope weight, changing pore pressure against normal stress and changing inherent material strength(Mccoll, 2015). The influence of groundwater in the landslide has also been considered in many physical based models to analyse slope stability(Kim et al., 2015; Sorbino et al., 2010; Iverson, 1990) and reducing its effect is one of the remedial measures in stabilising slopes (Popescu, 2002). Previous work by Rouse, (1986) and Rouse, (1990) in Dominica island argued the main cause of shallow slide in allophane soil and other soil types was a rise in pore pressure due to the increase of groundwater table that reduced effective stress and shear strength of the soils along failure surfaces. But they also indicated that the highly porous and highly water content capacity of Dominican soils needs high rainfall to rise pore water pressure in the soils.

**vi) Weathering**

A physical and chemical weathering processes reduce the intrinsic strength of slope materials, increase pore pressure and permeability and contributes to landslide(Mccoll, 2015). In general overview, shallow failures occur on a weathered mass of steep residual soils and deep failures occur on highly weathered soil mass(Calcaterra & Parise, 2010). Dominica, having humid tropical climate have intense chemical weathering by which the soil of the area was formed(Reading, 1991; Degraff, 1987; Rouse et al., 1986). Hence, the weathering process is one of the factors that influence landslide of the present study area.

**vii) Vegetation effect**

Vegetation can have both positive and negative influences on slope instability. The positive aspect is maintaining drier soil and reducing pore water pressure through rainfall interception and groundwater

transpiration. It can also negatively influence by changing soil infiltration and evapotranspiration, adding weight to slope mass which causes slope failure(Popescu, 2002). In Dominica, most of the areas where vegetation cover became sparse due to the previous hurricane and tropical storms were more affected by landslides than areas with dense vegetation as observed during fieldwork. However, the fast-growing vegetation in the area covered some of the fresh landslide scarps which make it challenging to establish the relation between observed landslide and vegetation cover. Van Westen (2016) also mentioned the absences vegetation on potential landslide areas as interpreted from stereo images during inventory landslides preparation but commented on lack of statistical relationship between landslide occurrence and vegetation cover of the area because of lack of detailed vegetation characteristic data.

**viii) Removal of lateral support**

Lateral support of slopes can be removed either by human activities, incisions of river flow, increased throughflow, reductions of glacier volume, wave action along the shore or related factors (Crozier, 2010). Once lateral support starts to be removed, landslide could continuously occur, and each previous failures removes support of stable slope leading to reduced lateral stress and strength and causing progressive failure(Popescu, 2002). Existing inventory landslide produced by Van Westen, (2016) showed a dense landslide close to stream channels and road which indicated the removal of lateral support is another factor influencing landslide occurrence of the study area.

**ix) Frost action**

Temperature change in cold climates leads to thawing of ice between rock fractures and soil pores that reduces the strength of the slope mass and facilitates slope failure (Crozier, 2010; Mccoll, 2015). This factor has little or no influence in inducing landslides of the present area because of its geographic location in the tropical climate.

## 1.4. Problem statement

Dominica is one of the active landslide areas of the Caribbean islands which is hit by frequent tropical storms and hurricane. Most of the resulting slides happened through the soil mass and caused frequent property damages and threatened human lives. Hence, the influence of soil depth in landslide initiation is undeniable in the area while it is difficult to obtain accurate information. Many researchers developed various models to study the influence of soil depth in landslide analysis. However, there is minimal research which explicitly gives a method that is used for site-specific condition and accurately predicts soil depth for slope stability assessment particularly for the large and data-poor area due to its associated uncertainties. That is also why issues of soil depth prediction are still open for further research.

Despite the presences of various soil depth prediction models, they are not without limitations. Liu et al., (2013) broadly classified models used for soil depth prediction into stochastic models, which assumes a statistical relationship between observed data and topographic variable and a physical based model, which focus on soil evolution process. Both methods require intensive data, and so far, their effectiveness was tested mostly on the small test area. Besides, most of the existing researches focused on the use of a single model from either of the broad model classes mentioned above and applied on small catchment where soil depth has a good relationship with the topography. However, Tesfa et al. (2009) stated the use of a single method could only show partial success because of the difficulty to incorporate various uncertainty parameters in a single model. Hence, the use of different models for soil depth prediction is believed to give more options to improve prediction results. For example, the applicability of empirical models like geo-statistics is limited to test area and require a significant amount of field data, but incorporating

physical based model will improve the prediction result(Liu et al., 2013). Presently, there is no research done on soil depth predictions in Dominica which is one of the most sensitive input parameters in slope stability analysis although the island is frequently affected by the landslides. In the present area, both the local government and the community are also interested to know the landslide probability of occurrence around settlements and infrastructures.

## 1.5. Objectives

### 1.5.1. General objective

This study intends to analyse the influences of different soil depth models on slope instability initiation using topographic predictor variables and field data.

### 1.5.2. Specific objectives

The following specific objectives are formulated to achieve the general objective of the present study.

i) To create soil depth maps using different techniques based on soil depth observations and topographic variables.

- Which spatial interpolation method gives the best results in assessing soil depth?

ii) To analyse the spatial relationships between soil depth and associated topographic variables.

- Which topographic variables explain well spatial variability of soil depth?
- Which locations have a soil depth that cannot be related to the topography, and why?
- Can we explain the uncertainty of soil depth predictions in relation to the quality of the variables used?

iii) To assess the sensitivity of slope instability of the area to the soil depth model results.

- What is the sensitivity of slope instability to soil depth relative to other variables?
- Is this influence of soil depth different in a year with average rainfall as opposed to a year with the extreme rainfall?

iv) To validate slope instability prediction results using existing inventory landslide data.

- Can the result of slope instability model be related to the landslide inventories?

## 1.6. Structure of the thesis

This thesis is structured as follow;

Chapter 1: Introduces the background and justifications of the study, problem statement, objectives and review of slope instability factors

Chapter 2: Describes the study area, the climate, the geology and landslides of the area (inventory landslide and field observations)

Chapter 3: Describes the available datasets and research methodology followed

Chapter 4: Presented the result of soil depth models and model validations through their relationship with the topographic attributes

Chapter 5: Presented the results of infinite slope model and its validation using inventory landslides.

Chapter 6: Discusses the results of soil depth and infinite slope model based on objectives achieved, concludes the key elements of the research and indicates possible future research in the form of recommendations.

# 2. STUDY AREA

## 2.1. Location and general description

The study area is located in the centre of the Lesser Antilles island arc, to the east of Caribbean sea and southern part of Dominica island, and covers an area of 43 square kilometres (Figure 1). The island is a volcanic formation with rugged topography and dense vegetation cover. The geology of the area is composed of various volcanic rocks which include ignimbrites, lava flows, lahar deposits, and volcanic ashes (Van Westen, 2016). The soil of the area is formed by weathering of tropical wet climate, and the rapid denudation caused slopes with thin soils and valleys filled up with debris over time, by erosion and mass movement (Jetten, 2016). The test area is defined by geographic coordinates of 15° 18' 26.7"N to 15° 12' 40.27"S latitude and -61° 20' 54.67"W to -61° 15' 38.19"E longitude, where the elevation reaches up to 1176m above sea level.

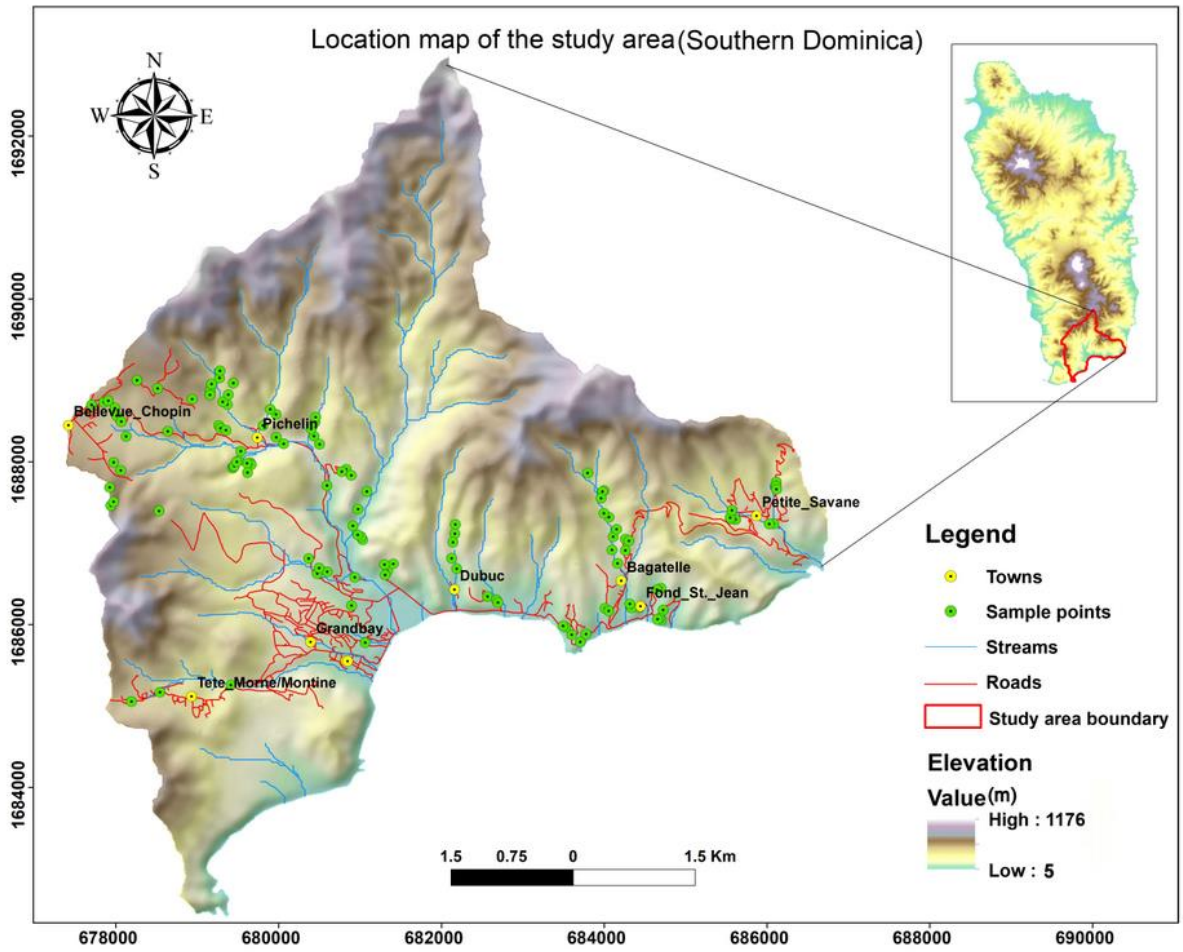


Figure 2.1 Location map of the study area

## 2.2. Climate

Dominica has a tropical climate with hot and humid air all year round. The rainfall patterns of the area from 1975 to 2013 showed the mean annual rainfall of 2620mm, which varies from a minimum of 1950mm to a maximum of 3937mm. The rainfall variation of the area is also highly seasonal. According to Reading (1991), rainfall which varies between the Western leeward coast that receives low rainfall and the perennial wet mountainous interior that receive high rainfall controls the soil distributions of the area. Also, rainfall variability caused rates of weathering variations over a short distance of the small island (Rad et al., 2013). Dominica has a dry season from January to mid-April and rainy season from mid-June to mid-November. Tropical storm and hurricanes most likely follow extreme rain of the area which occurs between August to October. Dominica has experienced many hurricane events at a different time out of which the two most destructive hurricanes were hurricane David and hurricane Maria which were category five hurricanes. Hurricane David which occurred in August 1979 caused many damages and generated many landslides, collapsed the economy and destructed infrastructures(Degraff, 1987) and similarly, hurricane Maria which happened in September 2017 also caused many disastrous damages to the island. The peak wind speeds were 280Km/hr and 282Km/hr for Hurricane David and Hurricane Maria respectively capable of producing severe losses.

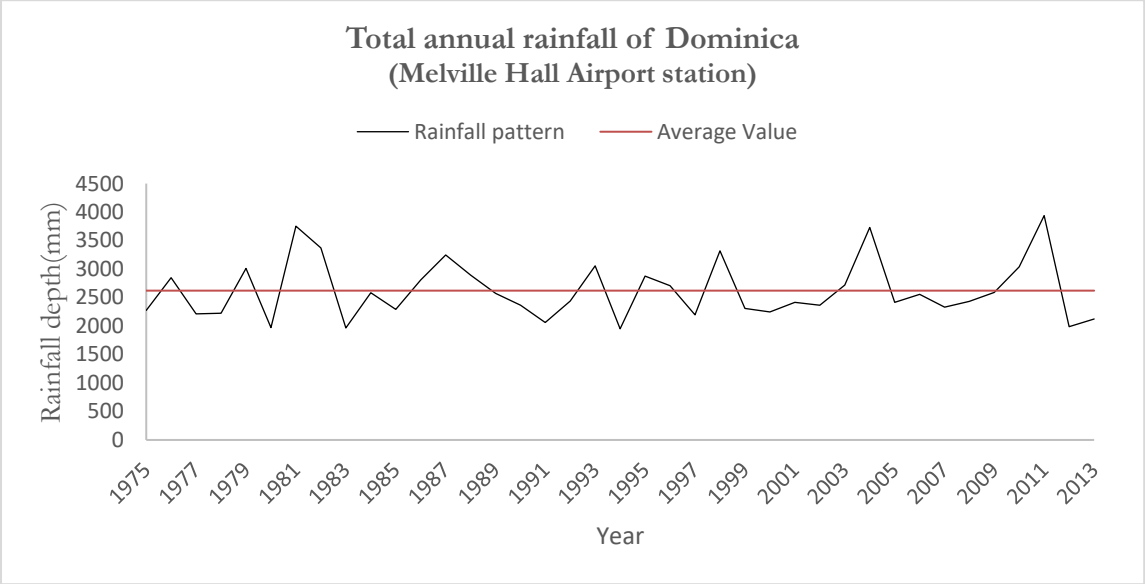


Figure 2.2 Rainfall pattern of Dominica (from 1975 to 2013)

## 2.3. Geology

Dominica is mostly made up of volcanic rocks of andesitic to dacitic rock types and their weathering by-products that formed rugged relief(Rouse, 1990). The volcanic products are mainly pyroclastic fall deposit types. In addition to the fall deposits, Pleistocene-recent dome forming pumiceous pyroclastic flow deposit form the mountain chains of the island (Howe et al., 2015). Because of such a close similarity in lithologic types and age of the island, soil formation is attributed to the climatic variability within the island(Reading, 1991).

Degraff (1987) described the geologic history associated with repeated volcanic eruption as the primary cause of landslides in the area. He argued, such a repeated and successive eruption has resulted in creating contacts (weak zones) between successive rock units dipping to either side of the highlands. Availabilities

of geological discontinuities between rock layers facilitate deep chemical weathering and influence soil formation and landslide occurrences.

## 2.4. Soils

Soils of the area are volcanic in origin and significantly vary as a result of variation in leaching effects in response to change in climatic factors, the age of the island and geology (Reading, 1991; Rouse et al., 1986). The present study area was large, and it was impossible to access all the soil types available within the test site. Hence, soil class information on the area was obtained from the previous works by Rouse (1986) who classified soils of the island into four major types as follows; (1) Smectoid soils also called black cotton soils, or tropical black clays were originated from pyroclastic volcanic materials, shallow in thickness and impermeable due to montmorillonite clay content. It occasionally has cemented silica pan at B-horizon that made it have high dry unit weight subsoil and low porosity. (2) Kandoid soils: A reddish to bright reddish soil because of dominant iron oxide mineral content are found around older volcanic areas, relatively thick, has no hardpan, susceptible to erosion or failure. (3) Allophane latosolic: Are deep, organic reach and covers the interior part of the young island reliefs and mostly formed due to slope erosion. (4) Allophane podzolics: Covers the wettest part of the island, high organic matter content and moderate thickness.

The available soil type map of the area is a generalised map which was prepared by Lang, (1967) and converted into GIS file by van Westen, (2016) (Figure 2.3B) for easy use. Soils were classified based on rates of chemical weathering that is enhanced by the tropical climate of the area. Regarding the degree of weathering, Protosols contain a large part of un-weathered minerals; young soil are at early stage of weathering, Smectoid soil is weathered clay, Allophane latosolic which is found in older volcanic deposits takes less time to be weathered compared to deeply weathered Kandoid latosoilcs clay (Rouse, 1986) (Figure 2.3A). These soils have unique engineering properties from transported or re-deposited soils (Reading, 1991), but the information was used as a soil texture from which soil hydraulic properties were generated for infinite slope input.

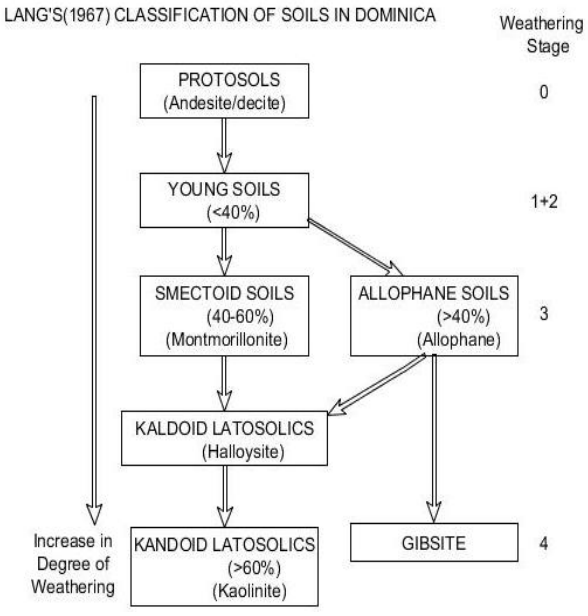


Figure 2.3A. Soil type of Dominica based on degree of weathering clay mineral content: Source: (Rouse et al., 1986) (Percent in the bracket shows the proportion of clay mineral)

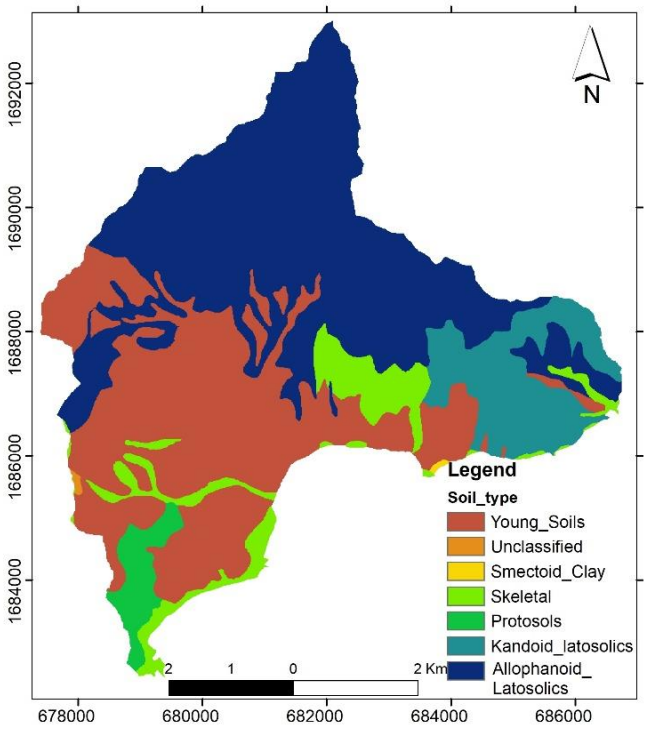


Figure 2.3B Soil type map of the area: Source:(Lang, 1967)

## 2.5. Vegetation and land use

Dominica has diverse vegetation type which varies with elevation variation and climate. Despite the agricultural expansion, charcoal and wood production which are the primary threat to the forest cover of the island, its undisturbed forest cover is estimated to be more than sixty per cent (ECU, 2000). The steepness of the slopes and rugged mountainous nature of the area also hindered fast expansions of agricultural land and contributed to conservations of the undisturbed forest cover. Forest cover type and variation which was reported by FRA, (2014) shows the semi-deciduous forest dominated by shrubs is found at the lower elevation and on the west coast of the island. Mature Rain Forest which is a dense forest occurs toward the interior of the island and between the elevations of 270m and 430m a.s.l. Montane forest dominantly occurs on thin soil-covered slopes and above 610m altitude while the Secondary rain forest distribution is controlled by shifting agriculture. The evergreen forest is dominant on the dry side of the island. However, there is no recent and detailed land use data for the island at present. The existing land use data obtained from physical planning division department of Dominica shows general information about the distributions of settlements, infrastructure, locations of resource site like quarry and various forest type of the area.

The vegetation cover of the area is usually affected by the frequent hurricane and tropical storm occurrences as shown in (Figure 2.4). The picture on the left shows the drying tree which was strongly hit by tropical storms, and the picture on the right side indicates trees recovering after tropical storms. The recovery is a mixture of new leaves and vines that overgrow dead trees. The change in vegetation cover is also believed to have effects on the occurrence of landslides through the root system and weight of the plant. The impact of plant weight is difficult to incorporate in the present study while the cohesion of plant root is recognised in slope stability system.

Figure 2.4 Effects of hurricane Maria on the vegetation cover (on the left, photo from Dominica News online) and the tropical rainforest after recovery (on the right, photo from Jetten, 2018)

## 2.6. Landslides of the area

Dominica is one of the most landslide prone areas of the Lesser Antilles in West Indies island groups, but there is not much information on landslide occurrences. The geologically active volcanic nature coupled with steep mountainous terrain and frequent extreme rainfall events made the country susceptible to landslides. Degraff, (1987) analysed landslide occurrences of the area considering topography, geology and hydrology as essential factors. He used aerial photography for landslides interpretation and classified the movement types into a slide, fall and flow based on materials involved. Accordingly, more than 980 individual landslide points have been identified in the island. As part of validation work, Degraff et al.

(1990) conducted fieldwork on selected portions of the island (present study area was involved) and identified additional 183 slope failures where the influences of slope steepness, soil types and vegetation cover was recognised. Since then different attempts were made to record landslides of the area for specific work objectives, but it was not organised into a common database until van Westen, (2016) collected historical landslide data and incorporated into their work in 2016.

## 2.7. Drainage networks

The area has a dense drainage density that cut through the young volcanic terrain. Erosion materials are accumulated within the drainage channels forming thin to thick deposits. Drainage channels of flat valley areas were filled with debris flow deposits because the drainage channel width increases from source to the outlet areas near the coast and energy of flowing water ceases. Most of the drainage channels of the study area also contain dense landslides because of slope undercuttings. In particular, soft volcanic deposits are highly susceptible to slope base erosion and caused several landslides.

## 2.8. Settlements

Dominica has an estimated population size of over 73,000 people. Majority of these people lives near coastal areas because of the topographic nature of the island. Many settlement areas are located in the southern part of the island (present study area) as it is near the coast. The area is also one of the active landslide areas of the island, which is hit by frequent hurricanes and tropical storms. Most people of the study area dwell in local villages of Pichelin, Grand Bay and petite savanne (Figure 2.5).

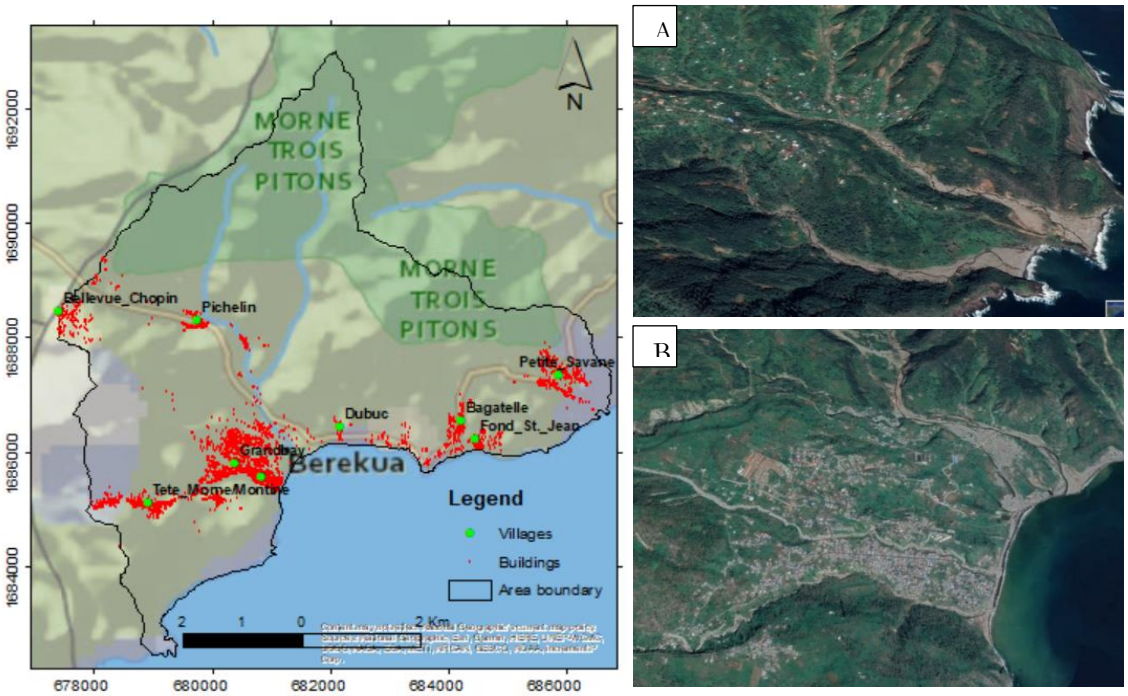


Figure 2.5 Settlement map of the area. Google earth images showing housing of A) Petite_savanne area and B) Grand bay area

# 3. MATERIALS AND METHODS

## 3.1. Introduction

Presently, many models are developed for estimations of soil depth spatial distribution. Liu et al., (2013) broadly classified models used for soil depth prediction into stochastic models, which assume a statistical relationship between observed data and topographic variable and physically based models, which focus on soil evolution process. In this study, three different soil depth prediction techniques; decision tree, Multiple regression and general soil balance equation which assumes a statistical relationship between soil depth and topographic variables were used. Then, the model results were separately used as the principal input parameter in an infinite slope model to analyse soil depth influence in slope instability initiations. Soil depth maps and other infinite slope model input parameters were run in a PCRaster script for daily time steps under normal and extreme rainfall condition scenarios for one year. Eventually, infinite slope model results produced using different soil depth maps from the three soil depth prediction techniques was validated against an existing inventory landslide polygon.

## 3.2. Methods for assessing soil depths

The complex topographic nature of the area, lack of strong correlation between observed soil depth and predictor variables and lack of dense field data forced soil depth to be predicted by three alternative methods. Multiple soil depth maps were believed to give an option for better soil depth maps which gives better landslide prediction results in the infinite slope model.

**(1) decision tree**

The decision tree is a decision rule based system of digital soil mapping which correlates dependent and independent variables and produces an output map according to the developed tree structure partitioning (Taghizadeh-Mehrjardi et al., 2014). In this study, soil depth is assumed as the dependent variable which varies based on independent topographic variables (Slope gradient, profile curvature, distance to river and TWI). Topographic variables were classified first into different classes based on their presumed relationship with soil distribution. This relationship was assumed to follow soil catena regardless of the origin of the topography. Accordingly, the soil continuum was divided into five artificial soil depth classes (very shallow to very deep) based on the work of Schaetzl (2013) to build a tree structure for different depth classes. The first vertical bar (from left to right) (Figure 3.1) represent the relative soil depth on the respective slope position.

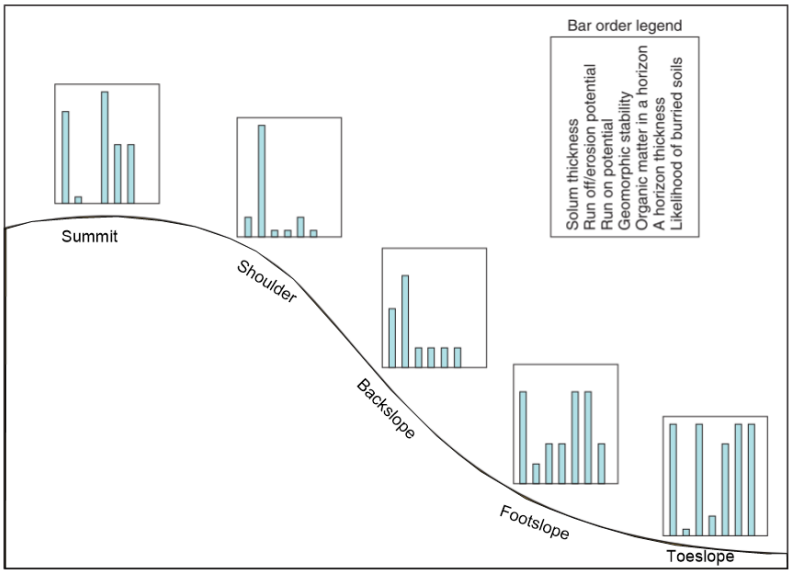


Figure 3.1 Soil depth variation along catena in a tropical humid climate. Source (Schaetzl, 2013).

The decision tree structure of the model was shown in (Chapter 4) under the decision tree model setup and result. The performance of the model was later checked by performing validation through the statistical correlation of observed depth in the field and predicted soil depth map.

**(2) Multiple linear regression model**

The model predicts the spatial variance of the dependent variable based on linear combinations of independent variables (Yilmaz & Kaynar, 2011). Here, it was used as a predictive analysis of a continuous soil depth based on the independent topographic variable. The same topographic variables used in the decision tree model were used in regression analysis to have a comparable result. Multiple regression was modelled using SAGA GIS 2.3.2, but the output is influenced much by the significant independent variables used for prediction. Soil depth was predicted based on the equation of the form below.

$$\hat{y} = b0 + b1X1 + \ldots + bnXn + \varepsilon \quad \text{----------(3. 1)}$$

where $\hat{y}$ =predicted variable (soil depth), x1-4=independent topographic variables (gradient, curvature, distance to river and TWI), b0=constant and b1-n=regression coefficients, $\varepsilon$=error term.
Soil depth observation points were divided into model calibration and validation datasets to check the predictive power of the model.

**(3) General soil balance equation**

The model was initially used by Dietrich et al. (1995) to predict the distribution and variations of colluvial soil depth for shallow landslide analysis based on soil mass balance between soil production by weathering and soil removal by erosion. Later, Kuriakose et al. (2009) tested the model on the Ghats mountains of Southern India using environmental variables based on the original work of Dietrich et al. (1995). In this study, the model was used because the previous test area is very similar to the present study area in terms of topography and landslide process the present model considers but differs geologically. It was also intended to have multiple soil depth maps to justify the influences of soil depth in slope instability initiations. The model used the same parameters as the two models above; slope gradient, distance to the river, slope profile curvature and TWI as an input parameter to produce soil depth. The model works in a principle of multiple regression above but with an adjustable coefficient (Equation 3.2). The following equation was used to create soil depth.

$$\text{Soil depth} = (1\text{-}a*G - b*\text{Driver}/\text{Driver}_{max} + c*\text{Curvature} + d*\text{TWI}/\text{TWI}_{max})^{e} \quad \text{----------(3.2)}$$

Where, G = slope gradient, Driver = is the relative distance to the river channel on the slope, Curvature=Profile curvature, TWI=topographic wetness index. The values for parameters (**a) to (e)** are optimised based on the one on one correlations of field soil depth observations and the topographic factors derived from DEM. Hence, the topographic variable with a higher correlation with soil depth is given higher weight. Multiple iterations were made to bring about a good correlation of soil depth and topography which is the basis of the present soil depth models.

## 3.3. Slope instability assessment

### 3.3.1. The infinite slope model

The infinite slope model is a limit equilibrium based slope instability analysis and widely used shallow landslide analysis (Iverson, 1990). The model determines the balance between shear stress and shear

strength of slope materials. The ratio between strength and stress factors is expressed as a factor of safety to assess the potential sliding surface as the stable or unstable slope (Kim et al., 2015). The classical infinite slope model has been applied mostly to a small area. Also, it was included in a GIS environment to be used for the large area where the factor of safety is calculated at pixel-based (Lee & Park, 2016, Segoni et al., 2009). The Factor of safety is calculated for individual pixels based on equation 3.3 below where the slope planar failure plane is assumed as shown in Figure 3.2.

$$FS = \frac{c+cr+(\gamma D-\gamma wzw)\cos^2\alpha \tan\varphi}{\gamma D sin\alpha cos\alpha} \text{----------(3.3)}$$

Where c = cohesion of soil (Kpa), cr = cohesion of plant root (Kpa), γ = unit weight of the soil (KN/m$^3$), D = soil depth (m), γw = unit weight of water (KN/m$^3$), zw =groundwater pore pressure (m), α = slope angle (degree), φ = soil friction angle (degree).

In addition to the factor of safety of a cell of a raster map, infinite slope model also gives a cumulative number of days in a year when the slope is unstable (equation 3.4).

$$FSDays = FSDays + if(FS < 1, 1, 0) \text{----------(3.4)}$$

Where FSDays = cumulative days in a year when the slope is unstable and FS = Factor of safety.

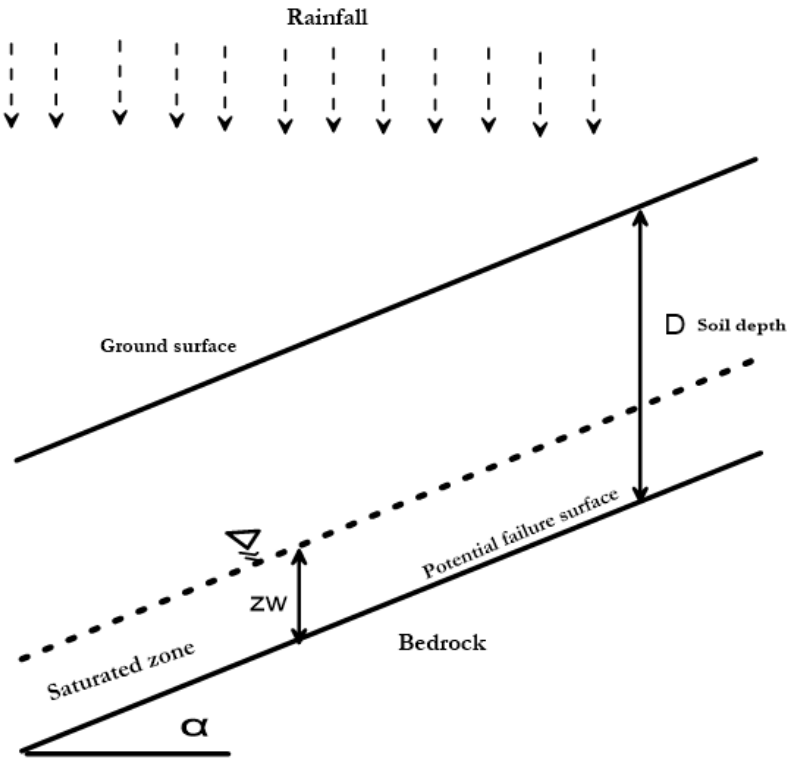


Figure 3.2 Infinite model diagram. Source (Kim et al., 2015)

In this study, the infinite slope model is implemented in the PCRaster modelling language (Karssenberg et al., 2009) and the code is added in Appendix 2. The model calculates the water balance for a single layer of soil on a daily basis, whereby part of the soil profile can be saturated with groundwater, creating a saturated and unsaturated zone. Figure 3.3 shows the flow chart of the model with hydrological fluxes and stores. The daily groundwater fluctuations are coupled to slope stability per pixel (Appendix 2). Input maps used includes DEM and its derivatives (local drainage direction, river width, outlet maps), soil units,

daily rainfall station and soil depth maps. The soil depth maps were raster maps produced using three techniques explained above. Besides, soil and land use data were used as an input constant. Daily rainfall data and potential Evapotranspiration data (calculated) were input as time series files which changes daily within the years considered (2004 and 2009).

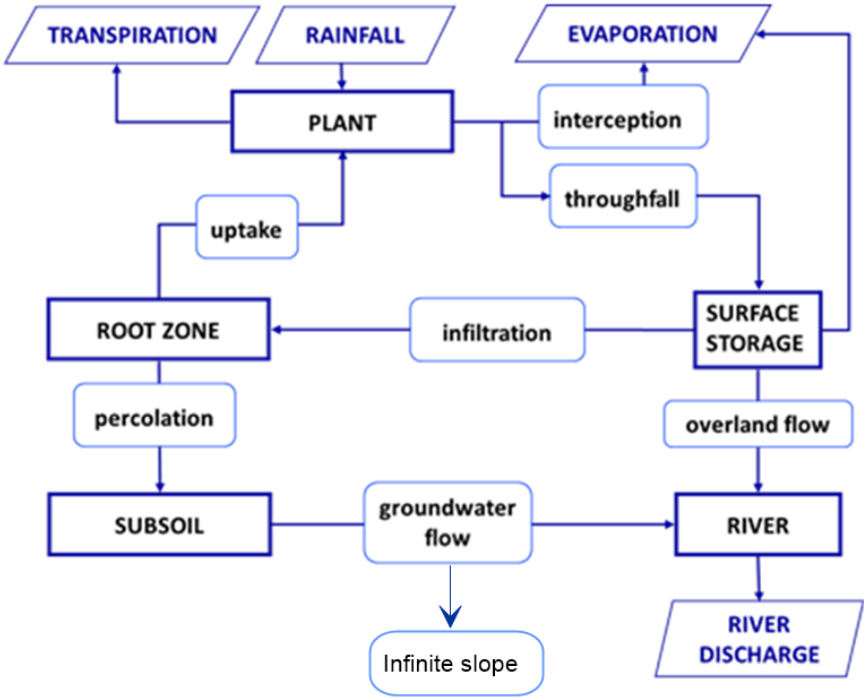


Figure 3.3. Flow diagram of water balance and infinite slope model process in PCRaster.

The infinite slope model involves a dynamic process, and it was modelled in a daily time step. The dynamic modelling also involved groundwater as one of slope destabilising force. The pore water pressure (Figure 3.2) reduces effective normal stress on the slope and causes slope failure. The initial groundwater depth was defined in the model based on the soil depth. Then, it varied per day based on soil depth, rainfall intensity of selected year and soil hydraulic conductivity for the whole year. The outputs of the PCRaster infinite slope model are a daily factor of safety and number of unstable days in a year.

### 3.3.2. The direct influence of soil depth in infinite slope model

Soil depth directly influences the infinite slope model in different ways. In the factor of safety equation (equation 3.3) and model diagram (Figure 3.2), soil depth is specified as parameter D which influence the mass of the slope and depth of failure surface. Besides, soil depth also affects the water balance part in an infinite slope model. It is shown in Figure 3.2 that an increase of vertical rainfall infiltration increases soil saturation which also decreases soil strength and facilitates slope failure. However, Kim et al. (2015) stated that if the soil is fully saturated up to the surface (D < depth of (zw)), saturated overland flow occurs (Figure 3.3). In addition, rainfall infiltration also causes different levels of soil saturation based on soil depth of the slope (Chae et al., 2015). The slopes having shallow soil cover can quickly be saturated with rainfall infiltration, and shallow slope failure happens. However, it takes a longer time for deep soil to get fully saturated by direct rainfall infiltration and soils are assumed to be saturated by the rise of groundwater table which causes deep slope failures. Also, there are significant effects of plant zoot zones

in slope stability of vegetated soil slopes as shown in the process above (Figure 3.3). At a given soil depth, vegetation controls the initial moisture content of the topsoil through plant root water uptake and plant evapotranspiration. According to Leung & Ng (2013), the influence of vegetation in slope stability varies based on the hydrogeological response of soils during wet and dry seasons. Hence, the plant root zone at a given soil depth influences the porewater pressure in the soil and controls slope stability (Figure 3.3). Therefore, the direct influence of soil depth in the infinite slope model is in several ways, and presently the process is included in PCRaster to model slope instability of the area.

### 3.3.3. Model calibration and validation

Soil depth models were calibrated and validated based on field soil depth values while infinite slope model was calibrated using input constants obtained from field and literature. Unlike cohesion of some soil types measured in the field there was no laboratory analysis made for soil strength parameters. Hence, the values of constants related to soil shear strength and land use data obtained from secondary sources were varied between the minimum and maximum to use in the infinite slope model calibration. Infinite slope model calibration also involved defining groundwater threshold value through an iterative process to avoid overestimation of FS results which was checked by comparing with inventory landslide validation datasets. Hence, infinite slope model validation involved existing intensive landslide inventory data and Google earth images. Example of the existing inventory landslide including runout part is shown in Figure 3.4 below. However, this study is focused on landslide initiation areas of the slope, and the runout part of the inventory landslide was removed before used in the infinite slope model as model validation.

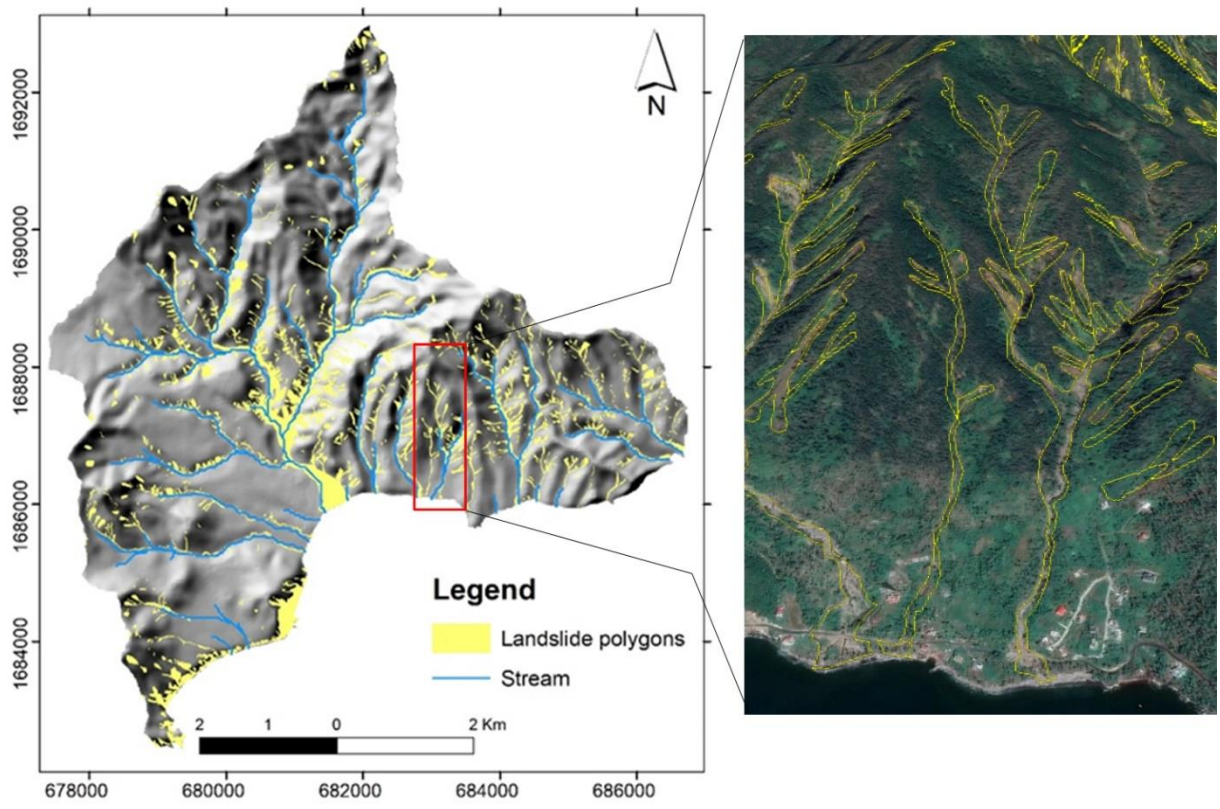


Figure 3.4 Landslide inventory map and example of google earth image with landslide polygon. Source:(van Westen, 2016)

## 3.4. Data collection and preparation

Many datasets were used in this study despite the quality issues associated with some of them. Soil depth was the primary data collected from the field. Topographic factor maps were derived from DEM of 10m resolution. Long-term daily rainfall data was obtained from Melville Hall Airport station which is near the study area due to unavailability of rainfall station in the study area. Most of the soil physical properties were obtained from secondary sources while cohesion measurement was made using a shear vane test in the field. Also, the land use data was collected from the secondary source, and canopy cover percentage was calculated using (equation 3.5). Potential evapotranspiration was calculated based on the geographic location of the area and daily temperature data. The descriptions of data used in this study are given as follows.

### 3.4.1. Topographic data

The significance of topographic data in soil depth model has been mentioned in studies of (Kuriakose et al., 2009; Sarkar et al., 2013; Tesfa et al., 2009) and its significance in landslide model was elaborated in the work of (Cascini et al., 2017; Fu et al., 2011; Lanni et al., 2013). However, the quality of topographic data significantly affects the results of both soil depth and infinite slope model. Three sources of topographic data were available for the study area (radar, ALOS PALSAR and DEM interpolated from contour). However, none of them showed the ground truth of the area where steep slope and sharp ridges are prevalent. All the DEMs are smooth, and some of them also contain artefacts. In this study, DEM derived from contour is chosen to be used throughout this study because of the minimum artefacts it possesses compared to the other two DEM types. This DEM was produced in the CHARIM project by a kriging operation using a Gaussian semi-variogram on contour line data. However, these contour lines were themselves a product from ArcGIS (automatically generated) because the original digitised data was no longer available(Jetten, 2016). Hence the DEM lacks terrain details.

### 3.4.2. Soil data

Soil cohesion was measured in the field as mentioned above while porosity, field capacity, wilting point and bulk density were obtained from pedo-transfer functions by Saxton & Rawls (2006) based on soil texture class. Soil cohesion was measured in the field on a vertical soil profile, and an abrupt change in soil strength was used to define soil depth. Soil cohesion values measured in the field are assigned to the different soil types based on the existing soil type map of the area (Figure 2.2B) and its descriptions. Later, the soil cohesion values were varied between the minimum and maximum to decide their optimum value used in infinite slope model for model calibrations. Soil cohesion values of those soil types not encountered in the field and the soil friction angle were obtained from a website called www.geotechdata.info that provides standard geotechnical parameters for soil according to USCS classification. It gives a range of soil cohesion and friction angle values for normally consolidated soil.

### 3.4.3. Land use data

Analysis of slope stability per land use, particularly for settlement areas is helpful to reduce its consequences, but the existing land use data obtained from physical planning division department of Dominica is from the unknown date and of poor quality. So, detailed slope stability assessment for each land use type is not possible. However, an overlay map of land use data and inventory landslide is shown in Appendix 1 to inspect the locations of settlements relative to landslide areas visually. Vegetation types are also obtained from the same department, but the canopy cover percentage was calculated based on NDVI from Landsat 8 Operational Land Imager (OLI) and Thermal Infrared Sensor (TIRS) image

obtained in 2018 by USGS. The NIR and Red bands were used to calculate the NDVI. NDVI values were later converted to canopy cover based on the cover equation (equation 3.5) after (Van der Knijff et al. 1999). Vegetation controls both hydrological and mechanical process of a landslide that could be a positive or negative effect(Ghestem et al., 2011).

$$\text{Cover} = 1 - \exp\left(-\alpha \frac{NDVI}{(\beta - NDVI)}\right) \quad (3.5)$$

Where $\alpha$ and $\beta$ are 2 and 1 respectively

### 3.4.4. Rainfall data

Long-term daily rainfall data from 1974 to 2013 was obtained from Melville Hall Airport station. The values range from zero to an extreme of more than 400mm which shows the presence of significant rainfall variability in the area. However, the assumption of no slope failure occurs during the dry season was made for the slope stability analysis. Hence, the considerable rainfall amounts assumed to trigger slope failure are from the year with average rainfall and the year with extreme rainfall values caused by hurricanes and tropical storms. This is also helpful to obtain comparable slope instability result for two different rainfall scenarios. Then, the year 2009 was chosen as a year with an average daily rainfall of the area based on the absence of extreme event during that period. The year 2004 contains an extreme rainfall event which amounts 422mm/day (Figure 3.5), and this value is also close in amount to category five of hurricane Maria of September 2017 that generated thousands of landslides. The total annual rainfall values are 2590.9 and 3731.8 for 2009 and 2004 respectively. The daily rainfall data was used as a time series file in the infinite slope model. Potential evapotranspiration was also used as the time series data in the model.

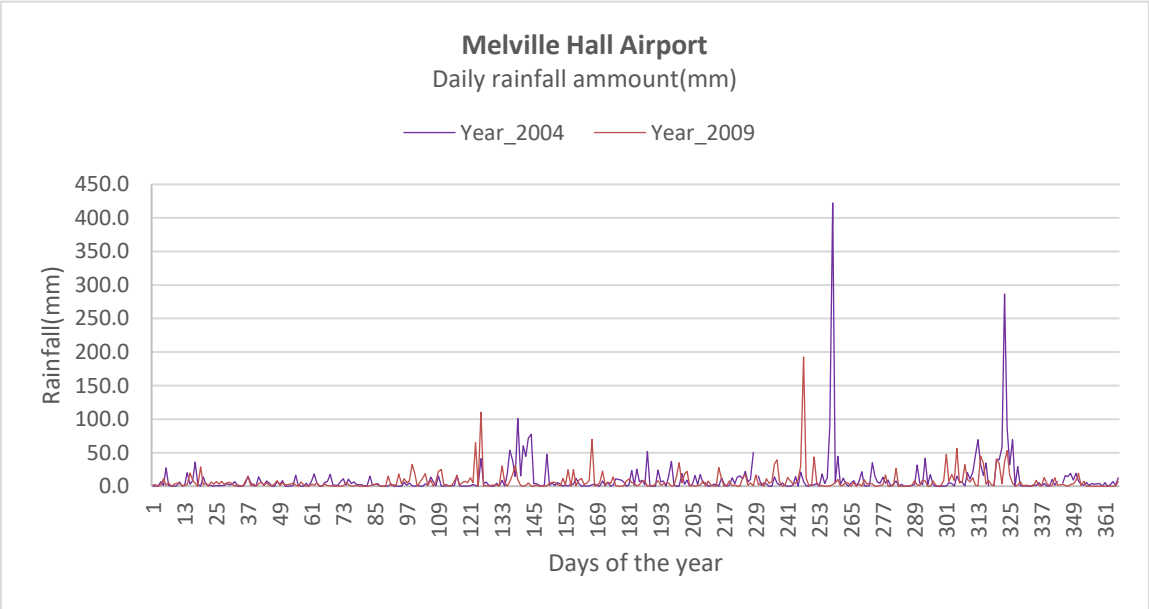


Figure 3.5 Daily rainfall amount (mm) of Extreme year (2004) and Normal year (2009)

### 3.4.5. Landslide inventory data

The most intensive landslide inventory of the area was made by van Westen, (2016) from historical information on landslide occurrences and multi-temporal visual image interpretation. They identified more than 1,600 landslides for the whole island and combined it with historical landslide data to produce landslide inventory database. Also, landslides which occur from the tropical storms Erika in 2015 and hurricane Maria in 2017 are included in the inventory landslide.

### 3.4.6. Field data collection methods

Sampling strategy for fieldwork was developed using an application called QField in QGIS in which shapefile of an existing landslide inventory data was loaded for finding landslide scarps in the field. Besides, road cuts and river incisions were followed for soil depth measurements.

Fieldwork was conducted in October 2018 to collect data on soil (soil depth, cohesion) and landslides. The purpose of obtaining data from the landslides is also for model validation. Different landslide characteristics and sizes were observed during fieldwork (Figure 3.6).

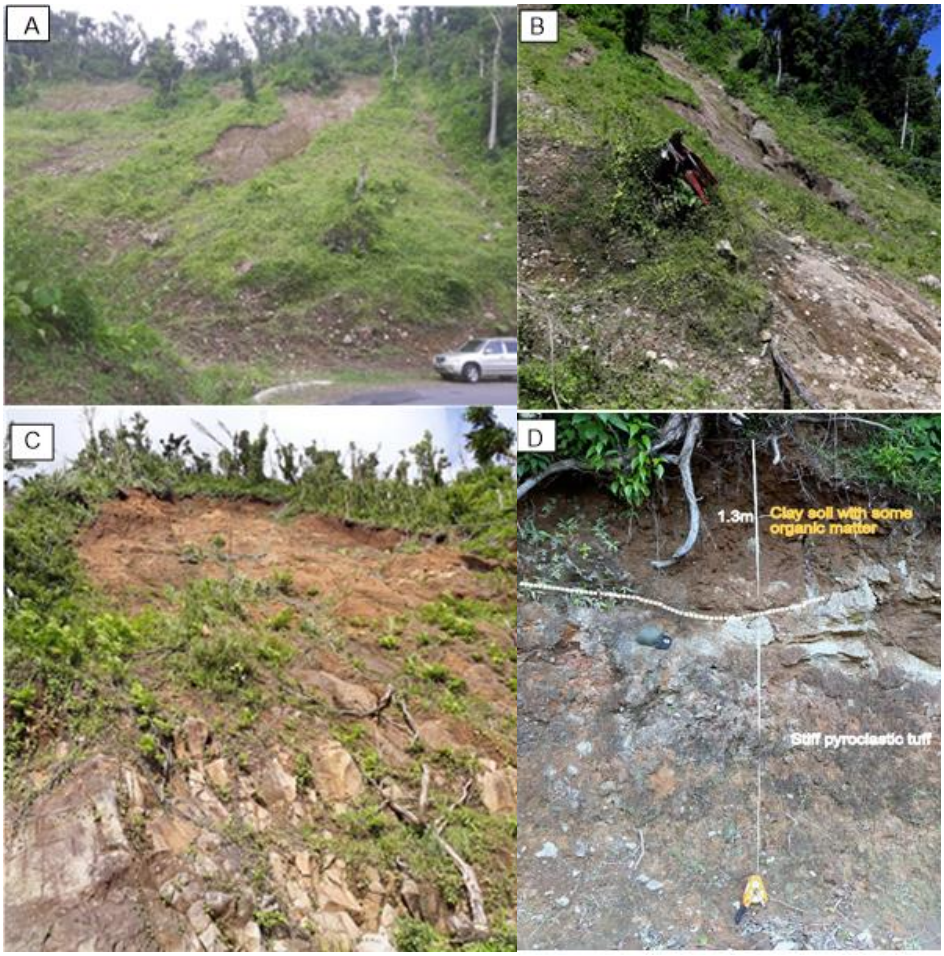


Figure 3.6 Typical landslide and soil depth in the study area

It was challenging to find depth to hard surface or bedrock most of the landslide scarps during fieldwork. In such case, depth to slip surface was measured but considered as soil depth for further soil depth model and later in infinite slope analysis. Stream incisions were also followed to find exposed depth to bedrock.

Because of the complex volcanic terrain nature of the area and lack of a detailed geological map, identifications of exact volcanic deposit boundaries were not possible both before and during fieldwork. The very steep slope nature of terrain which was very slippery during rainfall and dense vegetation cover restricted soil depth measurements close to the road network, stream channels, landslide scarps close to either stream cut or roads. Few points were measured using soil Auger penetration. Accordingly, one hundred nineteen soil depth points were collected during the fieldwork for calibration and validations of soil depth models.

### 3.4.7. The use of Pedo-transfer functions (PTF)

PTF transform easy obtained soil information (texture in this case) into both soil hydraulic properties and soil water capacity where water in soil vary between field capacity and wilting point. It is used to fill a gap between existing soil properties and soil properties required in modelling. In this study, soil properties like saturated hydraulic conductivity, wilting point, field capacity, a bulk density of soils and soil porosities were parameterised using soil texture based on the work of Saxton & Rawls, (2006). These parameters were used as input of soil properties in infinite slope model.

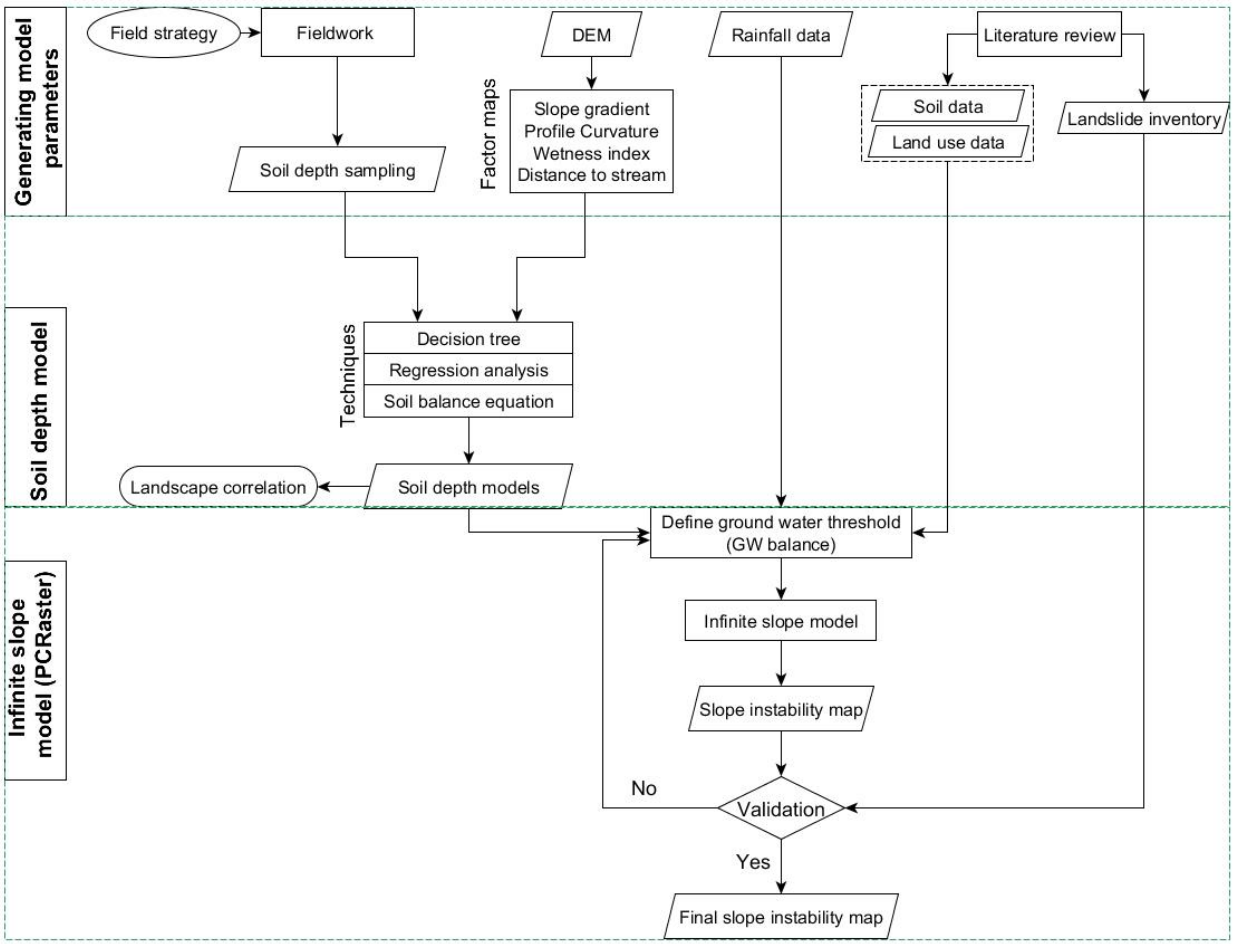


Figure 3.7 Flow chart of research methodology

# 4. RESULTS OF SOIL DEPTH MODELS

Three different methods described in chapter 3 were used to produce soil depth maps, and their spatial relationships with topographic variables were analysed through which the first and second specific objectives of the research are achieved.

## 4.1. Performance of field observation points

A total of 119 soil depth and landslide slip depth points were collected during fieldwork (Figure 4.2B) and later, all the points were considered as soil depth for modelling purpose. However, the number and distributions of soil depth points were not significant enough to make point interpolations through commonly used methods of creating a surface from observation points like geostatistical interpolations. Hence, the present soil depth interpolations were made based on the assumption that soil depth distribution pattern on topography has spatial relationships with the topography as described in chapter three. In this way, four topographic variables were extracted from DEM (Figure 4.4) and correlated with field-based soil depth observations as shown in (Table 4.1) to establish a basis for the present soil depth models.

Table 4.1 Correlation between all soil depth observations and the predictor variables (n=119)

| | *Soil depth observations* | *Profile curvature* | *Distance to river* | *Slope gradient* | *TWI* |
|---|---|---|---|---|---|
| *Soil depth observations* | 1 | | | | |
| *Profile curvature* | -0.14 | 1 | | | |
| *Distance to river* | -0.10 | 0.37 | 1 | | |
| *Slope gradient* | -0.01 | -0.13 | 0.20 | 1 | |
| TWI | 0.17 | 0.03 | -0.09 | 0.11 | 1 |

As shown in the correlation table above (table 4.1) there is no significant relationship between soil depth and topographic variables used because of high spatial variabilities of soil depth in the area. The correlation result showed a maximum correlation of 17% (between soil depth and the TWI) and a minimum of 1% (between soil depth slope gradient) which is insignificant. This weak correlation can be associated with both the complexity of the area and limitations of the DEM used as indicated in section 3.4. Since the soil depth models were based on the assumptions that soil depth and topographic relationships, such a lack of correlation between them led to the removal of some sample points regarded as outliers. The outliers, in this case, are those points which do not fit into the present model assumptions, and they are not predicted accordingly.

The outlier points accounted for 20% (n=24) of the total sample points and picked based on the bins of the histogram (Figure 4.2B). In addition to lack of correlation with the topography as indicated above, the points also highly deviate from mean soil depth measurements in the field. For instance, a bottom of a side valley can be an erosive and incision site, and the soil depth is minimal while extreme accumulation is expected in the valley bottom because it is in the centre of a debris flow/landslide lobe. Example of the characteristic outlier points was shown in (Figure 4.1) for the soil depth prediction using the decision tree model. The scatter plot shows the predicted soil depth and observed soil depth are diametrically opposite on locations where outlier points were collected. That is, the model might have predicted shallow soil depth while in reality it was measured as deep soil. The specific locations for the outlier points collected

include; very deep debris flow deposit in the valley or outcrop exposure in the valley due to river incision, and thick ash deposit on the slope in all cases were extreme values based on soil depth and slope relationship.

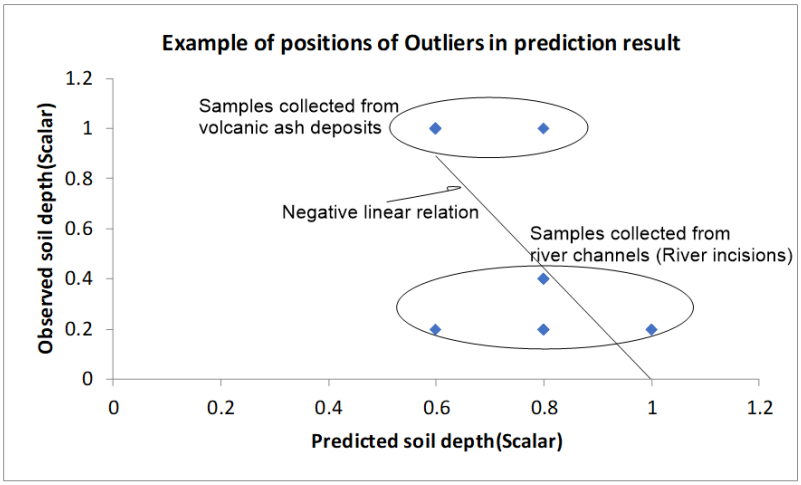


Figure 4.1 Scatter plots of outlier datasets (total number=24 points)

After identifying the outlier points, the rest of the sample points were assumed to meet the models' assumption and correlate with the topography even though the spatial variability of soil depth is still and the correlation is weak. Hence, the sample points were divided into 60% for developing the models and 40% for model validation which was randomly selected from all accessed locations during fieldwork (Figure 4.2A). Then, all the models were first developed based on a scalar range (0,1) and later converted to a quantitative value for the infinite slope model input because of the weak correlation recorded as mentions above. This qualitative class reduces soil depth spatial variability. Field observation points were also aggregated into the scale of (0,1) to have a comparable result with soil depth model predictions and to reduce its spatial variability. Hence, all the statistical analyses were made based on the scalar ranges. Soil depth prediction maps were also produced based on the scalar classes but later converted to quantitative maps to use in infinite slope model for the slope stability assessment.

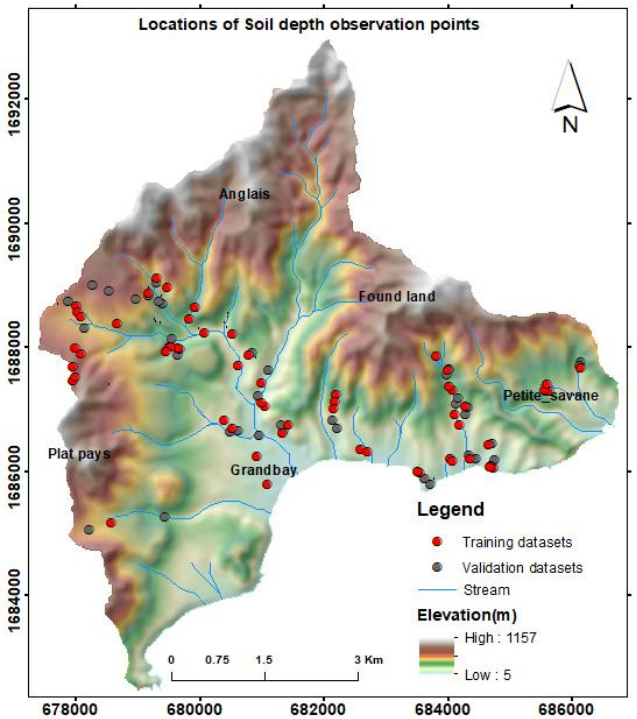


Figure 4.2 A) Locations of field observation points

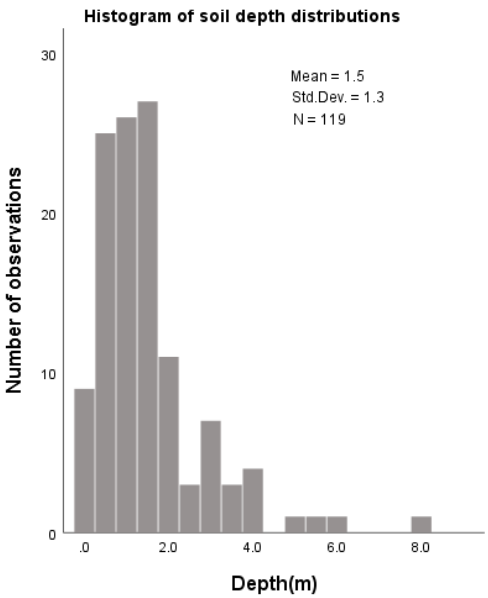


Figure 4.2 B) Distributions of all soil depth observation points

## 4.2. Soil depth predictor variables

The predictor variables were extracted from 10m resolution DEM. Slope gradient, profile curvature, distance to the river and topographic wetness index (TWI) (Figure 4.3) were considered as significant predictor topographic variables in soil distribution or redistribution on landform in the present study. Slope gradient is shown in a tangent with a value reaching up to 1.7 or about 60 degrees. TWI and profile curvature area expressed in values. Distance to the river is computed over the surface and shown in meters.

Topographic variables are related to soil depth in different ways. The natural erosive force of water removes soil from higher slope gradient and accumulates on the lower slope gradient where thick soil is expected to develop. Also, on the steeper slope gradient, the rate of infiltration decreases and contributes to soil erosion. So, the slope gradient affects the potential and kinetic energy of water movement that changes sediment flux and contributes to soil redistribution. In this way, the slope gradient is related to denudation and accumulation processes and comply with the present model assumptions.

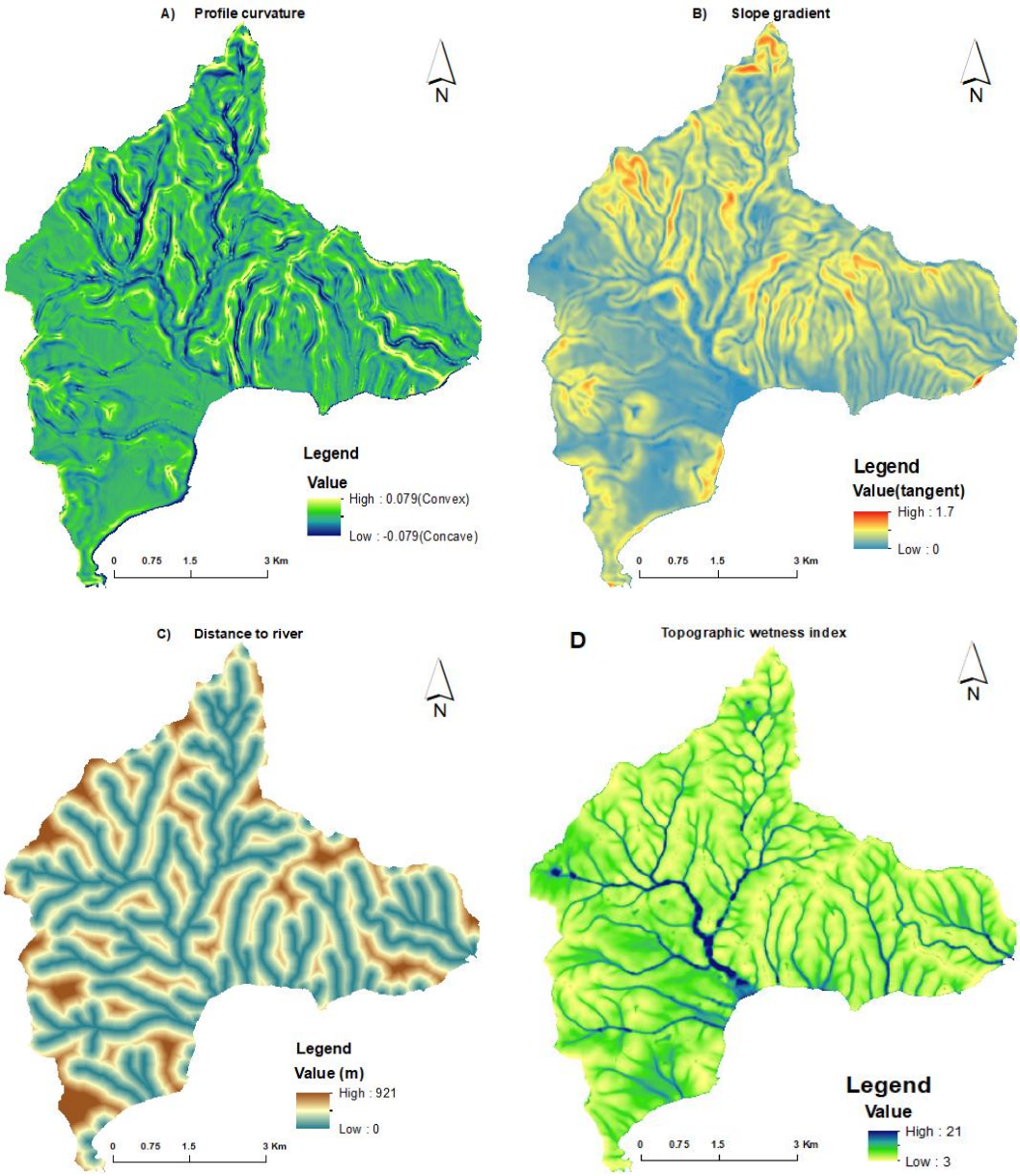


Figure 4.3 Factor maps of soil depth predictions

Slope profile curvature controls soil depth variability through convex and concave shapes (Figure 4.3). The convex profile curvature corresponds to an increased slope gradient and high erosive power of water while the concave profile curvature shows a decrease in slope gradient and corresponding soil deposition site where deep soil are expected. Hence, profile curvature affects soil distribution, and it is a useful parameter for the present soil depth model assumption. On the other hand, topographic wetness index shows where water accumulates in the landscape and is related to soil distribution. Hence, the lower wetness index value shows ridges and crests where soil erosion happens, and thin soil are expected while the higher value indicates landscape depression and accumulation of sediment and deposition where thick soil are expected. Distance to the river is also related to soil distribution because stream channels are erosional material accumulation site and the accumulation materials decrease as we go to the source area. Thus, four of the topographic factors mentioned above were used in the soil depth prediction models.

## 4.3. Results of Soil depth prediction techniques

### 4.3.1. Decision tree result

Soil depth map using the decision tree model was produced based on the decision rules by applying topographic parameters of slope gradient, profile curvature, distance to the rivers and topographic wetness index in soil depth prediction. The decision tree (Figure 4.4) was developed based on a conceptual model of soil distribution on landform or soil catena regardless of the origin of the landform. Then, the soil continuum was divided into five artificial soil depth classes (very shallow to very deep) related to natural soil distribution on a slope. For instance, shallow soil depth is expected on a steep slope because of soil erosion, and deep soil on flat areas due to accumulation. Slope gradient was classified into five classes based on (FAO, 2006) as; Flat to very gently sloping ( 0-2%), sloping (2-5%), Moderately steep (15-30%), Steep (30-60%) and very steep slope (>60%). Slope profile curvature classes were made to accommodate minor slope irregularities. On steep slopes, soil movement is controlled more by slope gradient than slope curvature. Hence, for slopes which are more than 30% steep, profile curvature was not included in the decision rule. Distance to the river and TWI values were subjectively classified based on its histogram frequency distribution and possible location on the slope as shown in Appendix 4.

Several other possible combinations of the decision rule system can also give different results of soil depth. However, the best possible combinations were selected based on the likelihood of soil depth expected using the different topographic factor map combinations, and soil depth map was created using a script in PCRaster (Appendix 3). The decision tree can be read as follows. For example, combinations of slope gradient = 20%, profile curvature = 0.005, distance to the river = 100 and TWI = 5.5 gives moderate soil depth. However, the lower class for any variable takes precedence and determine soil depth class.

Base on the decision rule (Figure 4.4) below, qualitative soil depth map with a qualitative class between (0 and 1) was produced (Figure 4.5) and later stretched to quantitative classes based on Soil survey (1951) to be used in the infinite slope model. The equivalent quantitative classes based on Soil survey (1951) are classified as very shallow (<0.25m), shallow (0.25-0.75m), moderate (0.75-1.25m) deep (1.25-1.5m) and very deep (>1.5m). The observed soil depth values were also aggregated into (0 to 1) scale to compare with the qualitative soil depth class and accordingly, the correlation was made between 40% of observed and predicted depth results (Figure 4.8A) for model validation.

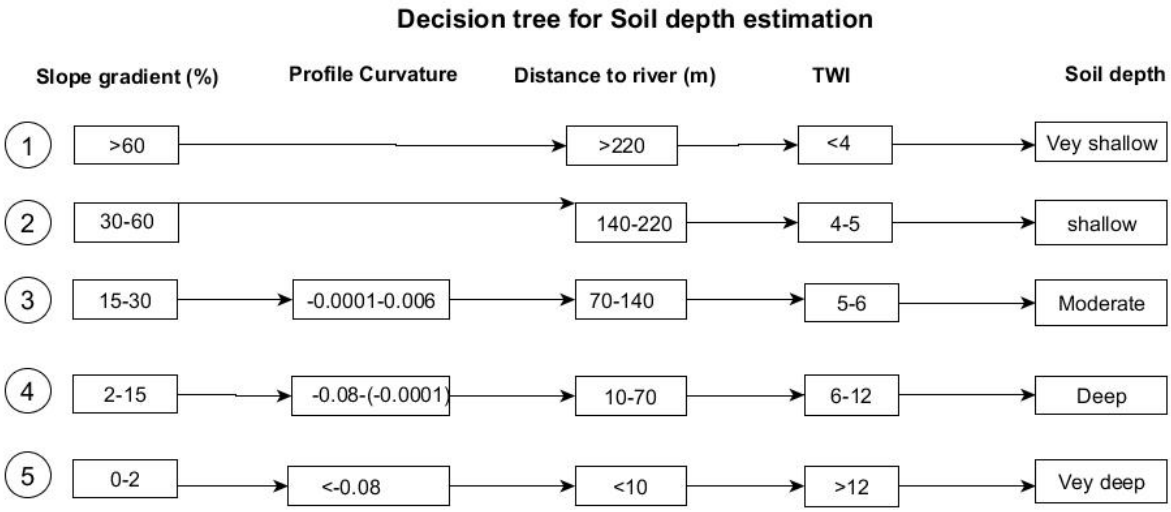


Figure 4.4 Decision tree for soil depth prediction

The result of the decision tree below (Figure 4.5) showed deep soil within the stream channel of flat valley areas which also comply with field observations. Also, the model predicted moderate to deep soil on narrow valleys of the upstream sides while in reality it was covered by bedrock exposure because of deep river incision as observed during the fieldwork and contrary to the prediction results. But all the narrow valleys were not exposed bedrocks, and debris flow deposits covered some areas because of the variation in topography and local lithology. Besides, the steep part of the slope near the water divide was covered with either shallow soil depth or moderately deep soil. The flat part of the top of the hills was predicted as deep to very deep soil. This top part of the mountain is also used for agriculture purpose by the local dwellers.

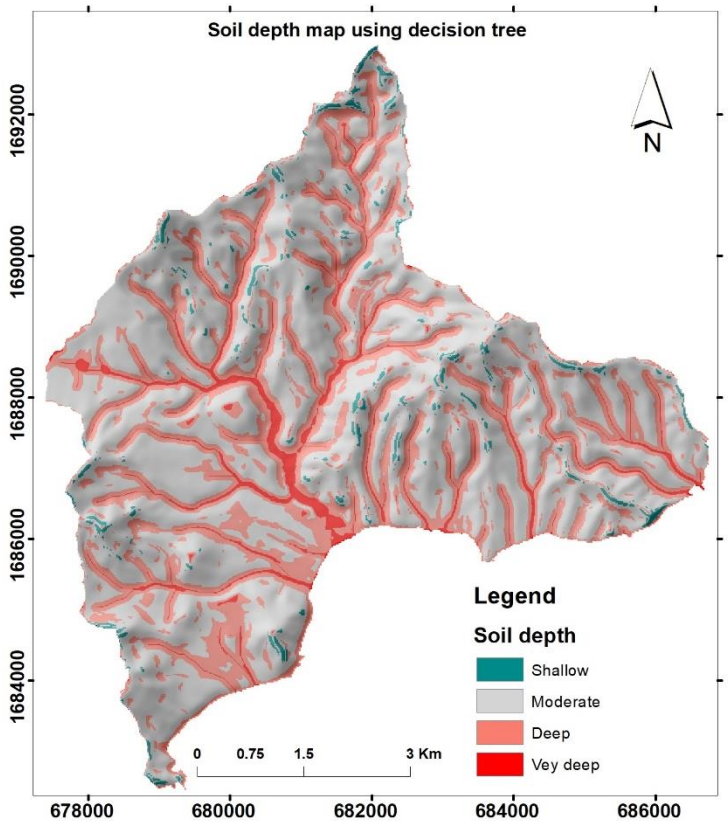


Figure 4.5 Soil depth prediction maps using decision tree

Based on the results of decision tree above (Figure 4.5), statistical one on one correlation between the predicted soil depth and predictor factor maps used in prediction was computed for the training dataset to check the relative contributions of each factor maps in defining soil depth on the area (Table 4.2). The result showed that the slope gradient has low power of explaining soil depth distributions which are expected because of smooth DEM used. The high correlation with TWI is an indication that zones of accumulation greatly influences soil depth. The negative signs of the correlation coefficients show the inverse relationships between the predicted soil depth and predictor variables.

Table 4.2 Correlation of predictor variables and predicted soil depth using decision tree(n=57(60%))

| | *Predicted soil depth* |
|---|---|
| *Predicted soil depth* | 1 |
| *Profile curvature* | -0.57 |
| *Distance to river* | -0.58 |
| *gradient* | -0.20 |
| *TWI* | 0.71 |

### 4.3.2. Multiple regression analysis result

Multiple regression analysis was performed using SAGA GIS (2.3.2) with the intent to have additional soil depth prediction result apart from decision tree prediction. The model predicted the spatial variance of the dependent variable (soil depth) based on linear combinations of independent variables (topographic factors). Soil depth map was influenced highly by the factor map with high correlation (Table 4.2) and relatively significant (Table 4.4).

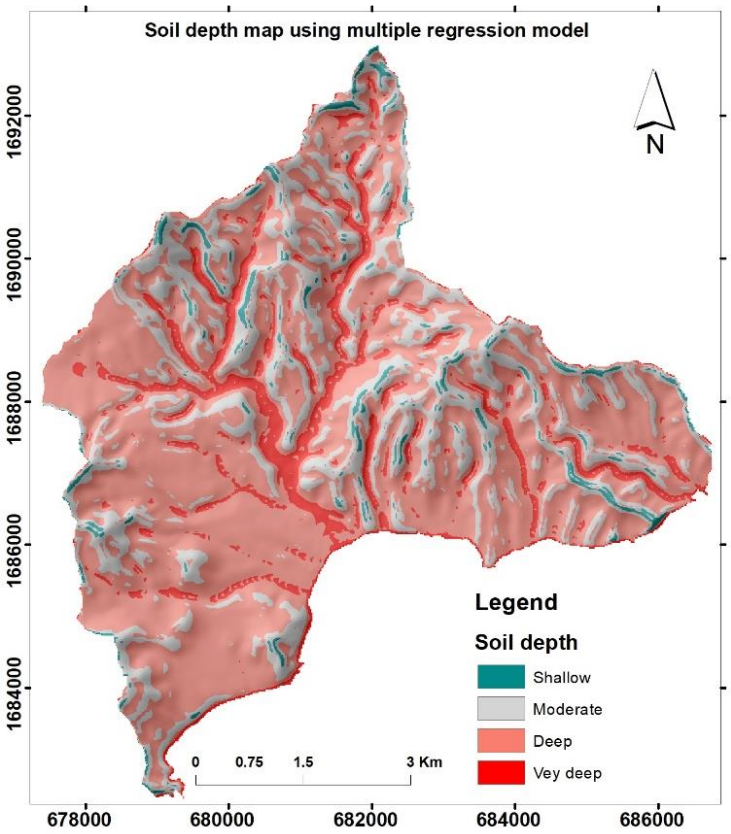


Figure 4.6 Soil depth prediction maps using multiple regression

The prediction results of the multiple regression (Fig 4.6) showed moderate and shallow soil depth cover close to ridges, but it does not follow slope gradient (Table 4.2). However, the model result underrated the deep soil to the downstream side and overestimated on the upstream side of the river channels. The flat part of the valley bottoms was covered by debris flow deposit as observed in the field. The underrated deep soil zone is attributed to the fact that the model considers the most significant factor maps for soil depth prediction and hence, the significant factor map was slope curvature. Unlike the decision tree model prediction which showed a progressive downstream increase of soil depth due to accumulation, the multiple regression result closely follows significant curvature differences for deep and very deep soil predictions. In this way, it predicted deep soil where very deep soil are expected due to lack of considerable surface irregularity variation shown by slope curvature on the valley bottom.

The less significant factor maps in the multiple regression prediction models were slope gradient, distance to the river and TWI as mentioned above. The statistical relationship between the prediction result and the predictor variables (Table 4.4) also show the significance levels of each predictor variables. Hence, slope gradient was very smooth and had little effect in prediction result because the of the smooth DEM used. Similarly, distance to the river factor map was also less significant because it was computed as the distance on the slope surface which again depend on the topographic surface or DEM quality. The profile curvature and TWI factors were the influential factors, but profile curvature was the most influential factor considered by the model and greatly influenced the soil depth prediction result. So, the correlations of training datasets showed the spatial relationship of 87% with profile curvature followed by 74% with TWI, 39% with distance to the river and 33% with a slope gradient. However, the results of the regression analysis (Table 4.2 and 4.3) based on regression coefficients showed all the factor maps were insignificant except curvature despite they all were forced in regression analysis to have a comparable result with other prediction model results. That is why decision tree and other techniques of predictions were sought for in such data poor area. The sign before the numbers shows the directional effects of the models. The strong correlation along a few observed points also does not make the model best over the other model, and its performance should be judged based on how accurately it predicts a landslide. Summary of the regression model and regression coefficients are shown in Table 4.2 and Table 4.3 below.

Table 4.3 Summary of multiple regression model (n=57)

| Model Summary[b] | | | | | |
|---|---|---|---|---|---|
| Model | R | R Square | Adjusted R Square | Std. Error of the Estimate | Durbin-Watson |
| 1 | .485[a] | .235 | .175 | .1993 | 1.367 |
| a. Predictors: (Constant), Gradient TWI, Curvature, Distance to a river | | | | | |
| b. Dependent Variable: Observed depth | | | | | |

Table 4.4 Regression coefficients

| **Coefficients[a]** | | | | | | | | |
|---|---|---|---|---|---|---|---|---|
| | | Unstandardized Coefficients | | Standardized Coefficients | | Correlations | | |
| Model | | B | Std. Error | Beta | Sig. | Zero-order | Partial | Part |
| 1 | (Constant) | .713 | .177 | | .000 | | | |
| | Curvature | -22.5 | 7.854 | -.426 | .006 | -.459 | -.372 | -.351 |
| | Distance to river | .000 | .000 | -.066 | .624 | -.235 | -.069 | -.060 |
| | Gradient | -.091 | .185 | -.084 | .627 | -.091 | -.068 | -.060 |
| | TWI | .005 | .015 | .058 | .754 | .284 | .044 | .039 |
| a. Dependent Variable: Observed soil depth | | | | | | | | |

Table 4.4 shows the presences of correlations between predicted soil depth and topographic variables. However, the overall low $R^2$ and many irrelevant predictor variables are what is expected given the complexity of the area, presences of outliers in the data and concentrations of sample points in narrow zones (like roadcut).

Table 4.5 Correlation of predictor variables and soil depth using Multiple regression analysis (n=60%)

| | *Predicted soil depth* |
|---|---|
| *Predicted soil depth* | 1 |
| *Profile curvature* | -0.87 |
| *Distance to river* | -0.39 |
| *gradient* | -0.33 |
| *TWI* | 0.74 |

### 4.3.3. Soil mass balance between soil production and erosion

The model was first tested by Dietrich et al. (1995) and later in India by Kuriakose et al. (2009). Soil depth map was produced using equation 3.2 mentioned before.

$$\text{Soil depth} = (1\text{-}a*G - b*\text{Driver}/\text{Driver}_{max} + c*\text{Curvature} + d*\text{TWI}/\text{TWI}_{max})^{e}$$

Where, G = slope gradient (0-1), Driver = is the relative distance to the river channel on slope (0-1) and Scaling parameters: a=0.7, b=0.6, c=0.7, d=0.3, e=0.9. These scaling parameters were determined through multiple iteration processes and decided based on stage where soil depth observation points and topographic parameters showed significant correlation.

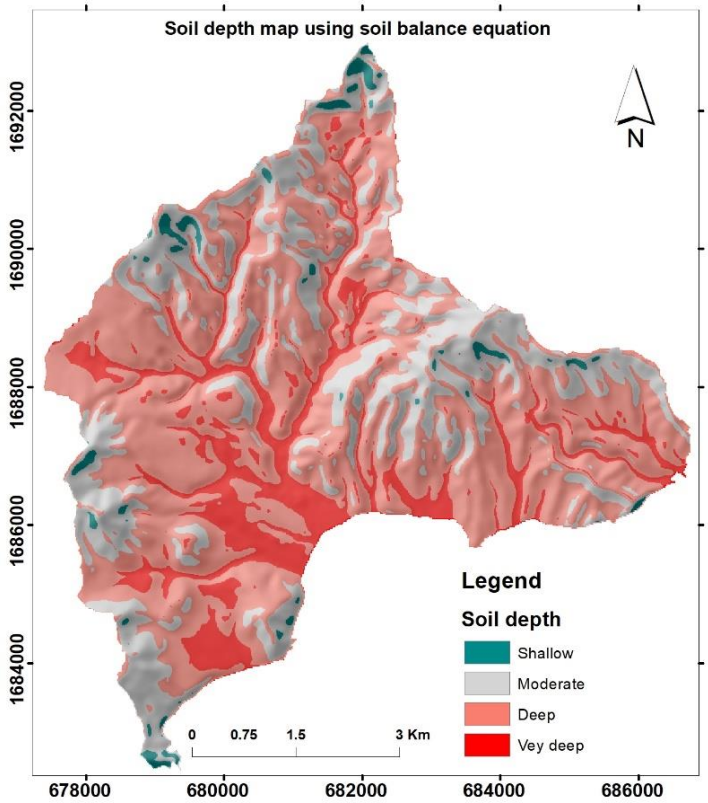


Figure 4.7 Soil depth prediction maps using soil balance equation

The prediction result of soil balance equation has pronounced the significances of slope gradient and TWI than the other variables although its general pattern is closely related to the other two model results (Fig 4.7). The model predicted very deep to shallow soil following the slope gradient as shown in (Table 4.6) where the correlation is very high. Unlike the other model, it predicted very deep soil on large areas of the flat valley floor. Shallow soil prediction near the sharp edges of the hillslope sides and the large area cover of the deep soil predicted is related to the quality of the DEM in which flat areas are more pronounced than steep slopes of the area. The correlations of the predicted soil depth with topographic factors (Table 4.5) also shows the significances each factor maps used.

Table 4.6 Spatial relationships of predictor variables and predicted soil depth using soil balance equation for model building(n=57(60%))

| | *Predicted soil depth* |
|---|---|
| *Predicted soil depth* | 1 |
| *Profile curvature* | -0.17 |
| *Distance to river* | -0.30 |
| *gradient* | -0.90 |
| *TWI* | 0.77 |

## 4.4. Validation of soil depth models

The predictive power of the model has to be checked by comparing the predicted and observed datasets for the models to be transferred to the final user (Beguería, 2006). In this case, the model results would be used in landslide analysis. The predicted soil depth values were expected to meet the assumptions made to build the models based on soil depth-hillslope relationships despite lack of statistically good correlation between observed datasets and predictor variables at the start of the analysis. After exclusions of the outliers from the observed datasets, 40% of the normally distributed sample were used for validating all the three models used for prediction. The correlation matrix table below (Table 4.7) showed correlation coefficients among observed and predicted soil depth for each prediction models used and the predictor variables. The soil-hillslope position relationship assumption made to build the model has now shown a statistically good relationship at a point. The variations in the significances of each predictor variables and its correlation coefficient under different models are also an indication of the unpredictability of which variable most influences the soil depth distributions in the study area. Hence, it is possible to say that the predictive powers of all the models used were reasonable and can be used further in an infinite slope model.

Table 4.7 Correlation matrix among soil depth models and topographic attributes(n=40)

| ***Pearson Correlations*** | | |
|---|---|---|
| | | *Observed soil depth* |
| *Observed soil depth* | | *1* |
| *Predicted soil depth using:* | *Decision tree* | *.825*** |
| | *Soil balance equation* | *.670*** |
| | *Multiple regression* | *.786*** |
| *Predictor variables* | *Profile curvature* | *-.506*** |
| | *Distance to river* | *-.592*** |
| | *gradient* | *-.518*** |
| | *TWI* | *.730*** |

| |
|---|
| ***. Correlation is significant at the 0.01 level (2-tailed).* |

In addition to the correlation matrix results, the variability of the validation datasets is shown in Figure 4.8 below. The scatter plots show that it is rare for shallow soil depth to be observed in the field and predicted by the model because of the model assumptions. For instance, most of the field data were collected from the lower slope and valley area where the model predicted as deep soil but in reality where shallow soils were also found. These reduced $R^2$ values and the points included as outliers are shown in Figure 4.1. Also, the predictive models predicted soil depth into the next class; for example, an observed shallow soil depth might have been classified as moderate depth by the models, which contributed to reducing $R^2$ values. Such a difference in prediction result also indicates the differences in sensitivity of the models used to input factor maps. However, the correlations made for points collected from landslides indicate no relation with an observed depth points (Figure 4.8D) which shows high spatial variability of landslides in the area. Because of the spatial distributions of measured soil depths in the field and the limited number of sample points compared to landslide density on the area, the weak correlation result presented cannot distract the role of the big picture that slope parameters influence landslide occurrence besides soil depth.

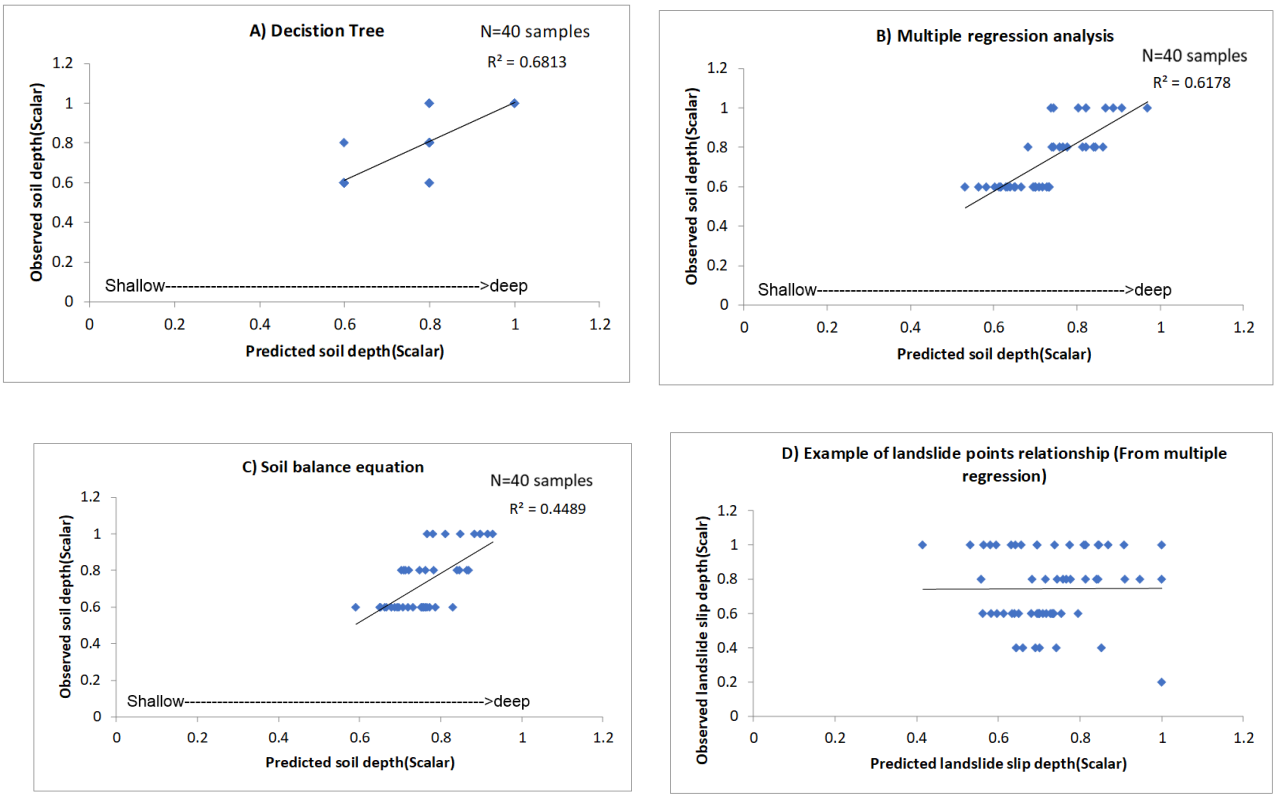


Figure 4.8 Scatter plots for model validations

Compared to the number of field data and quality of the available DEM, the predictive powers of the models are all at best (Figure 4.8). Besides, each of the models was sensitive to different factor maps (Table 4.7) which are also indications of where to expect slope failures in slope stability assessment results.

In addition to the correlations made on the qualitative classes of field observation and predicted soil depths, correlation is made on the quantitative soil depths. For the predicted qualitative soil depth classes, an equivalent quantitative classes were assigned based on Soil survey (1951) soil depth classes as mentioned above. Quantitative classes of the observed soil depth are soil depth values measured in the

field. Accordingly, the scatter plot was produced between the real data as shown in Figure 4.9 below for the same sample points shown in Figure 4.8 as a validation dataset. The $R^2$ values of soil depth from the multiple regressions show a higher value while the equivalent qualitative classes showed higher $R^2$ value for decision tree. This occurred because the qualitative class values which range from 0 and 1 were an integer number for the decision tree model while it was a fraction for the multiple regression model. Hence, one on one correlation between the integer value gave higher correlation compared to the fraction values on a qualitative soil depth class. However, for the real quantitative soil depth, the fraction number got higher value because of the significant spatial variabilities of soil measurements in the field. Based on the results of both the qualitative and quantitative classes it is possible to say that decision tree and multiple regression models predicted soil depth better than soil balance equation. The results were also validated later based on the predictive power of the models in slope instability initiations.

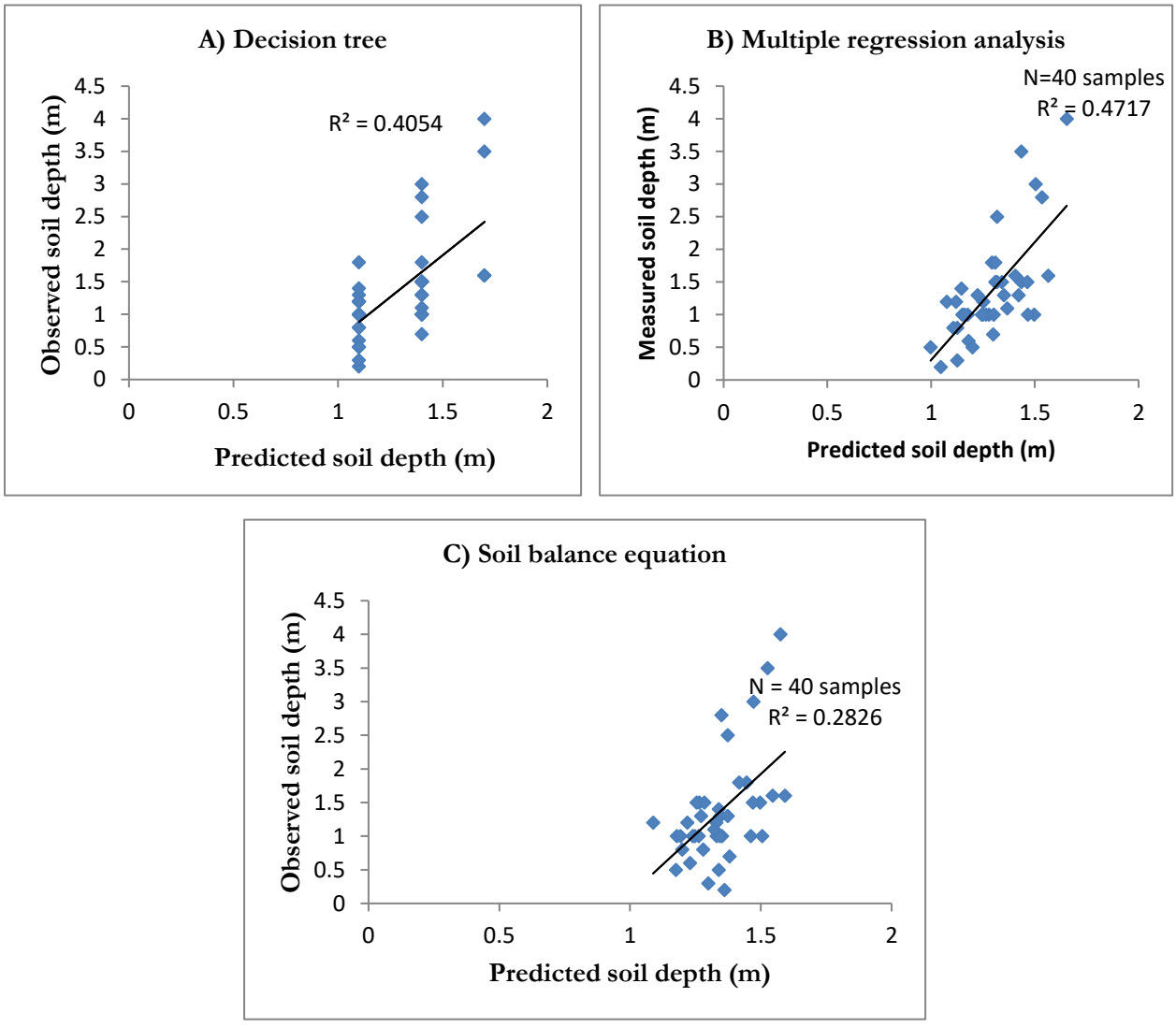


Figure 4.9 Scatter plot for model validation using quantitative data

# 5. RESULTS OF INFINITE SLOPE MODEL

## 5.1. Introduction

In this section, the results of the spatial infinite slope model using different soil depth maps are presented. Topographic factors, land use, soil characteristic and rainfall data are used as an input in the infinite slope model under different scenarios. Soil depth maps produced using various techniques (Chapter 4) were used separately in the infinite slope analysis to check their influences in slope instability. Then, the prediction results of the infinite slope model were tested against existing landslide inventory data to validate the model output. After validation, the best model are selected and the number of unstable days of the model is presented separately.

## 5.2. Infinite slope model input parameters

The input parameters of the infinite slope model in PCRaster was described under chapter 3, and the values of specific parameters obtained from different sources is shown in Table 5.1. The input parameters were optimised by varying the values between minimum and maximum and the optimum values are used to calibrate the infinite slope model. For example, there was no slope failure observed when maximum values of soil strength parameters are used. Hence, the minimum values were used for soil shear strength parameters and average values for parameters obtained from pedo-transfer functions to calibrate the infinite slope model. The minimum soil shear strength values were selected because most slope failure happens during the rainy season and rainfall reduces shear strength values as observed in the field. Parameters obtained from pedo-transfer functions were soil texture dependent, and the was no need of changing the values sought. Eventually, all the constants, maps and time series files as described in chapter 3 were run by scripts in PCRaster to produced infinite slope model results.

Table 5.1 soil classes and input parameters

| Soil type | Soil class | Ksat (mm/hr) | Porosity (%) | Field Capacity (%) | Wilting Point (%) | Cohesion (Kpa) | Friction Angle ($^0$) | Bulk Density (KN/m$^3$) |
|---|---|---|---|---|---|---|---|---|
| Skeletal | Gravelly sandy loam | 25.2 | 0.45 | 0.18 | 0.08 | 3.3 | 36 | 14.3 |
| Kandoid latosolics | Silty clay | 3.8 | 0.53 | 0.42 | 0.28 | 4.5 | 34 | 12.1 |
| Protosols | Sandy loam with less fine matrix | 61 | 0.45 | 0.16 | 78 | 3.8 | 33 | 14.2 |
| Young soil | Sandy loam | 50 | 0.45 | 0.18 | 50 | 4 | 32 | 14.2 |
| Smectoid soil | Clay | 0.76 | 0.49 | 0.42 | 49 | 6.5 | 28 | 13.3 |
| Allophane latosolics | Sandy clay loam | 7.9 | 0.43 | 0.28 | 18 | 5 | 31 | 14.8 |
| Unclassified soil | - | - | - | - | - | - | - | - |

Sources: Ksat, Porosity, Field capacity, Wilting point and Bulk density are obtained from the pedo-transfer function by Saxton & Rawls, (2006), Cohesion (measured in the field) and Friction angle (www.geotechdata.info).

## 5.3. Infinite slope model results

The results of an infinite slope model were a time series raster maps with each pixel representing a factor of safety (FS) values and the number of unstable days in the year. However, the factor of safety of two days each from the year with average rainfall (2009) and extreme rainfall (2004) were selected for further analysis. The two days with the rainfall amount of 192.6 for 2009 and 422.3 for 2004 are the maximum rainfall in respective years (Figure 5.1). The two days were selected because rainfall triggers slope failure and no slope failure is expected under dry condition. In this study, the emphasis was given to identify how soil depth influences slope failure initiations under two different rainfall conditions. Hence, the infinite slope stability model using 2009 rainfall is considered as modelling under normal rainfall conditions because it was from the year with average rainfall condition. Whereas the FS model using 2004 is considered as modelling under heavy rainfall condition because of the presence of the extreme rainfall presence.

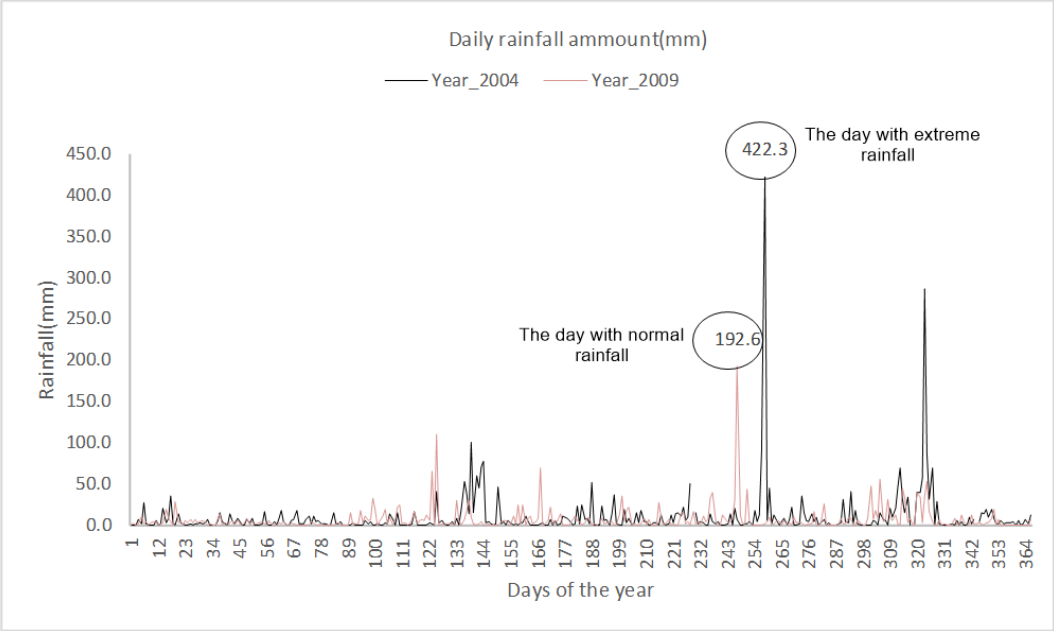


Figure 5.1Selected rainfall days for FS analysis under different scenarios

### 5.3.1. Factor of safety under normal rainfall conditions

The results of infinite slope analysis considering different soil depth models under normal rainfall condition for the area is presented in Figure 5.2. Similarly, the same input parameters were used in infinite slope analysis under extreme rainfall conditions to evaluate the influences of different soil depth models on slope instability initiations.

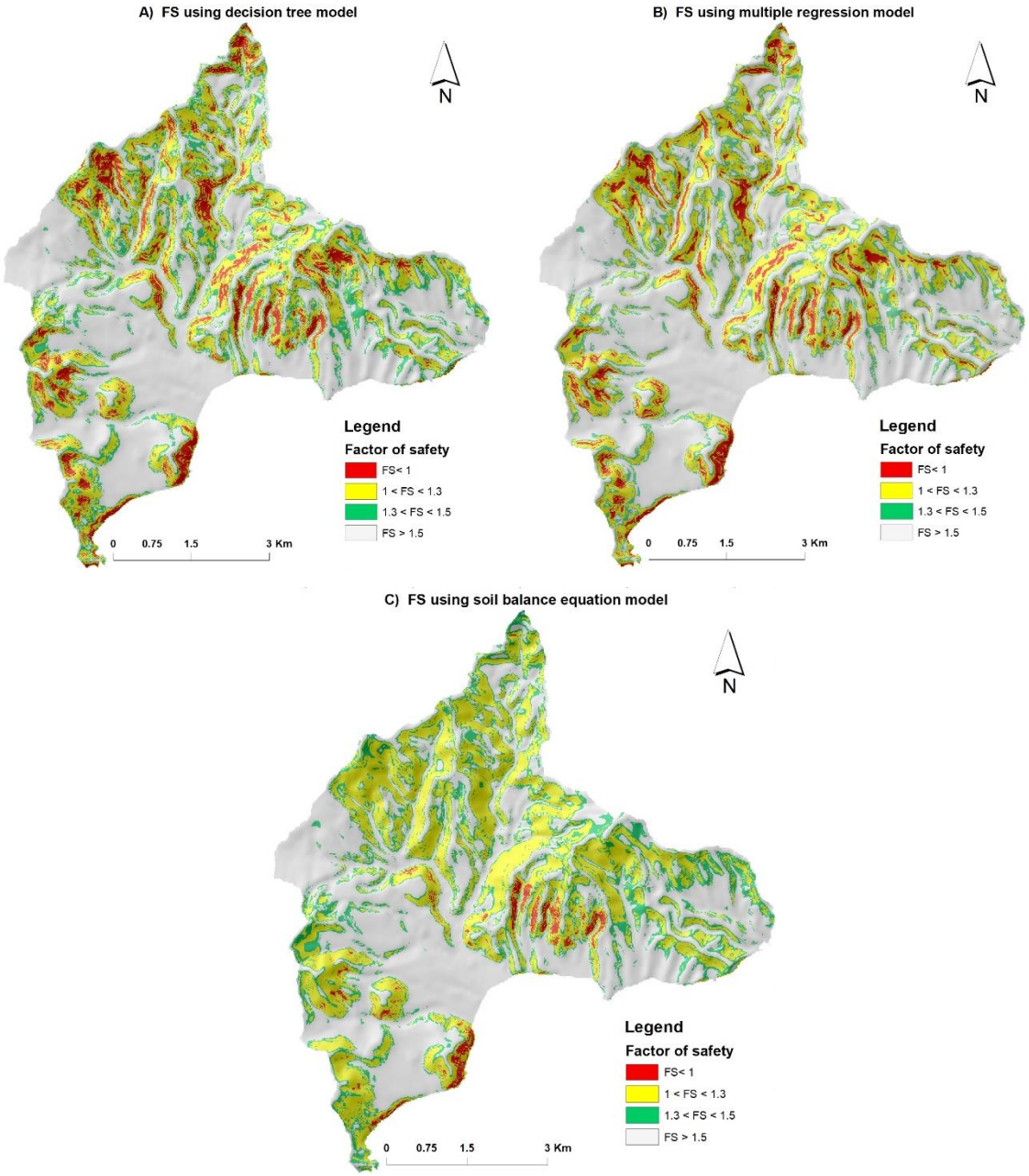


Figure 5.2 FS of slope using different soil depths and under normal rainfall condition on day which has the max daily rainfall (192mm) for that year

The FS result (Figure 5.2) showed that deep soils require a high amount of rainfall to get fully saturated and cause many slope failures. The predicted dense slope failures on a steep slope by decision tree and multiple regression models are associated with predicted shallow to moderately deep soil depths by the respective models. But the soil balance equation predicted deep soil on the same steep slope and only a few slope failures occurred. Based on the result it is also logical to say that low rainfall intensity causes shallow slope failures than deep slope failures because it can not quickly saturate deep soils.

### 5.3.2. Factor of safety under heavy rainfall condition

The factor of safety was analysed for the extreme daily rainfall intensity in the year 2004. The daily rainfall intensity of the year was 422.3mm (Figure 5.1), and this was selected from the results of time series files of FS to evaluate how heavy rainfall affects slope instability compared to normal rainfall for the same soil

slope. Slope stability under extreme rainfall were modelled for different soil depth methods given all the other input parameters set constant to check the significance of soil depth in slope failure initiation. Unfortunately, there is no report on landslide occurrence in the year 2004, but the rainfall intensity was close to category five or equivalent to category four of hurricane Maria, which occurred in 2017. Hence, based on previous facts it was assumed that slope failure would presumably happen if the area receives such high rainfall. The FS result for the heavy rainfall are shown in (Figure 5.3).

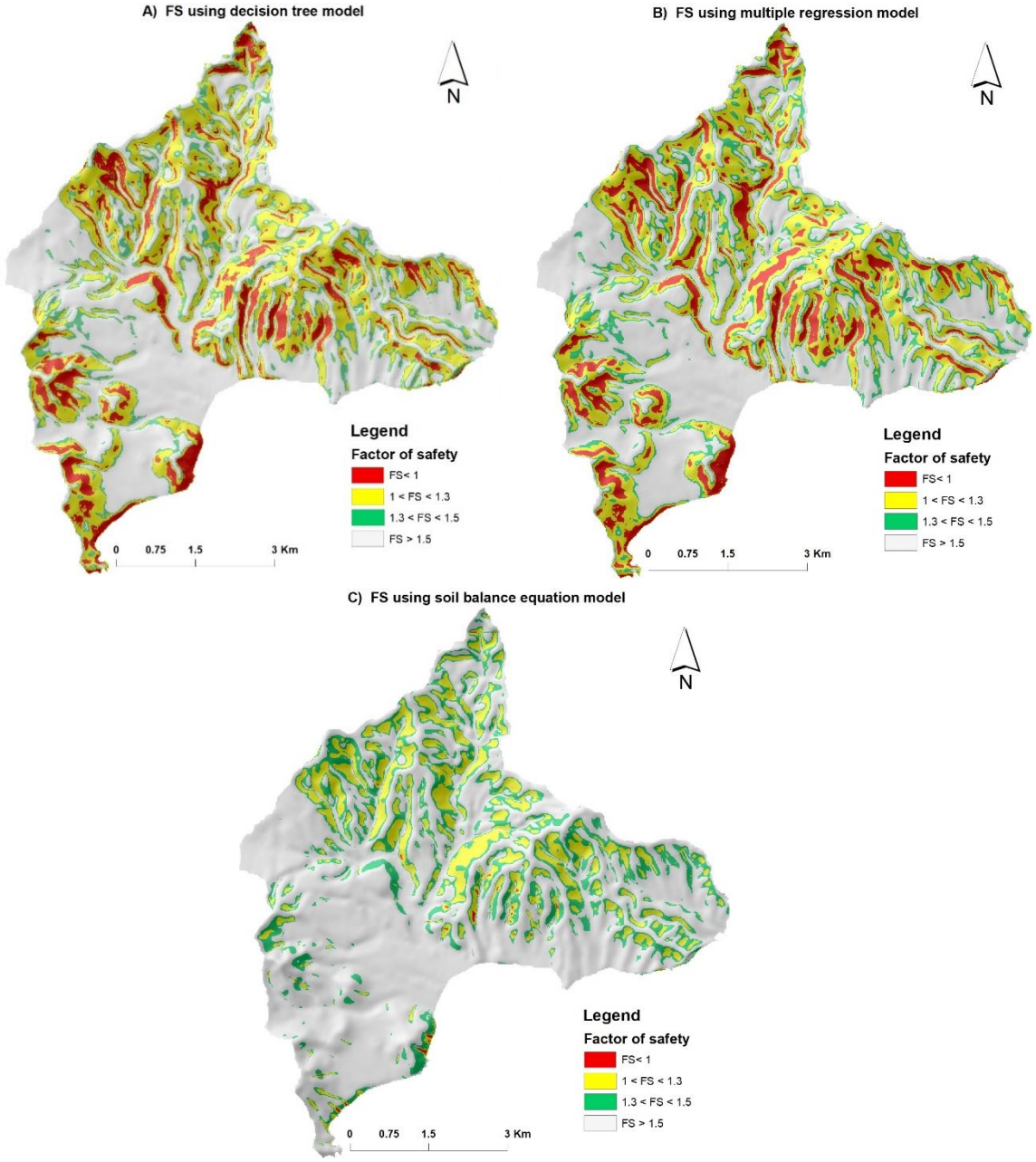


Figure 5.3 FS of slope using different soil depths under extreme rainfall condition and the extreme rainy day considered

The FS result showed several slope failures for decision tree, and multiple regression soil depth models under heavy rainfall conditions(Figure 5.3A & B) compared to the normal rainfall while there were minimal failures for deep soil(Figure 5.3C). Still, there was no major slope failure occurrence for slopes covered by thick soil under heavy rainfall condition. However, the time series result showed more slope

failures occurrences after one or two days compared to the slope failures during the extreme rainy day. This is also logical that deep soils require time to get fully saturated and for slope failures to occur while the result shown in (Figure 5.3C) is FS result of the extreme rainy day only.

## 5.4. Infinite slope model validation

Results obtained by applying infinite slope models were validated with the goal to know how good the models' predictive power is compared to an existing landslide inventory of the area (excluding the runout part of the landslide inventory). There were no predefined threshold values set for the predictive models; instead, the emphasis was given to examining the FS results produced from each soil depth and selections of the best model with good predictive power. Accordingly, the outputs were first visually inspected based on their spatial distributions compared to the inventory landslide map. It was observed that soil depth maps predicted low slope failures close to stream channels and near flat valley areas. It was noted also that the spatial locations of the predicted slope failure initiations are sensitivity to slope gradient. Besides visual observations of the results, the models were validated using quantitative statistical based error matrix or confusion matrix analysis. The error matrix were performed between the raster maps of reference inventory landslide maps and slope failure maps from the predicted model results.

### 5.4.1. Sensitivity of slope failure to soil depth models under normal rainfall condition

Inventory landslide and predicted FS overlay showed several slope failures occurred on shallow to moderately deep soil under normal rainfall conditions as shown in the example of FS result using decision tree prediction (Figure 5.4A) and multiple regressions while only few slope failures occurred on deep soil slope predicted using soil balance equation (Figure 5.4B). Majority of the deep soil slopes were marginally unstable.

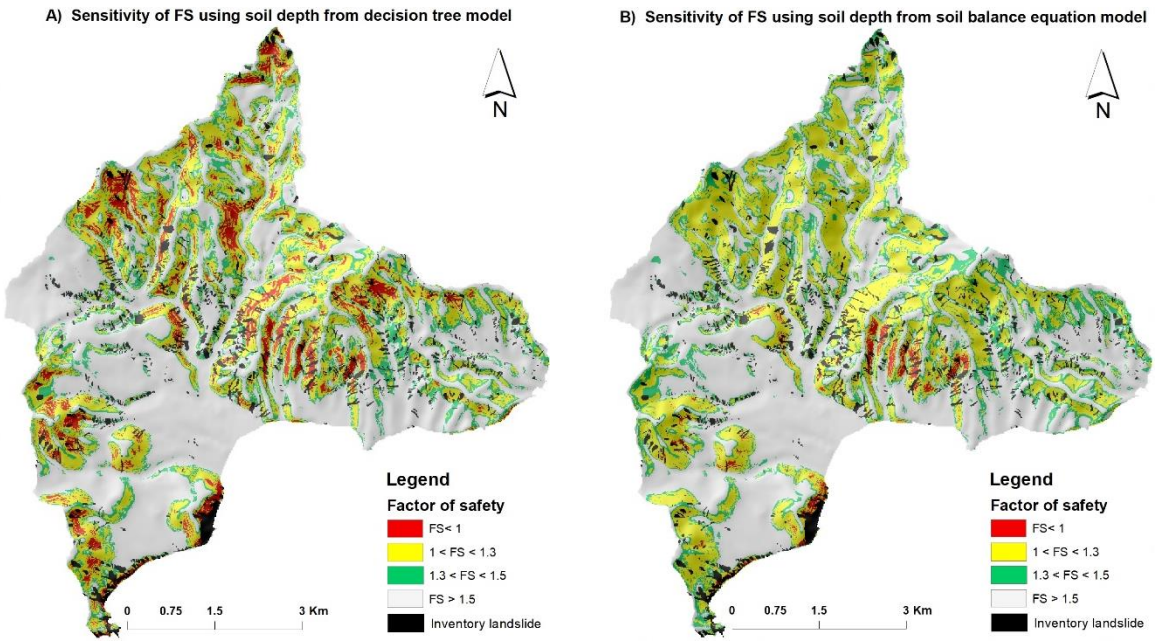


Figure 5.4 Example of FS model validation under normal rainfall condition using inventory landslide

Besides, statistical accuracy assessment for all the three soil depth models was conducted using the error matrix (Table 5.2) between inventory landslide and slope failure maps under normal rainfall conditions.

Both inventory landslide and predicted slope failure maps (maps with FS < 1) are converted to Boolean maps of 0 and 1 for pixels with FS > 1 and FS < 1 respectively. Accordingly, the pixel-based confusion matrix were made between the landslide and non-landslide areas of two maps where the per cent of errors in the table indicate the numbers of pixels involved and omitted during classification. Besides, the overall accuracy per cent reported was calculated based on whether the classified total of landslide and non-landslide pixels has been classified correctly into the category. The available inventor landslide map is a collection from several sources and years combined. However, the present infinite slope model was performed for one year based on a daily time step and the result of an extremely rainy day is presented. Hence, this fact needs to be considered before generalisations of the output. However, the results are also good indicators of how soil depth influences slope failure initiations. The numbers in the rows and columns of the confusion matrix (Table 5.2) shows the numbers of respective pixels.

Table 5.2 Accuracy assessment of predicted FS maps using different soil depth under normal rainfall condition

| Error Matrix | | Inventory landslide | | | | |
|---|---|---|---|---|---|---|
| | | FS > 1 | FS < 1 | Row sum | Commission error(%) | User's accuracy (%) |
| Prediction FS map using soil depth model<br>A. **Decision tree** | FS > 1 | 371327 | 22657 | 393984 | 5.75 | 94.25 |
| | FS < 1 | 28166 | 5180 | 33346 | 84.46 | 15.54 |
| | Column Sum | 399493 | 27837 | 427330 | | |
| | Omission error (%) | 7 | 81.4 | | Overall Accuracy=88.1 | |
| | Producer's accuracy (%) | 93 | 18.6 | | | |
| Prediction FS map using soil depth model<br>B. **Multiple regression** | FS > 1 | 374708 | 23101 | 397809 | 5.8 | 94.2 |
| | FS < 1 | 24785 | 4736 | 29521 | 83.95 | 16.5 |
| | Column Sum | 399493 | 27837 | 427330 | | |
| | Error of Omission (%) | 6.2 | 82.98 | | Overall Accuracy =88.8 | |
| | Producer's accuracy (%) | 93.8 | 17.02 | | | |
| Prediction FS map using soil depth model<br>C. **Soil balance** | FS > 1 | 394047 | 25815 | 419862 | 6.15 | 99.89 |
| | FS < 1 | 5446 | 2022 | 7468 | 72.92 | 13.91 |
| | Column Sum | 399493 | 27837 | 427330 | | |
| | Error of Omission (%) | 1.4 | 92.73 | | Overall Accuracy = 92.2 | |
| | Producer's accuracy (%) | 98.6 | 7.27 | | | |

For FS using soil depth from decision tree, about 84% of the predicted FS was incorrectly classified as slope failure while it was not present in the inventory map which shows the mismatch between the numbers of the pixel in reference and prediction maps. However, only 5.75% of the prediction landslide free area was reported as the landslide free area while it was not actually when compared with the inventory reference data. Besides, 81.4% of slope failure (FS<1) prediction using soil depth from decision tree was left out of the slope failure category. The result also means 81.4% of the inventory landslide area was classified as landslide free in the predicted map. Similarly, about 83% and 73% of landslide area were classified as landslide free area for FS prediction using Multiple regression and soil balance equation of the soil depth models. However, regarding the accuracy of the predictive model decision tree, multiple regression and soil balance equation models had 88.1%, 88.8% and 92.2% overall classification accuracies respectively.

The performances of all soil depth models in slope instability initiations under normal rainfall condition can be evaluated as a good prediction result based on the overall accuracy. However, the overall accuracy result alone is misleading as it shows how the performance of the model classifications. Hence, based on the number pixels class predicted slope failure classified into the inventory landslides, soil depth model using decision tree model showed good performance compared to the other soil depth models. Regardless of how well the slope failures are classified, the results were an indication of the influence of soil depth in slope instability initiations. Based on the results it is also logical to say that the average rainfall of the area induces slope failure mainly on shallow and moderate soil depths compared to deep soils.

### 5.4.2. Sensitivity of slope failure to soil depth models under heavy rainfall condition

Visual observations showed most of the predicted slope failures using soil depth models from the decision tree, and multiple regression falls within inventory landslide area (Figure 5.5 A & B). However, there were few slope failures predicted on deep soil (Figure 5.5 C).

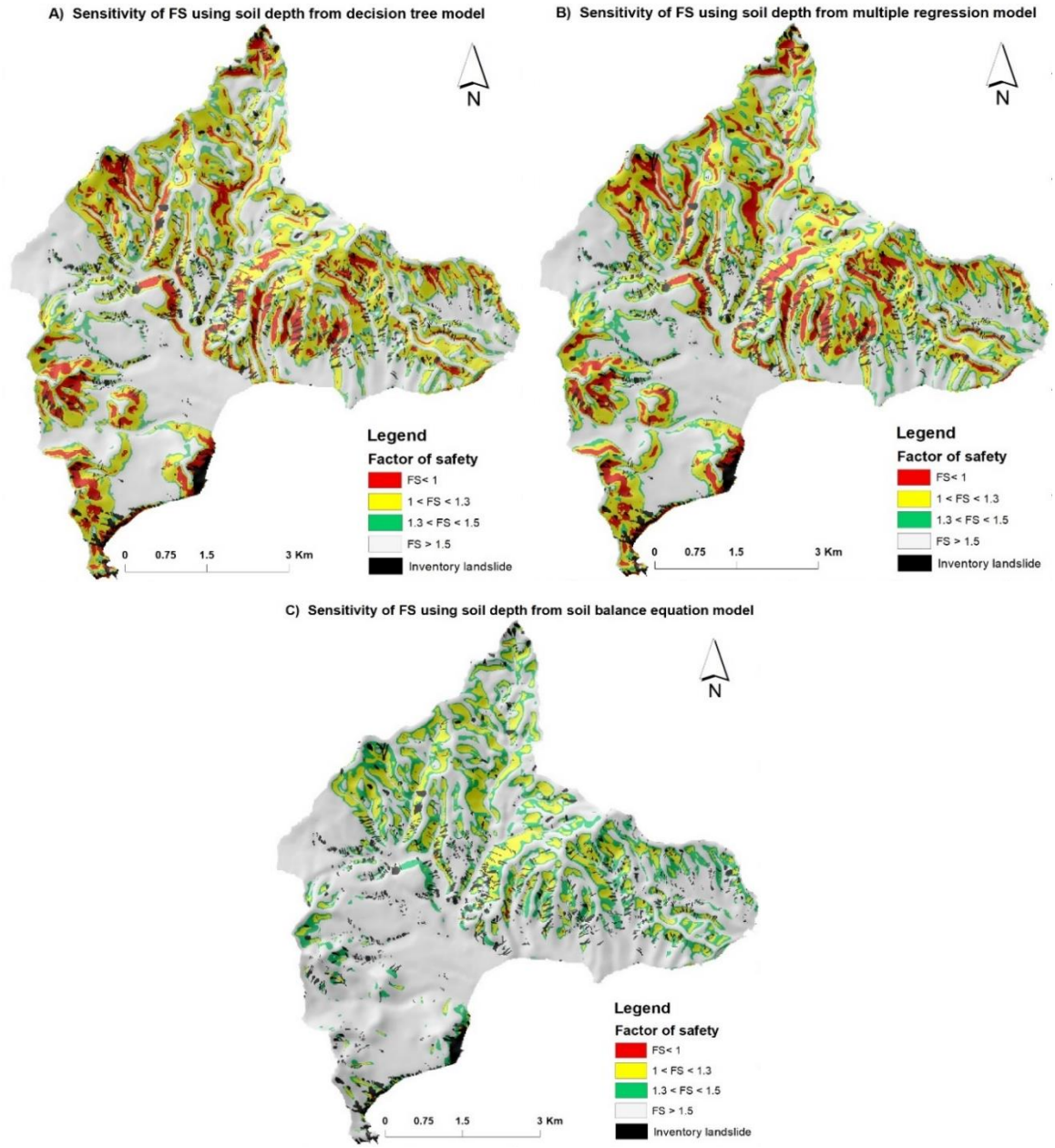


Figure 5.5 FS prediction under high rainfall for different soil depth models and inventory landslide used for model validation

The confusion matrix result between the predicted factor of safety and inventory landslide raster maps is shown in (Table 5.3). The result shows soil depth prediction using soil balance equation produced higher classification overall accuracy (93.45%) for slope instability compared to decision tree model (85.57%) and multiple regression model (84.8%). However, the goal of this study is mainly to evaluate the influence of soil depth in slope failure with less emphasis on the stable slope. Hence, pixel-based evaluations show soil depth model using decision tree has predicted better slope failure that was classified into inventory landslides than the other soil depth models.

Table 5.3 Accuracy assessment of predicted FS maps using different soil depth for extreme rainfall condition

| Error Matrix | | Inventory landslide | | | | |
|---|---|---|---|---|---|---|
| | | FS > 1 | FS < 1 | Row sum | Error of Commission(%) | User's accuracy (%) |
| Prediction FS map using soil depth model A. **Decision tree** | FS > 1 | 357838 | 20007 | 377845 | 5.3 | 94.7 |
| | FS < 1 | 41655 | 7830 | 49485 | 84.2 | 15.8 |
| | Column Sum | 399493 | 27837 | 427330 | | |
| | Error of Omission (%) | 10.42 | 71.87 | | Overall Accuracy = 85.57 | |
| | Producer's accuracy (%) | 89.58 | 28.13 | | | |
| Prediction FS map using soil depth model B. **Multiple regression** | FS > 1 | 354566 | 20041 | 374607 | 5.3 | 94.7 |
| | FS < 1 | 44927 | 7796 | 52723 | 85.21 | 14.79 |
| | Column Sum | 399493 | 27837 | 427330 | | |
| | Error of Omission (%) | 11.24 | 71.99 | | Overall Accuracy = 84.8 | |
| | Producer's accuracy (%) | 88.76 | 28.01 | | | |
| Prediction FS map using soil depth model C. **Soil balance** | FS > 1 | 399059 | 27543 | 426602 | 6.4 | 93.6 |
| | FS < 1 | 434 | 294 | 728 | 59.6 | 40.4 |
| | Column Sum | 399493 | 27837 | 427330 | | |
| | Error of Omission (%) | 0.1 | 98.9 | | Overall Accuracy = 93.45 | |
| | Producer's accuracy (%) | 99.9 | 1.1 | | | |

Even though soil depth model using decision tree has produced a comparatively low value of overall accuracy, it is the best model based on the number of slope failure pixels classified into inventory landslide both under normal and extreme rainfall conditions. Furthermore, the close similarities between the number of pixels classified into inventory landslide for both decision tree and multiple regression soil depth models were also similar in general pattern as shown in (Figure 5.6) at a large scale view under heavy rainfall condition. However, the high overall accuracy classification using the soil balance equation was overrated by the dominant non-landslide area, and it showed fewer landslide initiations as shown in Figure 5.6. This are associated with the deep soil predicted by the model while the landslides were shallow or moderately deep as observed in the field.

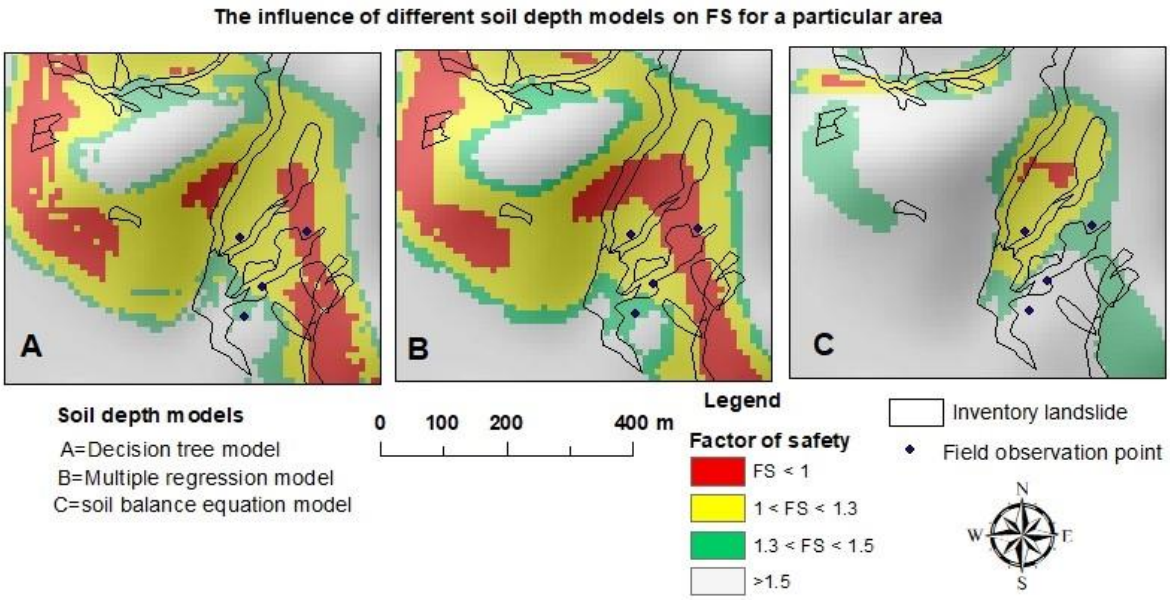


Figure 5.6 Example of large-scale FS maps for a particular area using different soil depth models under heavy rainfall

### 5.4.3. Number of unstable days of the slope under high rainfall

A factor of safety changes with time but no slope is expected to be unstable for the whole year. The number of unstable days of slope using soil depth from the model decision tree (Figure 5.7) showed many stable days for most of the flat and gentle slope and where deep soil dominate. Shallow soil depth zones found on steep slopes are unstable for many days in the year. However, artefacts on the DEM and very steep slopes were unstable for more than 300days in the year which reduce the confidence of the result on those positions.

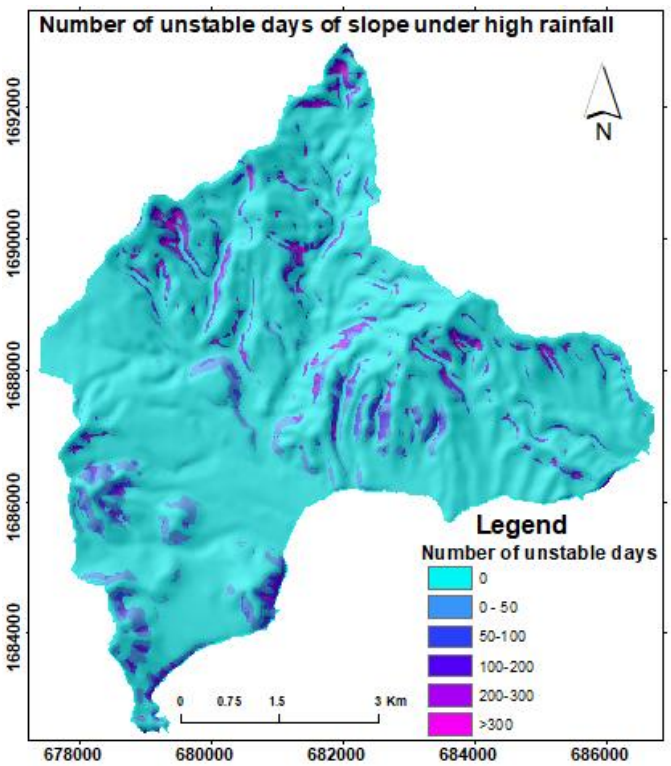


Figure 5.7 Number of unstable days of slopes under heavy rainfall using soil depth from decision tree

# 6. DISCUSSION, CONCLUSIONS AND RECOMMENDATIONS

This chapter discusses about the main finding of the research, the limitations of the models and data used, and draw conclusion based on the main question posed for the research objectives.

## 6.1. Discussion on soil depth models

The application of a different method for soil depth prediction gave different results which are attributed to the sensitivity of the models to different topographic variables. The source of input data for all the soil depth models used was DEM, which was not perfect as discussed below in the section on the limitations of the study. While the effects of the inputs data on model outputs are undeniable, efforts were made to calibrate each model using field observation to get the best possible result.

Soil depth results obtained using decision tree and multiple regression models were closely related. Both the models predicted deep soil (>1.5m) on the flat top of the mountains and valley bottoms as verified in the field. The result also complies with an estimation made by Rouse, (1990) on those specific positions. Model validation results also showed that both models had a weak correlation with slope gradient compared to other variables. Slope gradient showed only 20% correlation with decision tree prediction result and 33% with multiple regression result which in both cases were the lowest. However, the result is justifiable because of the poor DEM quality which did not show the actual nature slope geometry in the area. The main difference between the decision tree and multiple linear regression models was their sensitivity to different topographic input variables. In the decision tree, the model was forced to have the predefined values although it standardises the result based on the combined input variables the result had a correlation of 71% with TWI. However, multiple regression model result was sensitive to minor topographic irregularities having an 87% correlation with profile curvature due to its significance compared to other input topographic variables.

Soil balance equation comparatively predicted deep soil where the other two models predicted either moderate or shallow soil depth. It was caused by the calibrations of the model coefficients to find a good correlation between soil depth and topographic variables. Accordingly, the highest weight was given to the slope gradient that resulted in a 90% correlation with soil depth observations. The model prediction also showed a very weak correlation with profile curvature with only 17% which was the opposite of multiple regression prediction result relationship. Eventually, soil depth prediction using the decision tree showed a correlation of 82.5% with field measured soil depth which was a promising result in obtaining good slope instability result in such a poor data area. The sensitivities of each soil depth model to different topographic variables were also helpful to get different slope instability model caused by various slope instability contributing factors in addition to soil depth.

## 6.2. Discussion on infinite slope model

Sensitivity analysis was carried out by using different soil depth map in an infinite slope model while keeping constant all the other parameters. This resulted in different slope instabilities and confirmed the sensitivity of slope stability to soil depth as proved by several researchers (Montgomery & Dietrich, 1994, Segoni et al., 2011, Kim et al., 2016) and as assumed in this work. For all the three soil depth maps used in infinite slope model under different scenarios, the influence of deep soil were underestimated, and the importance of shallow and moderate soil depths were overestimated in the slope failure initiations (Figures

5.2 and Figure 5.3). The overestimations of slope failure by shallow soil depth were mentioned by Segoni et al. (2011) as the limitations of infinite slope model.

The infinite slope model under normal rainfall condition returned overestimation of the factor of safety for both decision tree and multiple regression soil depth models while the model underestimated FS for soil depth using the soil balance model. Overestimations of the FS by the two soil depth models were related to the high sensitivity of shallow slope failures to shallow and moderate soil depths. To the contrary, there were no significant slope failures predicted on deep soil due to normal rainfall. Also, Van Asch et al. (1999) stated that deeper landslides in soil needs larger amount of water for its triggering than shallow and moderate soil depths and justifies the low slope failure prediction on deeper soil balance model under normal rainfall. The result can also be related to what many researchers claimed that infinite slope better predicts shallow slope failures than deep failure. The quality of available inventory landslide data was also believed to have influenced the reality of the slope failure predictions because the inventory landslides were not a single event failure but rather a collection of multiple events from different sources.

The results of the infinite slope model under heavy rainfall showed the high number of landslide initiations as observed from the pixel-based statistical comparison with inventory landslide for both soil depths obtained from decision tree and multiple regression models. It is also logical that heavy rainfall triggers many shallow slope failures. On the other hand, Rouse, (1986) described the topsoils of Dominica as characterised by unique nature and requires a high amount of rainfall to be saturated due to their high porosity and high water holding capacity. In this way, deep soils need both a high amount of rainfall and time for slope failure to occur. Therefore, there were only a few unstable slopes observed using soil depth model that predicted deep soil (soil balance equation). It was proved also from a time series factor of safety maps that many slope failures happened after the extreme rainy day shown here as an analysis result (Figure 5.3C). This resulted because the maximum rolling set for rainfall in the dynamic model was one day and on the selected day (extreme rainy day) for infinite slope analysis, the soil could not be fully saturated to initiate huge slope failure.

Topographic variables are also identified as the most important controls for slope failure initiations in this study. The patterns and distributions of slope failure results also showed the influence of topographic factors in slope failure initiations in addition to soil depths. For example, the relationship of average values of slope gradient and factor of safety result under heavy rainfall condition (Figure 6.1) showed the sensitivity of slope instability to slope gradient. Hence, slopes higher than 37 degrees are susceptible to failure under heavy rainfall conditions. On the other hand, Reading, (1991) estimated the tropical residual soils of Dominica could be stable up to more than 40 degrees under normal conditions. In general, as the slope gradient increases, the chance of slope failure also increase.


Figure 6.1 Slope angle and factor of safety relationship for decision tree soil depth under heavy rainfall

For the other topographic variables like slope profile curvature and wetness indexes used in soil depth modes, there was no sensitivity analysis made on the infinite slope result maps. However, a simple overlay of the factor of safety maps on the topographic variables showed the locations of slope failure initiations as convex slope areas, low topographic wetness index and steep slopes far from the rivers.

## 6.3. Conclusion

This study presented the use of decision tree, multiple regression and soil balance equation as methods to predict soil depths of the area. Soil depth points was collected in the field from landslide scarps, road cuts, stream cuts and using Auger assuming to calibrate and validate soil depth model results. The present models assumed soil depth distribution is related to topography and it plays an essential role in slope failure initiations. Hence, topographic variables was extracted from DEM and soil depth maps were produced based on the relationship between soil depth points from the field and DEM derivative variables. The results of soil depth models were validated using soil depth points collected in the field, and consequently, soil depth map from the decision tree model showed higher soil depth spatial variability. Then, all the soil depth maps were entered into the infinite model which was developed in PCRaster. Infinite slope model were performed under an average rainy day and extreme rainy day of the years 2009 and 2004 respectively with an assumption of no slope failure during a dry season. The reliabilities of slope stability results was checked against an existing inventory landslide data, and in this way, soil depth prediction using the decision model produced a better factor of safety map under both rainfall conditions. Hence, soil depths predicted using decision tree was rated as the best model as the validation results of an infinite slope model showed a higher number of predicted slope failure predicted factor of safety classified into inventory landslides. The factor of safety maps predicted using multiple regression models showed closely similar results decision tree results both in terms of pattern and number of pixels. Slope stability assessment result also showed that a thick soil layer (soil balance model prediction) caused under predictions of slope instability and shallow soil depth caused slope instability over prediction.

The influences of slope gradient, soil strength and rainfall were also significant in slope failure initiations of the area in addition to soil depth. The sensitivity of a factor of safety result against slope gradient showed slope gradient as a useful index of slope failure locations in the area. Steep slopes were sensitive to slope failure compared to gentle slopes. Higher rainfall amount caused many slope failures as shown by pixel based statistical relationship with validation data. Infinite slope model was also susceptible to the changes in model calibration data values like soil cohesion and friction angle as soil strength determining factors. However, the influences of soil strength parameters were checked during infinite slope model calibration and there was no sensitivity analysis made for it.

The following section gives answers to the main questions asked for the specific objectives.

### (1) Which spatial interpolation method gives the best results in assessing soil depth?

The ratings of the models were made based on their accuracy assessment and predictive power of slope failure initiations. The accuracy of soil depth prediction results was tested against field observation points. The decision tree prediction result showed the best soil depth result compared to results obtained using the soil balance equation and multiple regression models. Besides, it also better-predicted slope failure initiations that makes the decision tree the best model used in this work. However, the researcher warns on the general ratings of the models as the validation points were not uniformly distributed in the study area.

**(2) Which locations have a soil depth that cannot be related to the topography and why?**

The present soil depth prediction methods assume the presence of a relationship between soil depth distribution and topography regardless of the origins of the materials. However, there are locations where the soil depth does not behave according to the soil depth model concepts used. In this way, the thick soils on volcanic ash deposits observed in the field were not predicted accurately by all the soil depth prediction methods. Also, river channels which are an accumulation site for erosion materials and were thick soil are expected were also affected by river incisions. So, bedrock was exposed in stream channels located in the narrow, and V-shaped gorges which gave soil depth prediction result different from the model assumptions. Hence, there is low confidence in the results of soil depth maps in those locations.

**(3) Which topographic variables explain well spatial variability of soil depth?**

Correlations of soil depth and topographic variables showed the three soil depth prediction results were sensitive to different topographic variables (Table 4.7). Soil depth map obtained from the decision tree model was sensitive to the topographic wetness index and distance to the river while the soil balance equation model was highly sensitive to slope gradient followed by topographic wetness index. The main controls of the multiple regression model are the most significant variables, and slope profile curvature was a relatively significant variable in this study. The variability and sensitivity of soil depth to different topographic variables is believed to be related to the quality of DEM data and number and positions of field depth observation points.

**(4) Can we explain the uncertainty of predictions of soil depth in relation to the quality of the variables used?**

The primary input parameters in the soil depth model were DEM derivative topographic variables which had quality issues as indicated under limitations of the research subtopic below. Soil depth prediction results and topographic relationships were correlated to check which variable better explains soil depth distributions of the area. Accordingly, the three soil depth prediction results showed different correlation with topographic input parameters used, but uncertainties of the variables were not quantified. Similarly, the uncertainty of field soil depth measurements is admitted also because of the complex geologic nature of the area. Soil depth models were calibrated based on field observations which admittedly contain uncertainty. Therefore, uncertainties associated with model input parameters can be explained for future improvements, but they are not quantified in this work.

**(5) What is the sensitivity of slope instability to soil depth relative to other variables?**

Sensitive input parameters influence any model, and soil depth was the factor that influenced most the slope failure initiations in this study. The sensitivity of slope instability to soil depth was checked by purposely keeping all the other infinite slope models inputs same (values were not varied when different models are used) for each soil depth models. Hence, the results showed high sensitivities of slope failure to shallow and moderate soil depths as opposed to deep soil both under normal and heavy rainfall conditions. In addition to soil depth, both topographic factors like slope gradient and soil strength parameters also played an important role in slope stability of the area. Even though sensitivity analysis was not made statistically for how soil strength parameters affected slope stability, it was checked during infinite slope model calibration as mentioned above. So, there were no slope instabilities observed at higher soil strength parameter values as opposed to low and average soil strength parameter values. The influence of slope gradient was significant in slope stability under both normal and heavy rainfall

conditions. For example, the average factor of safety of slopes under heavy rainfall occurred on a slope having an angle higher than $37^0$ is shown as an example of other factors affecting slope instability of an area (Figure 6.1). It also shows the positions of factor of safety range from unstable slope through marginal and stable slopes on the slope gradient. Besides, the importance of soil strength parameters on slope instability result was also undeniable as observed during model calibration under different rainfall condition. In general, rainfall increases soil saturation and decreases soil shear strength which also causes more unstable slopes.

**(6) Is this influence of soil depth different in a year with average rainfall as opposed to a year with the extreme rainfall?**

The occurrence of slope instability was in general positively influenced by the presence of rainfall as opposed to a dry season. However, there is a significant difference in the predicted factor of safety as shown model validations (table 5.2 and table 5.3) under normal and heavy rainfall conditions. The factor of safety result using soil depth from decision tree showed an overall accuracy of 88.1% under normal rainfall and 85.57% under heavy rainfall condition. In the same way, the soil depth map using multiple regression showed an overall accuracy of 88.8% and 84.8% under normal and heavy rainfall conditions respectively. However, soil depth map using the soil balance equation showed a higher overall accuracy of 92.2% under normal rainfall and overall accuracy of 93.45% under heavy rainfall while having small numbers of slope failure pixels classified into inventory landslide data. Hence, the difference between different soil depth models in influencing slope failure is based on the number of pixels classified into inventory landslide. In addition to the overall accuracy results, visual observations of the predicted factor of safety maps also showed lesser unstable areas under the normal rainfall conditions as opposed to the heavy rainfall condition which showed the difference in the influence of soil depth models on slope instability under different rainfall condition.

**(7) Can the results of the slope instability model be related to the landslide inventories?**

The statistical summary of correlations made among landslide and non-landslide classes showed the presence of significant correlations between the predicted slope instability results and the existing inventory landslide data. The focus of the statistical relationship was on soil depth as a sensitive parameter in the slope stability model. All the three soil depth models also showed the presence of a reasonable relationship with an existing inventory landslide data with an overall accuracy of more than 84%. Since the goal of this study was also to identify the best soil depth predictive model which gives the best slope instability model, the statistical summary of the best model chosen was also indicated. In this way, soil depth model using decision tree was selected as the best model for slope instability prediction (based on the number of the classified pixels) and showed an overall accuracy of 88.1% under normal rainfall and 85.57% under heavy rainfall with inventor landslide data.

## 6.4. Limitations of the research

The main limitations of the research were the quality of topographic data used from which model variables were extracted, and the number as well as the spatial distributions of soil depth measurements in the field. The available DEM data contains artefacts that influenced both soil depth and infinite slope models. The low resolutions of the DEM also underrated the actual slope geometry of the area. In addition, the number of soil depth observation points were limited, and its spatial distributions were not uniform compared to the size of the test area because of inaccessibility during fieldwork. The models also

had limitations because they underrated soil depth values on volcanic deposit and overestimated the values of river incision that also appeared in infinite slope results. Majority of the model calibration data were obtained from secondary sources while the models were sensitive to input data. There was no rainfall station in the study area as rainfall variability controlled soil distribution and believed to control landslide occurrences in the area. Therefore, the overall evaluations of the research should consider the indicated limitations.

## 6.5. Recommendation

In this study, several data from various sources were used to model both soil depth and slope stability of the area. However, most of these data lacks details as shown under the limitation of the study. For example, the DEM data which was the sources of topographic input variables lacked terrain detail and influenced the results of both soil depth and infinite slope model. This could be improved by using detailed topographic variables obtained from Lidar DEM data. In addition, soil strength parameters which are an important input parameter in slope stability analysis was derived from standard tables and literature, but detailed laboratory analysis is required in future to improve the results of the present study. Furthermore, many researchers in the area indicated that rainfall of the area is highly variable and such variability controls soil distributions of the area. Unfortunately, there was no rainfall station in the study area. So, rainfall data from the nearest station was used. Any future study on the area should consider detailed rainfall data on the test site. The number and distributions of soil depth sampling in the field were also not satisfactory compared to the size of the area. Therefore, dense soil depth data which is uniformly distributed in the study area give more detailed information about soil depth distributions of the area. Equally important is also the soil depth models used. The models assumed the presence of correlation between soil depth distribution and topography. However, the area is complex terrain and there are areas which do not fit into these model assumptions. Hence, future improvement can be made by segregating the topography of the area into the parts which satisfy the model assumptions and adopting other assumptions for the parts that are difficult be included.

# LIST OF REFERENCES


Beguería, S. (2006). Validation and evaluation of predictive models in hazard assessment and risk management. *Natural Hazards*, *37*(3), 315–329. https://doi.org/10.1007/s11069-005-5182-6

Bishop, T. F. A., Minasny, B., & McBratney, A. B. (2006). Uncertainty analysis for soil-terrain models. *International Journal of Geographical Information Science*, *20*(2), 117–134. https://doi.org/10.1080/13658810500287073

Calcaterra, D., & Parise, M. (2010). Weathering as a predisposing factor to slope movements: an introduction. *Geological Society, London, Engineering Geology Special Publications*, *23*(1), 1–4. https://doi.org/10.1144/EGSP23.1

Cascini, L., Ciurleo, M., & Di Nocera, S. (2016). Soil depth reconstruction for the assessment of the susceptibility to shallow landslides in fine-grained slopes. *Landslides*, *14*(2), 459–471. https://doi.org/10.1007/s10346-016-0720-8

Cascini, L., Ciurleo, M., Di Nocera, S., & Gullà, G. (2015). A new-old approach for shallow landslide analysis and susceptibility zoning in fine-grained weathered soils of southern Italy. *Geomorphology*, *241*, 371–381. https://doi.org/10.1016/j.geomorph.2015.04.017

Crozier, M. J. (2010). Deciphering the effect of climate change on landslide activity: A review. *Geomorphology*, *124*(3–4), 260–267. https://doi.org/10.1016/j.geomorph.2010.04.009

D'Odorico, P. (2000). A possible bistable evolution of soil thickness. *Journal of Geophysical Research*, *105*(B11), 25927–25935. https://doi.org/doi:10.1029/2000JB900253

Dai, F. C., & Lee, C. F. (2003). A spatiotemporal probabilistic modelling of storm-induced shallow landsliding using aerial photographs and logistic regression. *John Wiley & Sons, Ltd.*, *545(28)*, 527–545. https://doi.org/10.1002/esp.456

DeGraff, J. V., Romesburg, H. C., Ahmad, R., & McCalpin, J. P. (2012). Producing landslide-susceptibility maps for regional planning in data-scarce regions. *Natural Hazards*, *64*(1), 729–749. https://doi.org/10.1007/s11069-012-0267-5

Degraff, J. V. (1987). *Landslide hazard on dominica, west indies final report*. Washington, D.C., Department of Regional Development Organization of American States

Degraff, J. V, Service, F., & Mmary, E. S. I. (1990). *Post-1987 landslide on Dominica, West Indies: An assessment of landslide-hazard map reliability and initial evaluation of vegetation effect on slope stability*. Washington, D. C.

DeRose, R. C., Trustrum, N. A., & Blaschke, P. M. (1991). Geomorphic change implied by regolith — Slope relationships on steepland hillslopes, Taranaki, New Zealand. *CATENA*, *18*(5), 489–514. https://doi.org/10.1016/0341-8162(91)90051-X

Dietrich, W. E., Reiss, R., Hsu, M.L., & Montgomery, D. R. (1995). A process-based model for colluvial soil depth and shallow landsliding using digital elevation data. *Hydrological Processes*, *9*(3–4), 383–400. https://doi.org/10.1002/hyp.3360090311

Di Martire, D., De Rosa, M., Pesce, V., Santangelo, M. A., & Calcaterra, D. (2012). Landslide hazard and land management in high-density urban areas of Campania region, Italy. *Natural Hazards and Earth System Science*, *12*(4), 905–926. https://doi.org/10.5194/nhess-12-905-2012

ECU. (2000). *The Commonwealth of Dominica ' s First National Report on the Implementation of the United Nations Convention to Combat Desertification ( UNCCD )*. Roseau.

FAO. (2006). *Guidelines for soil description*. (R. Jahn, R., Blume, H.-P., Asio, V.B., Spaargaren, O., Schad, P., Langohr, R., Brinkman, R., Nachtergaele, F.O., & Pavel Krasilnikov, Ed.) (4th ed.). Rome: Viale delle Terme di Caracalla. Retrieved from http://www.fao.org/3/a-a0541e.pdf

FRA. (2014). *Global forest resources assessment 2015, Country report for Dominica*. Rome. Retrieved from http://www.fao.org/3/a-au190e.pdf

Fu, Z., Li, Z., Cai, C., Shi, Z., Xu, Q., & Wang, X. (2011). Soil thickness effect on hydrological and erosion characteristics under sloping lands: A hydropedological perspective. *Geoderma*, *167–168*, 41–53. https://doi.org/10.1016/j.geoderma.2011.08.013

Gariano, S. L., & Guzzetti, F. (2016). Landslides in a changing climate. *Earth-Science Reviews*, *162*, 227–252. https://doi.org/10.1016/J.EARSCIREV.2016.08.011

Geotechdata.info, Cohesion, http://geotechdata.info/parameter/cohesion (as of December 15, 2013).

Ghestem, M., Sidle, R. C., & Stokes, A. (2011). The influence of plant root systems on subsurface flow : Implications for slope stability, *61*(11), 869–879. https://doi.org/10.1525/bio.2011.61.11.6

Goetz, J. N., Guthrie, R. H., & Brenning, A. (2011). Integrating physical and empirical landslide susceptibility models using generalized additive models. *Geomorphology*, *129*(3–4), 376–386.

https://doi.org/10.1016/j.geomorph.2011.03.001
Gorsevski, P. V, Gessler, P. E., Boll, J., Elliot, W. J., & Foltz, R. B. (2006). Spatially and temporally distributed modeling of landslide susceptibility, *80*, 178–198. https://doi.org/10.1016/j.geomorph.2006.02.011
Gray, J. M., & Murphy, B. W. (1999). *Parent material and soils : a guide to the influence of parent material on soil distribution in Eastern Australia*. Sydney. Retrieved from https://www.researchgate.net/publication/277013099%0AParent
Guha-sapir, D., Hoyois, P., & Below, R. (2016). *Annual Disaster Statistical Review 2016: The numbers and trends*. *Review Literature And Arts Of The Americas*. Brussels, Belgium. https://doi.org/10.1093/rof/rfs003
Ho, J. Y., Lee, K. T., Chang, T. C., Wang, Z. Y., & Liao, Y. H. (2012). Influences of spatial distribution of soil thickness on shallow landslide prediction. *Engineering Geology*, *124*(1), 38–46. https://doi.org/10.1016/j.enggeo.2011.09.013
Howe, T. M., Lindsay, J. M., & Shane, P. (2015). Evolution of young andesitic-dacitic magmatic systems beneath Dominica, Lesser Antilles. *Journal of Volcanology and Geothermal Research*, *297*, 69–88. https://doi.org/10.1016/j.jvolgeores.2015.02.009
Iverson, R. M. (1990). Groundwater flow fields in infinite slopes, *40*(1), 139–143. https://doi.org/doi.org/10.1680/geot.1990.40.1.139
Jerome, D. V., James, A., & Breheny, P. (2010). The formation and persistence of the Matthieu landslide-dam lake, Dominica, W.I. *Environmental and Engineering Geoscience*, *16*(2), 73–89. https://doi.org/10.2113/gseegeosci.16.2.73
Jetten, V. (2016). *Dominica National Flood Hazard Map Methodology and Validation Report*. Enschede. Retrieved from http://www.charim.net/sites/default/files/handbook/maps/DOMINICA/DOMFloodReport.pdf
Karssenberg, D., Schmitz, O., Salamon, P., Jong, K. De, & Bierkens, M. F. P. (2009). Environmental Modelling & Software A software framework for construction of process-based stochastic spatio-temporal models and data assimilation. *Environmental Modelling and Software*, *25*(4), 489–502. https://doi.org/10.1016/j.envsoft.2009.10.004
Kim, M. S., Onda, Y., Kim, J. K., & Kim, S. W. (2015). Effect of topography and soil parameterisation representing soil thicknesses on shallow landslide modelling. *Quaternary International*, *384*, 91–106. https://doi.org/10.1016/j.quaint.2015.03.057
Kim, M. S., Onda, Y., Uchida, T., & Kim, J. K. (2016). Effects of soil depth and subsurface flow along the subsurface topography on shallow landslide predictions at the site of a small granitic hillslope. *Geomorphology*, *271*, 40–54. https://doi.org/10.1016/j.geomorph.2016.07.031
Kuriakose, S. L., Devkota, S., Rossiter, D. G., & Jetten, V. G. (2009). Prediction of soil depth using environmental variables in an anthropogenic landscape, a case study in the Western Ghats of Kerala, India. *Catena*, *79*(1), 27–38. https://doi.org/10.1016/j.catena.2009.05.005
Lanni, C., Mcdonnell, J., Hopp, L., & Rigon, R. (2013). Simulated effect of soil depth and bedrock topography on near-surface hydrologic response and slope stability. *Earth Surface Processes and Landforms*, *38*(2), 146–159. https://doi.org/10.1002/esp.3267
Lee, J. H., & Park, H. J. (2016). Assessment of shallow landslide susceptibility using the transient infiltration flow model and GIS-based probabilistic approach. *Landslides*, *13*(5), 885–903. https://doi.org/10.1007/s10346-015-0646-6
Leung, A. K., & Ng, C. W. W. (2013). Analyses of groundwater flow and plant evapotranspiration in a vegetated soil slope. Canadian Geotechnical Journal, 50(12), 1204–1218. https://doi.org/10.1139/cgj-2013-0148
Liu, J., Chen, X., Lin, H., Liu, H., & Song, H. (2013). A simple geomorphic-based analytical model for predicting the spatial distribution of soil thickness in headwater hillslopes and catchments. *Water Resources Research*, *49*(11), 7733–7746. https://doi.org/10.1002/2013WR013834
Lucà, F., Buttafuoco, G., Robustelli, G., & Malafronte, A. (2014). Spatial modelling and uncertainty assessment of pyroclastic cover thickness in the Sorrento Peninsula. *Environmental Earth Sciences*, *72*(9), 3353–3367. https://doi.org/10.1007/s12665-014-3241-6
Matori, A. N., & Basith, A. (2012). Evaluation of landslide causative factors towards efficient landslide susceptibility modelling in the Cameron Highlands, Malaysia. *WIT Transactions on Engineering Sciences*, *73*, 207–218. https://doi.org/10.2495/DEB120181
McColl, S. T. (2015). Landslide Causes and Triggers. In *Landslide Hazards, Risks and Disasters* (pp. 17–42). Academic Press. https://doi.org/10.1016/B978-0-12-396452-6.00002-1

Michel, G. P., & Kobiyama, M. (2016). Development of new equation to estimate the maximum soil depth by using the safety factor. *Associazione Geotecnica Italiana*. Retrieved from https://www.ufrgs.br/gpden/wordpress/wp-content/uploads/2014/10/Michel-and-Kobiyama-2016-ISL-MEMPS.pdf.

Montgomery, D. R., & Dietrich, W. E. (1994). A physically based model for the topographic control on shallow landsliding, *30*(4), 1153-i17. https://doi.org/doi.org/10.1029/93WR02979

Popescu, M. E. (1994). A suggested method for reporting landslide causes. *Bulletin of the International Association of Engineering Geology*, *50*(1), 71–74. https://doi.org/10.1007/BF02594958

Popescu, M. E. (2002). Landslide causal factors and landslide remedial options. In *Keynote Lecture, Proceedings 3rd International Conference on Landslides, Slope Stability and Safety of Infra-Structures* (pp. 61–81). Singapore.

Rad, S., Rivé, K., Vittecoq, B., Cerdan, O., & Allègre, C. J. (2013). Chemical weathering and erosion rates in the lesser antilles: An overview in guadeloupe, martinique and dominica. *Journal of South American Earth Sciences*, *45*, 331–344. https://doi.org/10.1016/j.jsames.2013.03.004

Ran, Q., Su, D., Qian, Q., Fu, X., Wang, G., & He, Z. (2012). Physically-based approach to analyze rainfall-triggered landslide using hydraulic gradient as slide direction. *Journal of Zhejiang University Science*, *13*(12), 943–957. https://doi.org/10.1631/jzus.A1200054

Reading, A. J. (1991). Stability of tropical residual soils from Dominica, West Indies. *Engineering Geology*, *31*(1), 27–44. https://doi.org/10.1016/0013-7952(91)90055-P

Reichenbach, P., Busca, C., Mondini, A. C., & Rossi, M. (2014). The influence of land use change on landslide susceptibility zonation: The Briga catchment test site (Messina, Italy). *Environmental Management*, *54*(6), 1372–1384. https://doi.org/10.1007/s00267-014-0357-0

Rouse, W. C., Reading, A. J., & Walsh, R. P. D. (1986). Volcanic soil properties in Dominica, West Indies. *Engineering Geology*, *23*(1), 1–28. https://doi.org/10.1016/0013-7952(86)90014-1

Rouse, C. (1990). The mechanics of small tropical flowslides in Dominica, West Indies. *Engineering Geology*, *29*(3), 227–239. https://doi.org/10.1016/0013-7952(90)90052-3

Sarkar, S., Roy, A. K., & Martha, T. R. (2013). Soil depth estimation through soil-landscape modelling using regression kriging in a Himalayan terrain. *International Journal of Geographical Information Science*, *27*(12), 2436–2454. https://doi.org/10.1080/13658816.2013.814780

Saxton, K. E., & Rawls, W. J. (2006). Soil Water Characteristic Estimates by Texture and Organic Matter for Hydrologic Solutions, *1578*, 1569–1578. https://doi.org/10.2136/sssaj2005.0117

Schaetzl, R. J. (2013). Catenas and Soils. *Treatise on Geomorphology*, *4*, 145–158. https://doi.org/10.1016/B978-0-12-374739-6.00074-9

Segoni, S., Leoni, L., Benedetti, A. I., Catani, F., Righini, G., Falorni, G., … Rebora, N. (2009). Towards a definition of a real-time forecasting network for rainfall induced shallow landslides. *Natural Hazards and Earth System Science*, *9*(6), 2119–2133. https://doi.org/10.5194/nhess-9-2119-2009

Segoni, S., Rossi, G., & Catani, F. (2011). Improving basin scale shallow landslide modelling using reliable soil thickness maps. *Natural Hazards*, *61*(1), 85–101. https://doi.org/10.1007/s11069-011-9770-3

Soil Survey. (1951). Soil Survey Manual (18th ed.). Washington DC: Agricultural Research Administration, United states department of Agriculture. Retrieved from https://www.nrcs.usda.gov/Internet/FSE_MANUSCRIPTS/alabama/soilmanual1951/soilsurveymanual1951file1.pdf

Sorbino, G., Sica, C., & Cascini, L. (2010). Susceptibility analysis of shallow landslides source areas using physically based models. *Natural Hazards*, *53*(2), 313–332. https://doi.org/10.1007/s11069-009-9431-y

Taghizadeh-Mehrjardi, R., Sarmadian, F., Minasny, B., Triantafilis, J., & Omid, M. (2014). Digital Mapping of Soil Classes Using Decision Tree and Auxiliary Data in the Ardakan Region, Iran. *Arid Land Research and Management*, *28*(2), 147–168. https://doi.org/10.1080/15324982.2013.828801

Tesfa, T. K., Tarboton, D. G., Chandler, D. G., & McNamara, J. P. (2009). Modeling soil depth from topographic and land cover attributes. *Water Resources Research*, *45*(10), 1–16. https://doi.org/10.1029/2008WR007474

Van Asch, T. W., Buma, J., & Van Beek, L. P. (1999). A view on some hydrological triggering systems in landslides. Geomorphology, 30(1–2), 25–32. https://doi.org/10.1016/S0169-555X(99)00042-2

Van der Knijff, J.M.F., Jones, R.J.A., Montanarella, L. (1999). Soil Erosion Risk Assessment in Italy. European commission directorate general jrc joint research centre Space Applications Institute European Soil Bureau p. 58.

Van Looy, K., Bouma, J., Herbst, M., Koestel, J., Minasny, B., Mishra, U., Montzka, C., Nemes, A., Pachepsky, Y.A., Padarian, J., Schaap, M. G., Tóth, B., Verhoef, A., Vanderborght, J., Martine, J.V., Lutz, W., Zacharias, S., Zhang, Y., Vereecken, H. (2017). Pedotransfer Functions in Earth System Science: Challenges and Perspectives. *Reviews of Geophysics*, *55*(4), 1199–1256. https://doi.org/10.1002/2017RG000581

Van Westen, C. J. (2016). *National Scale Landslide Susceptibility Assessment for Dominica*. Washington, D.C. https://doi.org/10.13140/RG.2.1.4313.2400

Wilford, J., & Thomas, M. (2013). Predicting regolith thickness in the complex weathering setting of the central Mt Lofty Ranges, South Australia. *Geoderma*, *206*, 1–13. https://doi.org/10.1016/j.geoderma.2013.04.002

Wösten, J. H. M., Pachepsky, Y. A., & Rawls, W. J. (2001). Pedotransfer functions: bridging the gap between available basic soil data and missing soil hydraulic characteristics. *Journal of Hydrology*, *251*(3–4), 123–150. https://doi.org/10.1016/S0022-1694(01)00464-4

Yilmaz, I., & Kaynar, O. (2011). Multiple regression, ANN (RBF, MLP) and ANFIS models for prediction of swell potential of clayey soils. *Expert Systems with Applications*, *38*(5), 5958–5966. https://doi.org/10.1016/j.eswa.2010.11.027

Zafra, P. (2015). *National Scale Landslide Susceptibility Assessment for Dominica and Saint Vincent*. University of Twente. https://doi.org/10.13140/RG.2.1.4313.2400

Zhang, W., Hu, G., Sheng, J., Weindorf, D. C., Wu, H., Xuan, J., & Yan, A. (2018). Estimating effective soil depth at regional scales : Legacy maps versus environmental covariates, 167–176. https://doi.org/10.1002/jpln.201700081

**Appendix 1**: The distribution of inventory landslide per land use of the area

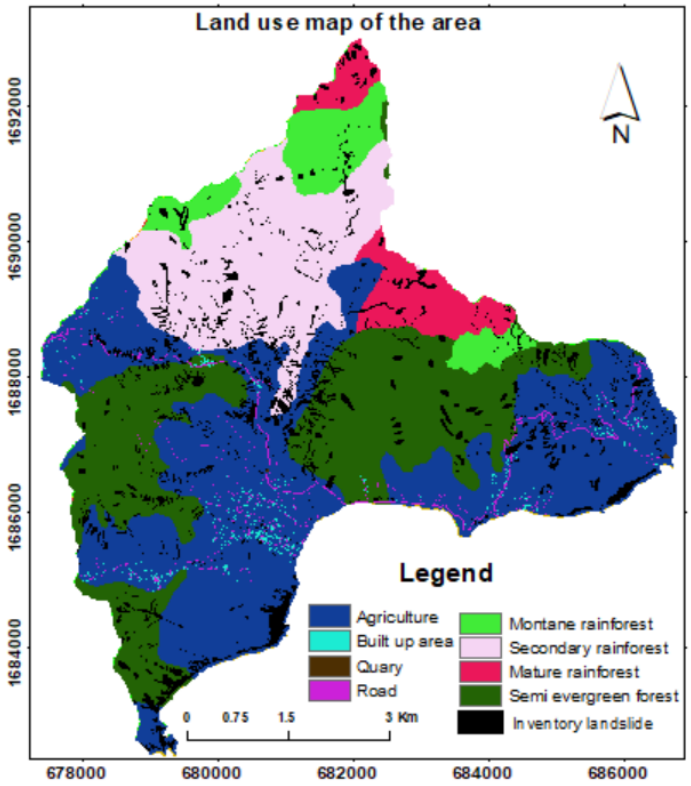

**Appendix 2**
**PCRaster code**

```
############################################################
# MSC thesis (groundwater balance and slope stability model)
# Version 4.1.0 #
# timestep: day #
# input : daily rainfall and daily ETp, dem, soiltypes, landuse types # #
############################################################
#! --matrixtable --radians --lddout
# global options, do not touch!
```

**binding**

```
### Input ###
dem = dem10mNew.map; # digital elevation model
stations = station2.map; # map with rainfall station(s)
LDD = ldd2.map;
soilunit = soils1.map; # main texture class units
rainfall_tss = prec2009.tss; # rainfall data in mm/day
ETP_tss = ETp2009.tss; # Potential evapotranspiration, based on Penman
soildata_tbl = soils.tbl; # 1 = ksat, 2=pore, 3=field capacity, 4=wilting point, 5 = c
# 6 = phi, 7= bulk density
Ksat = ksat2.map; # saturated hydraulic conductivity (mm/h)
soildepth = soildepth.map; # soil depth in mm
riverwid = rivw.map; # stream channel width (m)
landunit = landuse2.map; # land use types
landusedata_tbl = landuse.tbl; # 1=cover, 2=height, 3=ground cover
Outlet = outlet2.map;
#rivfract = rivfrac.map;
mask=mask.map;
### Output ###
#maps##
theta_s = pore.map; # porosity (fraction)
theta_fc = fieldcap.map; # field capacity (fraction)
theta_wp = wilting.map; # wilting point (fraction)
SoilMoisture = moist; # daily soil moisture maps (mm)
interception = intc; # daily interception (mm)
unsatdepth = unsdep; # deoth unsaturated zone (mm)
#graphs
p_tss = pavg.tss; # average daily rainfall (mm)
pcum_tss = pcumavg.tss; # average cumulative rainfall (mm)
ETpavg_tss = etpavg.tss; # average daily ETp (mm)
ETpcum_tss = ETpcumavg.tss; # average cumulative ETp (mm)

intccum_tss = intcum.tss; # average cumulative interception (mm)
ETfact_tss = ETfactor.tss; # average daily ratio ETa/ETp
eta_tss = ETaavg.tss; # average daily ETa (mm)
etacum_tss = ETacumavg.tss; # average cumulative ETa (mm)
perc_tss = perc.tss; # average daily percolation (mm)
perccum_tss = perccum.tss; # average daily cumulative percolation (mm)
```

```
infcum_tss = infilcum.tss; # average cumulative interception (mm)
rocum_tss = runoffcum.tss; # average cumulative interception (mm)

theta_tss = theta.tss; # average daily theta (-)
moisture_tss = moisture.tss; # average daily soil moisture (mm)
```

**areamap**

```
dem;
```

**timer**

```
1 365 1; # 365 days, 2004 and 2009, adjust when using different year!
```

**initial**

```
report mask = scalar(soilunit ne 0 and landunit ne 0 and dem gt 0);
# ensure the mask has the smallest cross section with all input maps

dem *= mask;
soilunit = if(mask eq 1,soilunit);
landunit = if (mask eq 1, landunit);

nrCells = maptotal(mask);
# nr cells in catchment
################################
### read soil related data ###
################################
rivfrac = min(1.0, riverwid/celllength());
# fraction of riverwidth in a stream gridcell, 0 elsewhere
#report rivfrac.map = min(1.0, riverwid/celllength());
dem = if(riverwid gt 0, dem-2*rivfrac,dem) + 10;
#burn in the river
report LDD = lddcreate(dem, 1e10,1e10,1e10,1e10);
report ws.map=catchment(LDD, pit(LDD));
# burn in the river, 2 m
outcrop = boolean(0); #soildep22.map eq 0;
# boolean map with true and false
Ksat = Ksat * 24 * mask;
#convert to mm/day
theta_s = lookupscalar(soildata_tbl, 2, soilunit);
# porosity in column 2 (-)
theta_fc = lookupscalar(soildata_tbl, 3, soilunit);
# field capacity in column 3 (-)
theta_wp = lookupscalar(soildata_tbl, 4, soilunit);
# wilting point in column 4 (-)
#m_param = lookupscalar(soildata_tbl, 8, soilunit);
#Van Genuchten n-param NOT USED
theta_s = theta_s * mask;
#porosity (-)
theta_fc = theta_fc * mask;
#field capacity (-)
theta_wp = theta_wp * mask;
#wilting point (-)
```

```
Cover = lookupscalar(landusedata_tbl, 1, landunit)*mask;
# constant plant cover (-)

TanPhi = lookupscalar(soildata_tbl,6,soilunit);
# tan of angle of internal friction
coh = lookupscalar(soildata_tbl,5,soilunit);
# regolith/soil cohesion kPa
bulk = lookupscalar(soildata_tbl,7,soilunit);
# specific density regolith kN/m3
##############################
### initialize variables ###
##############################

theta = theta_fc;
# initialize soil moisture theta at field capacity (arbitrary)
GWDepth = soildepth*0.2;
# groundwater intially at 0.2 of the depth

GWDepth = (1-rivfrac)*GWDepth;
GWDepth = if (outcrop, 0, GWDepth);
# initialize groundwater depth (mm)
soildepth = if(outcrop, 10, soildepth);

unsatdepth = soildepth - GWDepth;
#depth unsatirated zone (mm)
SoilMoisture = theta*unsatdepth;
# initial soil moisture in mm

### totals ###
ETacum = 0;
ETpcum = 0;
Pcum = 0;
percum = 0;
intccum = 0;
infilcum = 0;
peakcum = 0;
Tacum = 0;
Eacum = 0;
rocum = 0;
totbase = 0;
totpeak = 0;
interception = 0*mask;
Perc = 0*mask;
SafetyDay = 0*mask;
baseflow = 0*mask;
surplus = 0*mask;
FDays = 0;
dynamic
##########################
### meteo data input ###
```

```
#########################
Pinterpol = timeinputscalar(rainfall_tss, stations);
# get the rainfall values at the stations

P = Pinterpol*mask;
# restrict to area mask
report p_tss = maptotal(P)/nrCells;
# write a graph of the average daily rainfall

Pcum = Pcum + P;
#calculate cumulative P for outut
#report pcum_tss = maptotal(Pcum)/nrCells;
# write a graph of the average cumulative rainfall
ETp = timeinputscalar(ETP_tss, nominal(mask));
# read potential evapotranspiration from a file and give the whole area that value
# ETp is the potential evapotranspiration (in mm) report ETpavg_tss = maptotal(ETp)/nrCells;
ETpcum = ETpcum + ETp;
report ETpcum_tss = maptotal(ETpcum)/nrCells;
#####################
### Interception ###
#####################
Coverm = min(Cover, 0.95);
# maximize cover fraction to 0.95, to avoid infinite LAI
LAI = ln(1-Coverm)/-0.4;
# calculate LAI from Cover using Cover = exp(-0,4*LAI), WOFOST
Smax = max(0, 0.2856*LAI);
Smax = if(outcrop, 0, Smax);
Smax = Smax*(1-rivfrac);
# calculate Smax from LAI and avoid negative values becuse of logarithm
# formula from data in De Jong and Jetten (2008)

interception = interception + P - ETp;
# add rainfall and subtract evaporation from interception
interception = min(Smax, interception);
# fill up the interception with rain to a max of Smax
interception = max(0, interception);
# cannot be less than 0
Pe = max(P - interception, 0);
# effective rainfall is rainfall - interception, but larger than 0

ETp = if(interception gt ETp, 0, ETp - interception);
# decrease potential evaporation with interception evaporation
# if ETp is greater that interception, interception becomes 0

intccum = intccum + interception;
# report cumulative interception
report intccum_tss = maptotal(intccum)/nrCells;
# graph with spatial average cumulative interception (mm)
#####################
### Infiltration ###
```

```
#####################
store = max(1.0, (theta_s-theta)*unsatdepth);
cal = 1.0;

rof = if(Pe gt 0, exp(-cal*store/Pe), 0);
#runoff coefficient according to Shrestha and Jetten 2018, based on kirkby 1976
rof = if(unsatdepth gt 1.0, rof, 1.0);
# 100% runoff if soil is nearly full

Infilcap = min((1-rof)*Pe, store);
Infilcap = if(outcrop, 0, Infilcap);
Infilcap = (1-rivfrac)*Infilcap;
Runoff = accuthresholdflux(LDD, Pe, Infilcap)*mask;
Infil = accuthresholdstate(LDD, Pe, Infilcap)*mask;
# route the water to the outlet

infilcum = infilcum + Infil;
# report cumulative interception
report infcum_tss = maptotal(infilcum)/nrCells;

###################################
### Actual Evapotranspiration ###
###################################

# actual evapotranspiration ETa linear with soil moisture content (mm)
ETpoint = theta_wp + (theta_fc - theta_wp)*1/3;
ETfactor = if (theta gt ETpoint, 1.0, 0.0);
ETfactor = if (theta lt ETpoint and theta ge theta_wp,
(theta-theta_wp)/(ETpoint-theta_wp), ETfactor);
ETfactor = if (theta lt theta_wp, 0.0, ETfactor);
report ETfact_tss = maptotal(ETfactor)/nrCells;
Ta = ETp * ETfactor * Cover;
# actual transpiration (mm)
Ea = ETp * theta/theta_s * (1-Cover);
#actual soil evaporation (mm)
Ea = if(outcrop, 0, Ea);
Ta = if(outcrop, 0, Ta);
Ta = (1-rivfrac)*Ta;
Ea = (1-rivfrac)*Ea;
ETa = Ea + Ta;
# ETa sum of the Evap and Transp
ETa = min(ETa, SoilMoisture);
# cannot be more than soil moisture present

# graphs with average and cumulative average ETa of all cells
report eta_tss = maptotal(ETa)/nrCells;
ETacum = ETacum + ETa;
report etacum_tss = maptotal(ETacum)/nrCells;
#####################
### Percolation ###
```

```
####################
theta_e = (theta/theta_s);

# percolation based on Shrestha and Jetten, 2018, after Brooks Corey 1964
p_coef = if(Ksat gt 0.1, 5.55*((Ksat/24)**-0.114), 0);
# using characteristic values for ksat to get a coefficient for percolation decrease with moisture
Perc = if (theta gt theta_fc, Ksat*(theta_e**p_coef), 0);
# using the coefficient to calculate the percolation from Ksat and theta_e
# assume dH/dz = 1 percolation depends on unsaturated hydr conductivity

Perc = min(Perc, SoilMoisture);
# cannot have more percolation than soil moisture
Perc = if(outcrop, 0, Perc);
Perc = (1-rivfrac)*Perc;
report perc_tss = maptotal(Perc)/nrCells;
# graph with average spatial percolation

percum = percum + Perc;
#report perccum_tss = maptotal(percum)/nrCells;
# cumulative percolation

############################
### new soil moisture ###
############################
SoilMoisture = SoilMoisture + (Infil - ETa - Perc) * dt;
SoilMoisture = max(0, SoilMoisture);
SoilMoisture = if(outcrop, 0, SoilMoisture);
# update soil moisture (mm) with rainfall and evapotranspiration

surplus = max(0, SoilMoisture - unsatdepth*theta_s);
# the water balance can result in more soilmoisture than fits in the soil
SoilMoisture = SoilMoisture - surplus;

theta = if(unsatdepth gt 0, SoilMoisture/unsatdepth, theta_s);
# soil moisture content (cm3/cm3) = (-)
report theta = min(theta_s, theta);

# calc new soil moisture based on adjusted theta (mm)
#SoilMoisture = theta * unsatdepth;
# graph with average theta of all cells
report theta_tss = maptotal(theta)/nrCells;
report moisture_tss = maptotal(SoilMoisture)/nrCells;

############################
### Groundwater balance ###
############################
# Gravity based flow: potential differences
# between GW surface in NS and EW directions
# Total flow in/out cell is:
# Darcy : Q = q*A = K sin(a)*(h*dx)
```

```
# A is wet cross section of the flow
# dQ = SUM [ (K * sin(a)*h*dx) ] EW and NS
# dQ is in m3/timestep and is added to the central cell
# Converted to height by division by the cell area
#NOTE: everything is in meters and meters/day

dx = celllength();
# set up basic directions for groundwater movement
ldd2 = ldd(2*mask); #south, row + 1
ldd4 = ldd(4*mask); #west, col - 1
ldd6 = ldd(6*mask); #east, col + 1
ldd8 = ldd(8*mask); #north, row - 1
z = (dem-mapminimum(dem)+1) - soildepth/1000;
# gravity potential equals dem of bedrock, soildepth is in mmm, convert to m
# assume more averaged (smooth) subsurface DEM over which GW flows ?
GWDepth = GWDepth + if(theta < theta_s, Perc/(theta_s-theta), 0);
GWDepth = if (outcrop, 0, GWDepth);

GWDepth = min (GWDepth, soildepth);
# add percolation amount to GW depth (convert to height in mm)

h = GWDepth/1000;
# GW depth in mm, h = matric potential in m
SumGWbefore = maptotal(h);
# sum GW before movement

day = 0;
hours = 2; #from 6 to 2
frac = hours/24; #8 hour timestep
grad = sin(atan(slope(dem)));
# loop to make the GW flow in steps less than a day, e.g. 8 hours does 3 steps

repeat{
H = h + z;
# total hydraulic potential in m
dHdL2 = sin(atan((upstream(ldd2, H)-H)/dx));
dHdL4 = sin(atan((upstream(ldd4, H)-H)/dx));
dHdL6 = sin(atan((upstream(ldd6, H)-H)/dx));
dHdL8 = sin(atan((upstream(ldd8, H)-H)/dx));

# sine of potential differences between central cell
# dH/dx = tan so atan(dH/dx) is angle
# and cells in 4 directions EW ans NS (in m)
h2 = 0.5*(h+upstream(ldd2, h));
h4 = 0.5*(h+upstream(ldd4, h));
h6 = 0.5*(h+upstream(ldd6, h));
h8 = 0.5*(h+upstream(ldd8, h));

dQ = 10*frac*Ksat/1000 * dx * (h2*dHdL2 + h8*dHdL8 + h4*dHdL4 + h6*dHdL6);
# sum of all fluxes in m3/day, ksat in m/day, divide by 1000
```

```
h = h + dQ/(dx*dx);
# add in/out flow to the cell in m
day += hours;
### mass balance correction ###
SumGWafter = maptotal(h);
# sum GW after the movement
errorh = (SumGWbefore - SumGWafter)*mask;
#total mass balance error in GW depth (before - after)
wetcells = maptotal(scalar(h gt 0))*mask;
# calc which cells have GW
h = h + if(h gt 0, errorh/wetcells, 0);
# smooth out the error over all wet cells
SumGWafter = maptotal(h);
# report any remaining error in the mass balance

}until day gt 24;

report GWerror.tss = if (SumGWbefore gt 0.001,(SumGWbefore -
SumGWafter)/SumGWbefore,0);

#####################################
### back to hydrology, discharge ###
#####################################
GWDepth = h*1000;
# convert from m back to mm for comparison with the other fluxesin the model
GWDepth = max(0, GWDepth);
report surplus += if (GWDepth gt soildepth, (GWDepth-soildepth)*theta_s, 0);
GWDepth = min(GWDepth, soildepth);
#confine GWdepth between 0 and surface, surplus water becomes runoff
Runoff = Runoff + accuflux(LDD, surplus);
peak = Runoff*cellarea()*0.001;
#daily runoff in m3

GWloss = if(GWDepth gt 300, 0.01*GWDepth, 0);
GWDepth = GWDepth - GWloss;
# subtract a loss when GWDepth is above a threshold
GWDepth = if(outcrop, 0, GWDepth);
# no groundwater where outcrops
baseflow = (GWDepth*rivfrac*theta_s) + GWloss*theta_s;
base = accuflux(LDD, baseflow)*cellarea()*0.001;
#baseflow in m3/day
report Q = peak + base;

report q.tss = timeoutput(Outlet,Q);
report GWDepth = if(riverwid gt 0, GWDepth * (1-rivfrac) ,GWDepth);
unsatdepth = max(0, soildepth - GWDepth);
# hew unsaturated zone depth
#####################################
### slope stability SAFETY FACTOR ###
#####################################
```

```
grad = slope(dem)+0.005;
cosS = cos(atan(grad));
sinS = sin(atan(grad));
bulk_w = 9.8;
# bulk density water in kN/m3
Mu = GWDepth/1000;
#report Mu.map = GWDepth/1000;
# pore pressure in m
D = soildepth/1000;
# soil depth in m
cohroot = 1; #kPa, changed from 4 to 2
Tan_Phi = tan(TanPhi* 3.141592/180); # tan(angle *pi/180)
S = coh+cohroot+(D*bulk - Mu*bulk_w)*(cosS**2)*Tan_Phi;
# S = (coh+cohroot+(D*bulk - Mu*bulk_w)*(cosS**2)*TanPhi);
# shear strength
T = D*bulk*sinS*cosS;
# report T.map = D*bulk*sinS*cosS;
# shear stress kPa
F = S/T;
#safety factor, strength/stress, F >=1 means stable
report F = if(outcrop,0, F);#min(2,F);
# no instability on outcrops

report FDays = FDays + if (F lt 1, 1, 0);
# cumulative days in year when unstable
report FdayTot = FDays;
# report the last timestep, cumulative unstable days
```

**Appendix 3 Script to produce soil depth map using the decision tree**

```
rockexposure.map=scalar(if((grad.map ge 0.6 or distriva.map ge 290 or twi.map lt 0), 0,1))

very_shallowdepth.map=scalar(if(((grad.map ge 0.3) and (grad.map lt 0.6)) or ((distriva.map ge 220) and
(distriva.map lt 290)) or (twi.map lt 4), 0.2, 0))

shallowdepth.map=scalar(if(((grad.map ge 0.15) and (grad.map lt 0.3)) or ((curvp.map lt 0.05) and
(curvp.map gt 0)) or ((distriva.map ge 140) and (distriva.map lt 220)) or ((twi.map ge 4) and (twi.map lt
5)),0.4, 0))

moderatedepth.map=scalar(if(((grad.map ge 0.15) and (grad.map lt 0.3)) or ((curvp.map ge -0.0001) and
(curvp.map lt 0.006)) or ((distriva.map ge 70) and (distriva.map lt 140)) or ((twi.map ge 5) and (twi.map lt
6)),0.6, 0))

deepsoil.map=scalar(if(((grad.map ge 0.02) and (grad.map lt 0.15)) or (curvp.map lt -0.003) or
((distriva.map ge 10) and (distriva.map lt 70)) or ((twi.map ge 6) and (twi.map lt 12)),0.8,0))

verydeepsoil.map=scalar(if(((grad.map ge 0) and (grad.map lt 0.02)) or (curvp.map lt -0.08) or
((distriva.map ge 0) and (distriva.map lt 10)) or (twi.map ge 12),1, 0))
```

**Appendix 4 Frequency distributions of distance to river and TWI**

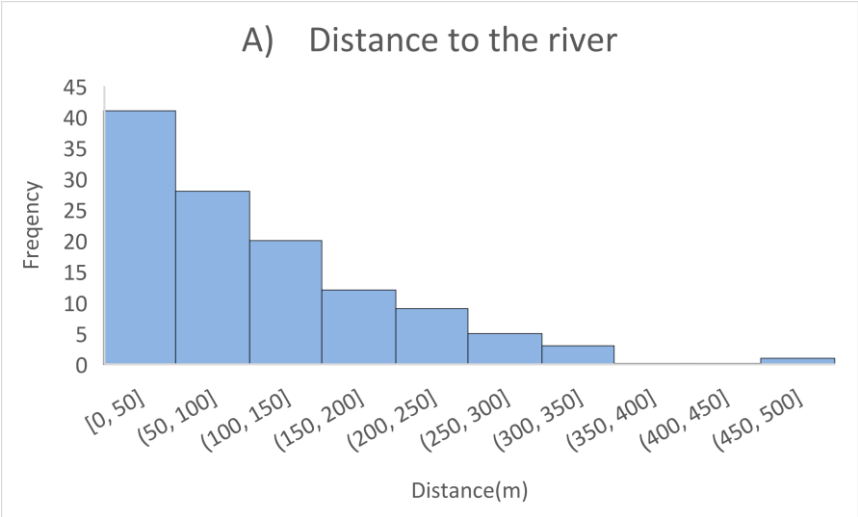


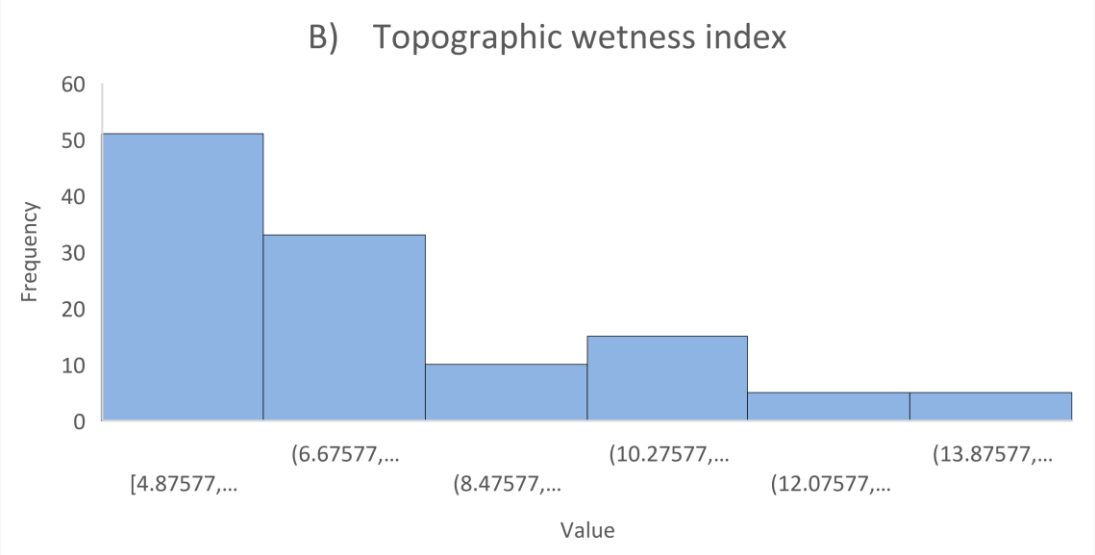


**Appendix 5 Soil depth scrip for soil balance equation model**

```
##########################################
# Model: Soil depth
# ##########################################
```

**binding**

```
mask=mask.map;
chanm = channelr.map;
soildepth=soildepth.map;
dem=dem10m.map;
distriv = distriv.map;
twi= twi.map;
curv=curvp.map;
grad=grad.map;
```

**initial**

```
#grad = min(1.0,slope(dem));
weight = grad; #weight for spreading, def 1.0. Grad gives steep slopes
coeff = 0.9; #higher than 1 gives narrow deep valley soils,
#< 1.0 gives broad deep valley soils
#report curv=profcurv(dem); #negative concave to positive convex)
#report distriv = spread(nominal(chanm gt 0),0,weight)*mask;
soild = cover(
1-0.7*grad # steeper slopes giver undeep soils
-0.6*distriv/mapmaximum(distriv) # closer to river gives deeper soils
+0.7*curv
+0.3*twi/mapmaximum(twi) # convex gives deeper soils
,0)*mask;
soild = (soild-mapminimum(soild))/(mapmaximum(soild)-mapminimum(soild));
soild = (soild)**coeff;
# m to mm for lisem, higher power emphasizes deep, updeep
soildepth = soild;#mask*(200+cover(windowaverage(soild,3*celllength()),mask));
report soildep3.map = soildepth*mask;
```